To the Graduate Council

I am submitting herewith a dissertation written by Saad Khattabi entitled "Separation of Selected Flavor Compound Enantiomers by Simulated Moving Bed Chromatography. Screening of 1-phenyl-1-propanol for Antimicrobial Activity" . I have examined the final copy of this dissertation for form and content and recommend that it be accepted in partial fulfillment of the requirements for the degree of Doctor of Philosophy, with major in Food Science and Technology.

Georges Guiochon, Major Professor

We have read this dissertation
and recommend its acceptance:

Sharon L. Melton

T. Ann Draughon

John R Mount

Accepted for the Council

Associate Vice Chancellor and
Dean of the Graduate School

Separation of Selected Flavor Compound Enantiomers by Simulated Moving Bed Chromatography

Screening of 1-phenyl-1-propanol for Antimicrobial Activity

A Dissertation
Presented for the
Doctor of Philosophy
Degree
The University of Tennessee, Knoxville

Saad Khattabi

December 1999

AG-VET-MED.
Thesis
996
.K47

Acknowledgments

First and foremost I would like to praise Allah the almighty, the merciful and the most compassionate for all his bounties. Then I would like to express my deepest gratitude to my major professor and advisor, Dr. Georges Guiochon, for his guidance, his help , and his patience throughout the course of my graduate research. I truly consider being a member of his research group for all these years as a tremendous honor and pleasure and I am grateful to him for the opportunity.

I would like to thank Professor Sharon Melton, Professor F. Ann Draughon and Professor John Mount for taking the time to serve in my doctoral committee. Special thanks for Professor F.A. Draughon for allowing me to conduct the last phase of my study in her lab, and for graciously making available to me all the material and equipment I needed. Many thanks also to Mondonna F. Cate, Mona Elgayyar, Willie Taylor, and Kay M. Trigiano for their help and assistance.

I would also like to acknowledge and thank the following group members, for their friendship and assistance, and for making our lab such a great work place: Zouhir Bensetiti, Tobias Bradshaw, Scott Broyles, Yibai Chen, Djamel Cherrak, Tivadar Farkas, Attila Felinger, Torgny Fornstedt, Jorg Fricke, Marianna Kele, Joon-ho Kho, Jayne Kubas, Kathleen Milhbachler, Kanji Miyabi, Igor Quinones-Garcia, Preshious Rearden, Peter and Hong Sajonz, Andrew Shalliker, Sue Smith, Tong Yun and Guoming Zhong. From the group cited above, Dr.

Djamel Cherrak deserves from me a special mention for all his help, his support and his friendship ever since he joined Dr. Guiochon's group. Dr. Marianna Kele also deserves a special thanks for being so kind and so disposed, never refusing to help.

Many thanks to Dr. Pierre Hilaireau and Dr. Henri Colin from Prochrom, Champineulles, France for graciously inviting me to spend a 2 week training period at their company. Thanks to Beatrice Joveniaux and to Pascal Jusforgues, also from Prochrom, for their kind help and assistance during my visit.

Last, but certainly not least, I would like to thank the members of my immediate and extended family:

* My dear parents for crossing the ocean to come and share with me the joyful event of graduating, for their continuous support and sacrifices, and most importantly for their everlasting prayers for me.

* My siblings Afifa, Chihab, and Taoufik and their spouses, my mother-in-law Janice Davidson, my sister-in-law Amy, and my friends Boualam & Farida for their support and encouragements.

* Our sons Aaron and Michael for enduring, and living through my frustration days.

* Finally, I thank my lovely wife, Zineb, for her love, and understanding throughout the whole ordeal. Without her support and countless sacrifices I would not have made it, so thanks Zineb.

Abstract

While the concept of simulated moving bed technology (SMB) has been known for almost forty years, its application to fine chemistry, and chiral separations in particular, did not really develop until recently. SMB is a continuous countercurrent chromatographic technique geared mainly toward production, limited to binary mixture separations. Such limitation becomes of no concern, when chiral separations are considered.

In the first phase of this study our objectives were to use SMB to separate enantiomers of selected flavor compounds under both linear and non-linear conditions. In the linear case, we confirmed that determining operating conditions for an SMB separation, is rather simple. The toughest hurdle seems to be obtaining columns with close characteristics. The importance of, periodically, testing SMB columns was experimentally proven. A lab-scale SMB, with eight column setting, was used to carry out enantiomer separations of three flavor compounds (benzoin, δ-octalactone and 1-phenyl-1-propanol), under linear conditions. The separation was successful, in all three cases, generating products with a purity higher than 97%, and nearing 100% in several instances.

To "upgrade" the separation to non-linear conditions (for 1-phenyl-1-propanol, or PP), adsorption isotherm parameters needed to be determined. A simple competitive Langmuir model was able to describe well both single component, and competitive behavior of PP on cellulose tribenzoate. The

isotherm parameters were used, in the context of the "triangle theory", to determine the SMB operating parameters, under non-linear conditions. Such an SMB run (total feed concentration 5g/l) generated a successful separation, with a purity >98% for the raffinate, and >95% for the extract. A production rate of 11.6 g of feed / day / kg of stationary phase, was achieved.

In the second phase of this study our objective was to screen PP enantiomers and their racemic mixture, for antimicrobial activity. All three exhibited strong activity against both bacteria and fungi. However, no significant differences ($P>0.05$) were found among the effectiveness of the three products. Among the bacteria, *Pseudomonas aeruginosa* and *Staphylococcus aureus* were the least inhibited, and the most sensitive, respectively. Among the fungi, *Rhodotorula glutinus* was found to be the least sensitive.

Table of Contents

I. INTRODUCTION....1

I-1. Generalities....1

I-1-1. Review of Chirality....1

I-1-2. Importance of Chirality....2

I-1-3. The FDA Position Toward Stereoisomers....4

I-1-4. Methods for Enantiomer Production....6

I-2. Objectives of the Study....7

I-3. Approaches to Reach Objectives....8

II. SIMULATED MOVING BED CHROMATOGRAPHY....10

II-1. Basic Principles of SMB....10

II-2. Advantages and Disadvantages of SMB....14

II-3. Enantiomer Separations Using SMB....17

II-4. Modeling of SMB....20

II-4-1. The Column Models....20

II-4-2. The Node Model....23

II-4-3. Estimation of Experimental Parameters....24

III. EQUIPMENTS AND EXPERIMENTAL PROCEDURES.....26

III-1. The Column Packing Procedure.....26

III-2. The SMB System.....27

III-3. The High Performance Liquid Chromatography System.....32

III-4. The PP Antimicrobial Activity Experiment.....34

IV. SEPARATION OF SELECTED FLAVOR COMPOUND ENANTIOMERS BY SMB UNDER LINEAR CONDITIONS.....35

IV-1. Introduction.....35

IV-2. Separation of Benzoin Enantiomers.....36

IV-2-1. Conventional HPLC Generated Data.....37

IV-2-2. SMB Operating Conditions.....40

IV-2-3. Results and Discussion.....43

IV-3. Separation of Octalactone Enantiomers.....56

IV-3-1. Conventional HPLC Generated Data.....58

IV-3-2. SMB Operating Conditions.....61

IV-3-3. Results and Discussion.....61

IV-4. Separation of 1-phenyl-1-propanol (PP) Enantiomers.....68

IV-4-1. Conventional HPLC Generated Data.....69

IV-4-2. SMB Operating Conditions.....71

IV-4-3. Results and Discussion.....71

IV-5. Summary 74

V. 1-PHENYL-1-PROPANOL ENANTIOMER SEPARATION BY SMB UNDER NON-LINEAR CONDITIONS: ADSORPTION BEHAVIOR STUDY.....76

V-1. Introduction.....76

V-2. Experimental Set-up.....78

V-2-1. Equipment and Materials.....78

V-2-2. Purification of PP Products.....80

V-2-3.Determination of Adsorption Isotherm for Single Component.....81

V-2-4. Determination of Competitive Adsorption Isotherms.....82

V-2-5. Fitting the Isotherm Data to the Isotherm Model.....83

V-3. Theory: Band Profile Calculations.....84

V-3-1 Equilibrium-dispersive Model.....84

V-3-2 Lumped Kinetic Model (transport-equilibrium).....85

V-3-3 Boundary Conditions.....86

V-4 Results and Discussion.....86

V-4-1. Modeling of Single Component Equilibrium Isotherms.....86

V-4-2. Modeling of the Competitive Equilibrium Isotherms.....92

V-4-3. Validation of the Isotherm Model.....98

V-5. Conclusion.....105

VI. 1-PHENYL-PROPANOL ENANTIOMER SEPARATION BY SMB UNDER NON-LINEAR CONDITIONS.....106

VI-1. Introduction.....106

VI-2. Optimization of a Chromatographic Process.....107

VI-2-1. Optimization Procedures.....107

VI-2-2. Optimization Parameters.....109

VI-2-3. The "Triangle Theory" as an Optimization Tool for SMB.111

VI-3. Experimental Results.....118

VII. INVESTIGATION OF ANTIMICROBIAL ACTIVITY OF 1-PHENYL-1-PROPANOL ENANTIOMERS.....129

VII-1. Introduction.....129

VII-2. Experimental Set-up.....132

VII-2-1. Chemicals, Microorganisms and Culture Media.....132

VII-2-2 .Procedure.....133

VII-3 Results and Discussion.....134

VII-3-1. Effect of PP on Bacteria.....134

VII-3-2. Effect of PP on Fungi.....138

VII-4. Conclusion.....143

VIII. SUMMARY AND GENERAL CONCLUSIONS.....145

REFERENCES.....147

VITA.....158

List of Tables

4-1 Characteristics for the 8 Closest Columns Obtained with Benzoin.....39

4-2 Two Sets of SMB Experimental Conditions for Benzoin Enantiomer Separation.....42

4-3 Characteristics for the 8 Closest Columns Obtained with Delta-octalactone.....59

4-4 SMB Experimental Conditions for δ-octalactone Enantiomer Separations.....62

4-5 Characteristics for the 8 Closest Columns Obtained with PP.....70

4-6 SMB Experimental Conditions for PP Enantiomer Separation.....72

5-1 Single Component Isotherm Coefficients for PP Enantiomers.....91

5-2 Competitive Isotherm Coefficients for PP Enantiomers.....93

5-3 Comparison of Simple Competitive Langmuir Isotherm Coefficients Determined from Single Component, Competitive, and Combined Data, for PP Products.....96

6-1 Characteristics for the 8 Closest Columns Obtained with PP (non-linear).....120

6-2 SMB Experimental Conditions for PP Enantiomer Separation under Non-linear Conditions.....124

6-3 Production Rate of Raffinate and Extract Produced During PP Enantiomer Separation by SMB under Non-linear Conditions.....127

7-1 Effect of PP Products on 5 Different Bacteria.....135

7-2 Effect of PP Products on 3 Different Fungi.....139

List of Figures

2-1 Schematic of an SMB Process.....13

2-2 Drawing of an SMB System Set-up.....15

3-1 Chemical Structure of Chiracel OB Stationary Phase.....26

3-2 The Column Packing Equipment.....28

3-3 A Photograph of the SMB System Used in this Study.....30

3-4 Inside of the SMB System Viewed from Above.....31

4-1 Normalized Production of Raffinate and Extract vs Cycle Rank

(a) Raffinate 44

(b) Extract.....45

4-2 Raffinate Start up Concentration Profile for Benzoin Separated by SMB.....47

(a) Calculated Profile

(b) Experimental Profile

4-3 Extract Start up Concentration Profile for Benzoin Separated by SMB.....48

(a) Calculated Profile

(b) Experimental Profile

4-4 Comparison Between Calculated and Experimental Elution Profiles inside the SMB System.....50

(a) Just before the Switch

(b) Just after the Switch

4-5 Analytical Chromatograms for Samples Collected During Benzoin Enantiomer Separation by SMB (Run 1).....54

4-6 Analytical Chromatograms for Samples Collected During Benzoin Enantiomer Separation by SMB (Run 2).....55

4-7 Analytical Chromatograms for Samples Collected During δ-octalactone Enantiomer Separation by SMB (total feed concentration =0.2 g/l).....64

4-8 Analytical Chromatograms for Samples Collected During δ-octalactone Enantiomer Separation by SMB (total feed concentration =0.4 g/l).....65

4-9 Analytical Chromatograms for Samples Collected During δ-octalactone Enantiomer Separation by SMB (total feed concentration =0.8 g/l).....66

4-10 Analytical Chromatograms for Samples Collected During δ-octalactone Enantiomer Separation by SMB (total feed concentration =1.0 g/l).....67

4-11 Analytical Chromatograms for Samples Collected During PP Enantiomer Separation by SMB (total feed concentration =0.5 g/l).....73

5-1 Injection Profile of Increasing Volumes of a Racemic PP Solution without Column.....87

5-2 Comparison of Single Component Experimental Data for PP Enantiomers on Chiracel OB, to the Best Fitted Langmuir Model.....88

5-3 Scatchard Plots of the Experimental Adsorption Data of PP Enantiomers.....90

5-4 Comparison of Experimental Competitive Adsorption Data for PP Enantiomers on Chiracel OB, to the Best Fitted Langmuir Model.....95

5-5 Experimental and Calculated Elution Profiles for 2 Injection Volumes of S-PP Solutions.....99

(a) V_{inj} =1.0ml

(b) V_{inj} =2.0ml

5-6 Experimental and Calculated Elution Profiles for 2 Injection Volumes of R-PP Solutions....101

(a) V_{inj} =1.0ml

(b) V_{inj} =2.0ml

5-7 Experimental and Calculated Elution Profiles for 4 Injection Volumes of Racemic PP Solutions

(a) V_{inj} =0.25 ml....102

(b) V_{inj} =0.5 ml....102

(c) V_{inj} =1.0 ml....103

(d) V_{inj} =2.0 ml....103

6-1 The (m_2, m_3) Plane with the 4 Different Regions for a System Characterized by a Linear Isotherm....114

6-2 Effect Of Increasing Feed Concentration on Complete Separation Zone in the (m_2, m_3) Plane....117

6-3 Separation Zone for PP Enantiomers in the (m_2, m_3) Plane....123

6-4 Analytical Chromatograms for Samples Collected During PP Enantiomer Separation by SMB under Non-linear Conditions....125

7-1 Illustration of the Effect of PP on 5 Bacteria....137

7-2 Controls (Sterilized Water) for Fungi....141

7-3 Illustration of the Effect of PP Products on 3 Fungi Grown on 2 Different Media..142

List of Symbols and Abbreviations

A	Column cross section
a_i	Henry's coefficient for compound i
$A_{i,j}$	Area under peaks i and j, respectively
b_i	Capacity factor for compound i (l/g)
C	Concentration in mobile phase (g/l)
$C_{F,T}$	Total feed concentration (g/l)
$C_{i,j}$	Liquid phase concentration of component i in section j (g/l)
C_x	Concentration of compound x in mobile phase (g/l)
$C_{x,ip}$	Concentration of compound x in intermediate plateau (g/l)
D_a	Apparent dispersion coefficient
D_L	Axial dispersion coefficient
DR	Desorbent requirement
dt	The length of time grid
dz	The length of space grid
F	Phase ratio
k_f	Mass transfer rate coefficient
K_i	Henry's coefficient of compound i (equivalent to a_i)
k'_i	Retention factor of component i
L	Column length

m_j	Ratio of liquid flow rate over adsorbed phase flow rate in section j
N	Number of theoretical plates, or efficiency
N_0	Efficiency calculated with non-retained compound
N_i	Efficiency calculated with compound i
N_d	Number of data points
P_i	Purity of compound i
PR	Production rate
q	Amount adsorbed on the solid phase
Q_j	Flow rate in section j, (j = I, II, III, or IV) (ml/min)
Q_d	Desorbent flow rate (ml/min)
Q_e	Extract flow rate (ml/min)
Q_f	Feed flow rate (ml/min)
$q_{i,j}$	Solid phase concentration of compound i in section j
Q_r	Raffinate flow rate (ml/min)
Q_s	Solid phase flow rate (ml/min)
q_s	Saturation capacity (l/g)
q_x	Amount of compound x adsorbed on solid phase
t^*	Switching time
t_0	Hold up time (non-retained compound residence time)
t_i	Retention time of compound i
u_j	liquid phase velocity
u_s	Solid phase velocity

V_0 Column void volume

V, V_t Total column volume

V_a Volume of adsorbent

V_f Retention volume of the inflection point

V_{inj} Sample injection volume

V_s Retention volume of enantiomer S

Y_i Recovery yield of compound i

Greek Symbols

α Separation factor

$[\alpha]$ Specific rotation

β Safety margin

δ Infinite small time intervals

ϵ Total column porosity

λ Wavelength (nm)

σ^2 Objective function minimized during fitting of regression models

Subscripts and Superscripts

1 Compound 1, the less retained compound

2 Compound 2, the more retained compound

in	Inlet
j	SMB section number (j = I, II, III, and IV)
ou	Outlet

Abbreviations

AN	*Aspergillus niger*
Bi-Lang	Bi-Langmuir
CSP	Chiral stationary phase
EC	*Echerichia coli O157:H7*
EtOH	Ethanol
GC	*Geotrichum candidum*
HPLC	High performance liquid chromatography
I.D.	Internal diameter
Lang	Langmuir
LM	*Listeria monocytogenes*
PA	*Pseudomonas aeruginosa*
PP	1-phenyl-1-propanol
RG	*Rhodotorula glutinus*
RSD	Relative standard deviation
SA	*Staphylococcus aureus*
SE	*Salmonella enteritidis*

SMB	Simulated moving bed
STD	Standard deviation
TTBB	Tri-tert-butyl-benzene

Chapter I

Introduction

I-1 Generalities

I-1-1 Review of Chirality

Chirality, or molecular asymmetry was first described by Pasteur in 1848, when he was able to separate, manually, crystals of Sodium Ammonium Tartrate enantiomers. A chiral molecule has two different non-superimposable forms which are mirror image of each other. The two forms (called enantiomers or optical isomers) display identical physical and chemical properties except in presence of chiral reagents (which react differently with the two enantiomers), or polarized light (light in which the electrical field vectors lay in the same plane after passage through a polarizer, or Nicol prism). Enantiomers, because of their optical activity, alter measurably the polarization plane of such light by rotating it either clockwise (Dextro-rotatory, D(+), or S enantiomer), or counterclockwise (Levo-rotatory, L(-), or R enantiomer). A polarimeter is usually used to measure the degree of the plane rotation from which the specific rotation [α], a more commonly used parameter (where concentration and path length are taken into account) is derived (Streitwieser and Heathcock, 1976).

Chirality can be caused by any stable chiral center (carbon, sulphur, nitrogen, phosphorous, or boron) with four different substituents. It can also be caused by chiral axes, or planes. However, chiral centers do not always confer optical activity as illustrated by " meso" molecules, which have chiral centers but are optically inactive because they have a center of symmetry within the molecules canceling any asymmetry generated by two chiral centers. Optical activity also disappears when an equimolar mixture of two enantiomers is considered as their effects cancel each other out. Such a mixture is called racemic.

I-1-2 Importance of Chirality

Most biosynthesis, metabolisms and other biological reactions depend on chirality. Enzymes are frequently specific to one optical isomer, unable to recognize the other isomer much less to react with it (White and Subramanian, 1994). Various types of industries depend on chirality and require chiral separation. Most of the time, the two enantiomers of many compounds behave differently, and some times even antagonistically (White and Subramanian, 1994).

The pharmaceutical industry is one of the industries where chirality can be very critical. The most famous example illustrating the importance of chirality was Thalidomide, which caused a tragedy in the early 1960's. At that time, it was

used as a sedative with anti-nausea properties. Later on, it was found that only the R-isomer had beneficial effects, while the S-isomer had a teratogenic effect causing serious malformations in newborn babies of women who took the drug in early pregnancy. Currently, Thalidomide is used only as anti-cancer drug mostly with men, since it was found that the body can convert R-isomer to the S-isomer and vice versa.

Several other drugs have shown the effect of chirality (Barbiturates, Opiates and Labetalol, to name a few). In 1982, a report showed that of 1675 drugs produced, only 28% were natural, or semi-synthetic with 98% of those being chiral and marketed as single isomers. However, of the remaining 72% (which are synthetic), 88% were sold as racemate or mixed isomers, while over 40% of them were known to be chiral (White and Subramanian, 1994); thus, there is a need to produce single isomer compounds either synthetically, or by separating the two enantiomers from a mixture (Anonymous, 1992; Stinson, 1995).

In the agrochemical industry, the need for most effective pesticide production with the minimum of toxic effects is leading to the production of single isomers whenever possible. Ninety eight percent of the 550 pesticides, used in 1981, were synthetics with 17% being chiral material, but less than 8% (of the 17%) being marketed as single isomers (White and Subramanian, 1994).

Finally, in the food and drink industry the importance of chirality and chiral separation is increasing as a result of differences between chemical and

biochemical processes, resulting in products with different isomeric compositions. Typical examples of that importance can be found in the control of fermentation process, in the production of artificial sweeteners (the S-asparagine a component of Aspartame is bitter while the R-isomer is sweet) (White and Subramanian, 1994), in the production of olive oil and orange juice, where chirality has been proven to be a valuable tool in the determination of naturalness (Mussinan, 1993, Mosandl et al.,1994). However, the importance of chirality has been most markedly illustrated in the field of flavors and fragrances. The fact that optical isomers can display different sensory properties has been known and reported for quite some time (Russel and Hill, 1971; Mosandl et al., 1986; Pickenhagen, 1989; Karl et al., 1992; Boelens et al., 1993; Mussinan, 1993; Dufosse et al., 1994; Koppenhoefer et al., 1994; Mosandl et al., 1994; White and Subramanian, 1994). Among the roles that can be played by chirality in food and beverage industries Armstrong et al. (1990) cited the following: identifying adulterated food, control and monitoring of fermentation processes, 50% less material to be use, and decrease of some compounds environmental persistence.

I-1-3 The FDA Position Toward Stereoisomers

The Food and Drug Administration (FDA) is trying to regulate, strictly, the status of enantiomers, especially in the pharmaceutical field. It is interesting to look back at the way the FDA position has evolved over the years. According

to Stinson (1997), it all started with the Drug Price Competition & Patent Term Restoration Act of 1984 (also known as Waxman-Hatch amendments to the Food, Drug & Cosmetic Act) which stipulates: "*If an application to FDA is for a new use for a drug containing an approved active ingredient, the new use gets only 3 years' marketing exclusivity. If the application is for a new chemical entity, then the use gets 5 years*". Stinson (1997) also reported that in 1989 the FDA , while setting the rules and regulations for the application of Waxman-Hatch amendments announced: "*FDA notes that a single enantiomer of a previously approved racemate contains a previously approved active moiety and is therefore not considered a new chemical entity*". By issuing such a statement, the FDA was approving single isomers every time it approved a racemate, considering them "in facto" as being the same chemical. The next phase, according to Stinson (1997), came in 1996 when the FDA required a myriad of tests (usually required only for new chemicals) from a pharmaceutical company seeking approval for a new application for an enantiomer of an already approved racemate. The FDA granted the approval, and with it the market exclusivity extension (for which only new chemicals are eligible). Then the FDA found itself in clear contradiction with its own policy defined in 1989. Nowadays, it becomes more obvious that active (or the enantiomers), and inactive (or racemic) forms of chiral compounds do behave differently in many cases, and should in fact be considered as different entities. It is then quite natural to see the FDA moving toward taking such a position; however, up to now, no ruling has been issued by the FDA except for

a set of guidelines published in 1992 (Anonymous, 1992).

I-1-4 Methods for Enantiomer Production

Given the aforementioned importance of chirality, and the still evolving FDA position toward enantiomers, the demand for new methods to obtain optically active compounds has been rapidly growing (Francotte, 1993). Enantio-specific synthesis remains always a possibility. However, synthesizing a racemate (50:50 mixture of both enantiomers) is often easier, cheaper and can be accomplished in a much shorter time (Francotte, 1993). Once the racemate is obtained, several techniques can be used to separate the two enantiomers, such as elution chromatography, closed loop recycling chromatography, closed loop recycling chromatography combined with column switching, and simulated moving bed chromatography (SMB). All these methods are variants of high performance liquid chromatography (HPLC) and can be used with various chiral stationary phases depending on the compounds. Armstrong and Han (1988) reported that other non-chromatographic methods can be used for enantiomeric separations, among them were: 1) conversion of the racemic mixture to a pair of diastereo-isomers with different physical and chemical properties, then use of conventional techniques for separation. 2) Use of enzymatic or microbiological digestion which can be (more often than not) enantio-selective. 3) Crystallization followed by mechanical separation. However most of these methods are

considered tedious and time consuming; thus, inefficient and not of interest in producing enantiomers in both high quantity and high purity (Armstrong and Han, 1988). In the early 70's gas chromatography (GC) showed some promising results for enantiomer resolution. However, the use of GC remained mostly confined to the analytical aspect with little, or no contribution to the preparative aspect. Such hindrance in preparative GC development originated, according to Armstrong and Han (1988), from several limiting factors, such as the requirement for the solute to be volatile, the often occurring racemization of the chiral stationary phase due to the required high temperature, which can also cause higher entropy and often affects the stability of the system, and finally the infeasibility of large scale preparative separations in GC. For these reasons, and others, HPLC offers the best alternative for separating enantiomers, especially at the preparative level.

I-2 Objectives of The study

Multiple objectives were set for this study. The first one was to determine the experimental conditions (and carry out the corresponding experiments) which would allow the separation of selected flavor compound enantiomers with different separation factors using Simulated Moving Bed (SMB) chromatography under linear conditions (where the equilibrium concentrations of a component in the stationary phase and the mobile one are proportional, usually achieved at

low concentrations (Guiochon et al., 1994)). The second objective was to choose one of the flavor compounds (namely, 1-phenyl-1-propanol) and study the adsorption behavior of its enantiomers (in both competitive and non-competitive environments) on a cellulose based chiral stationary phase. The third objective was to use the results from the experiments for objectives 1and 2, to carry out separation of 1-phenyl-1-propanol (PP) enantiomers by SMB under non-linear conditions (where the equilibrium concentrations of a component in the stationary phase and the mobile one are no longer proportional, and the isotherm of a given component depends on the concentration of all the other components present in the mixture (Guiochon et al., 1994)), and to optimize that separation in terms of purity and production rate. Finally the fourth objective was to investigate the potential antimicrobial activity of PP, and any potential difference(s) among the racemic, the R and the S enantiomers in that regard.

I-3 Approaches to Reach Objectives

To reach the first objective a set of preliminary experiments were carried out on a conventional HPLC system to determine thermodynamic (dead volume, retention times, phase ratio, separation factor) as well as kinetic (efficiency) characteristics of the sixteen columns packed in house (see later) with cellulose based chiral stationary phase. The obtained data were then used to determine the operational parameters for SMB through calculations and simulations using

programs provided by engineers in the group. Finally, the experiments were run for three different flavor compounds (benzoin, octalactone and PP), using an eight column SMB system, described in chapter III.

To reach the second objective all we needed was: a conventional HPLC system with at least a binary pump (described later in chapter III), one column from the set to be used in SMB with characteristics close to the mean values of all the columns, and the products to be studied (the racemic PP, the S and the R enantiomers) .

To reach the third objective, experimental data from previous experiments were needed, along with the SMB system in the same eight column configuration. Again computer simulations were useful in determining the experimental conditions and in optimizing 1-phenyl-1-propanol separation under non-linear conditions, however, some fine tuning was needed this time.

Finally to reach the fourth objective a simple screening method for antimicrobial activity was used. The assessment of such activity was based on measuring the diameter of an inhibition zone around a paper disk (with a drop of the tested chemical) placed in the center of a petri dish streaked with the assayed microorganism (see chapter VII).

Chapter II

Simulated Moving Bed Chromatography

Simulated Moving Bed (SMB) technology has been around for over thirty five years. It was invented and patented by Broughton and Gerhold in 1961 (Broughton and Gerhold, 1961). Since then, it has been extensively used in large scale fractionation of sugars and xylene isomer production (Ganetsos and Barker, 1993). However, until about ten years ago, its use has been very limited in the fields of fine chemistry, pharmaceutical, and agricultural research and production. Recently, those industries have been showing more interest in the technique, especially since its introduction for small scale purification seven to eight years ago. It has become more attractive as more research has been devoted to this domain shedding more light on its concept and principles, and emphasizing its advantages over conventional preparative chromatography techniques (Zhong et al., 1997).

II-1 Basic Principles of SMB

The fact that chromatographic separations could be drastically improved in a continuous countercurrent process led to the development of such

processes. True Moving Bed or TMB (where the stationary phase is physically moved in opposite direction of the mobile phase) was first proposed as true countercurrent process. However, TMB showed -rather quickly- its limitations, such as the difficulty to "move" the stationary phase without significant back-mixing, or excessive friction and attrition of the adsorbent particles, which markedly affect the column efficiency and ultimately the separation performance (Ganetsos and Barker, 1993). Furthermore high flow rates could not be used with TMB; otherwise, the mobile phase would push the solid phase back canceling the sought countercurrent effect. It is in this context, and in order to avoid those disadvantages that SMB was proposed as an alternative process to TMB.

SMB is also a solid-liquid countercurrent process; however, the solid phase is not physically moved. The countercurrent effect is achieved by simulating the solid phase motion, the feed and solvent inlets and the outlets of the purified fractions are periodically displaced within a system of several columns connected in series (Ganetsos and Baker, 1993). The result is a "virtual migration" of the solid phase by jumps taking place at constant frequency in opposite direction of the flow velocity of the liquid phase (Zhong et al.,1997). That migration of the solid phase, paced by a judiciously chosen switching time, confers to SMB a periodic rather than continuous nature (Yun et al.,1997).The mobile phase (or desorbent) and the feed (mixture to be separated) are continuously introduced into the column series, and two streams: the raffinate (the lesser retained component) and the extract (the more retained one) are

continuously withdrawn. Proper design and operating conditions (the different flow rates (feed, desorbent, extract and raffinate) and switching time) are the main keys for a successful separation with a high degree of purity for both the extract and the raffinate (Zhong et al.,1997). Furthermore, it is of critical importance to have the characteristics of the columns used in SMB as close as possible, since by design those columns are considered as equal subdivisions of ONE chromatographic bed. Thus, the need for taking extra care in packing columns for SMB by using a uniform procedure in order to minimize column to column variations.

Figure 2-1 shows a schematic of an SMB process. Roman numbers (I, II, III and IV) are the SMB sections which may contain 2,3 or 4 columns each. Conventionally Section (I) is located between the desorbent and the extract nodes, section (II) between the extract and the feed nodes, section (III) between the feed and the raffinate nodes, and section (IV) between the raffinate and the desorbent nodes. Sections (II) and (III) are the sections where the separation takes place; thus, the name "separation zones". On the other hand sections (I) and (IV) are called "regeneration zones" because they are, respectively, the sites of solid and liquid phase regeneration.

Beside columns, an SMB system has pumps (4 or 5) , valves and tubing connecting the columns to each other in a closed system: At the inlet of each column, four valves (feed, desorbent, raffinate, and extract) allow connections to the corresponding pumps (Nicoud, 1993). Such configuration is exhibited in

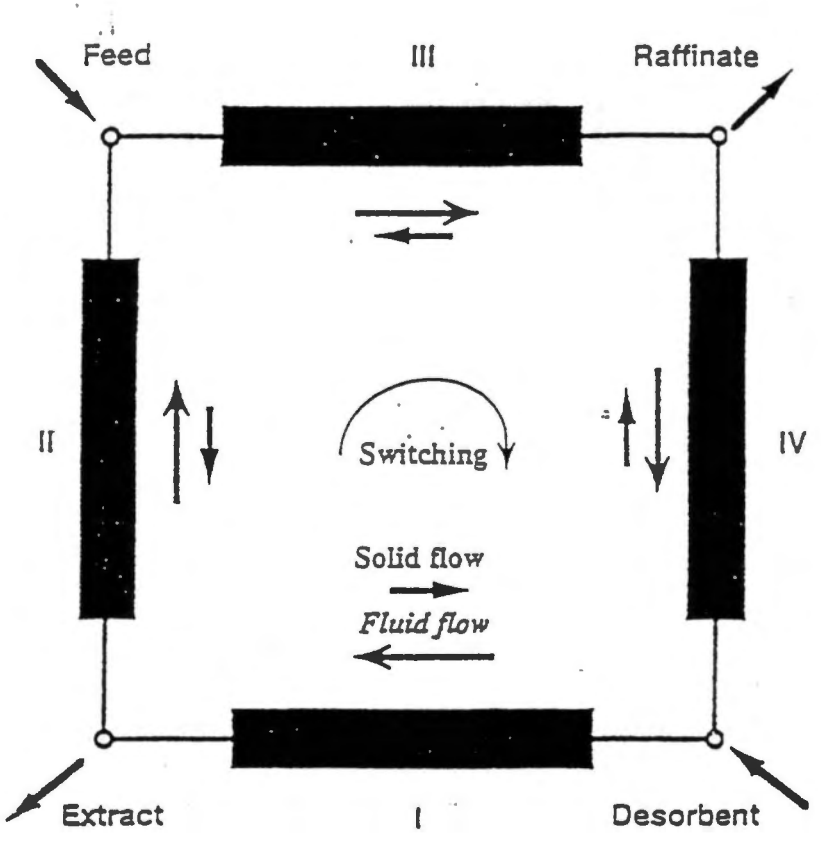


Figure 2-1: Schematic of an SMB Process

Figure 2-2 (reproduced with permission from Yun, 1996). An optional fifth pump can be used for recycle. The flow rate of each pump has to be carefully determined since the choice of the different flow rates is critical to a successful separation. One of the flow rates has to be chosen arbitrarily (usually the feed), then the other flow rates can be calculated using simple formulas (see paragraph II-4-3).

II-2 Advantages and Disadvantages of SMB

The advantages of an SMB chromatographic system over conventional batch chromatography are numerous, among them are:

1) Larger sample amount of the feed can be processed allowing higher degree of overloading; thus, a higher throughput and an important increase of the separation power of the entire system.

2) The concentration profiles of the components to separate do not need to be completely resolved within the columns to actually yield high purity products, since they are virtually migrating in opposite direction, one with the mobile phase, and the other with the stationary phase (Zhong and Guiochon, 1996). Thus, SMB appears to be ideal for chiral separations which traditionally have to deal with small separation factors.

3) Substantial reduction in the volume of mobile phase can be achieved since the process allows recycling of the mobile phase. Likewise, a more efficient

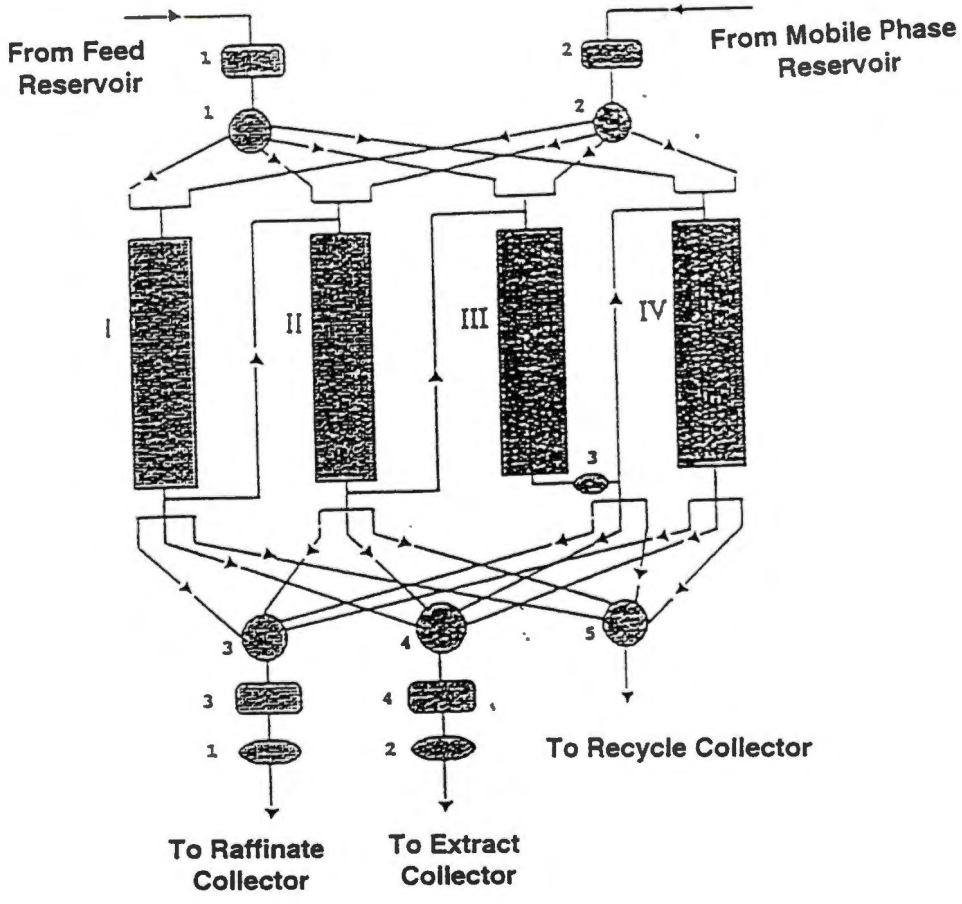


Figure 2-2: Drawing of an SMB System Setup

(Reproduced, with permission from Yun, 1996)

Rectangle: **Column** (I, II, III, and IV).

Circle: **Valve** (1: Feed, 2: Solvent, 3: Raffinate, 4: Extract, and 5: Recycle).

Round Rectangle: **Pump** (1: Feed, 2: Solvent, 3: Raffinate, and 4: Extract).

Ellipse: **Detector** (1: Raffinate, 2: Extract, and 3: On-Line Detector).

use of the stationary phase is achieved, since concentration profiles are more expanded inside the columns, while a large portion of the bed is not used during a batch chromatography run (Pynnonen, 1998).

4) The components to be separated are not only obtained with higher purity, but also with higher yield than conventional batch chromatography.

5) In SMB the feed is continuously injected, and the raffinate and the extract are continuously collected. The process can be run around the clock without any significant operator intervention which maximizes the production capacity and reduces labor cost (Pynnonen, 1998).

On the other hand, SMB also presents some disadvantages, such as the complexity of the design and applications, and the original cost of the equipment. The main disadvantage of SMB, though, is its inability to be used with multi-component mixtures. Indeed, unless several SMB systems are available and mounted in series, SMB is a technique restricted to separating binary mixtures. However, this disadvantage is no longer of concern when we consider the separation of enantiomers, making SMB the (potentially) ideal process for enantioseparations (Zhong et al., 1997). Another drawback of SMB comes from its lack of versatility: being designed for long term production, SMB is economically unable to compete with batch chromatography in solving small production problems (Nicoud, 1993).

II-3 Enantiomer Separations Using SMB

Enantioseparation using SMB has been in a rise for almost a decade now, especially since the development of small and medium range units. The trend should continue, as deeper and deeper understandings of the process' concept and design are brought about, and optimization tools are developed for this technique. Furthermore, the costs of chiral stationary phases are generally very high making the use of SMB (and its better utilization of the chromatographic bed) much more attractive (Ching et al., 1993). As more and more pharmaceutical and chemical companies are trying to set up their own SMB system, and start taking advantages of this seemingly beneficial technique, the few companies which design and commercialize SMB systems, are trying hard to keep up with such increasing demand.

Nowadays literature about chiral separations using SMB abounds. That was not the case just seven years ago when Negawa and Shoji (1992) reported what was, according to the authors, the first separation of optical isomers by SMB. Those authors were successful in separating 1-phenyl-1-ethanol enantiomers using cellulose based Chiral Stationary Phase (CSP). They performed the same separation using conventional HPLC, then compared the two techniques from both productivity (per unit of packing material), and solvent consumption standpoints. They reported that SMB outperformed HPLC on both fronts, allowing a productivity 61 times higher and a solvent consumption 87

times lower. Furthermore, they reported that the least retained enantiomer (the raffinate) was 200 times more concentrated at its collection port allowing a reduction of the cost of solvent recovery and concentration of the sample. Ching et al. (1993) used SMB to separate enantiomers of praziquantel (an anthelmintic drug used to treat the parasitic disease, schistosomiasis) on microcrystalline cellulose triacetate CSP. The authors used four columns (44.5 x 1.25 cm I.D.), and reached a production rate of more than 400 mg per hour of both enantiomers, with an optical purity that exceeded 90%. Their racemic feed (50 mg per ml) was continuously injected into the system at a flow rate of 0.3 ml per min. Using the same type of CSP(cellulose triacetate based), Nicoud et al. (1993) were able to separate enantiomers of a chiral epoxide (an intermediate used in numerous enantioselective synthesis) on an SMB system with 12 columns (11 x 2.6 cm). They, too, conducted a comparative study between SMB and batch chromatography. They reported that both processes performed comparably well from enantiomeric excess (ee) stand point (>99% for batch and 98% for SMB). When solvent consumption was considered, SMB outperformed batch by a factor of 7.5 (3 liter per gram of racemate processed for batch versus 0.4 liter for SMB). However, when productivity was considered, the authors reported that batch chromatography performed better by a factor greater than 3.4 (5 mg per gram of CSP per hour versus 1.46 mg for SMB). To explain such an apparently poor performance of SMB, the authors argued that for SMB columns they used a CSP with an average particle size twice the average size of the particles used in the

batch chromatography, and that an improvement of productivity by a factor of 4 should be expected if the particle size used was reduced by half. Similar results were reported by Küsters et al. (1995) when they separated the same compound (chiral epoxide), but on a different CSP (chiracel-OD). Again, SMB performance was superior with respect to eluent consumption by a factor of 5.4, while batch chromatography yielded a higher productivity. However, the authors reported that their SMB experiment was not fully optimized, and argued that even if it were, the saving in solvent use may be a justifiable factor, in itself, to choose SMB because solvent consumption is (in many cases) the largest portion in the production cost of a chemical by preparative chromatography. This argument was also given by Francotte and Richert (1997) who emphasized the importance of solvent consumption, especially for low solubility compounds, such as formoterol (an anti-asthmatic drug). By comparing the separation of formoterol enantiomers by SMB and by batch chromatography on chiracel-OJ stationary phase, Francotte and Richert (1997) reported a saving of 81% of the solvent used in favor of SMB. The same authors were able to achieved 84% in solvent use reduction when they separated another drug (guaifenesin, an antitussive medicine) on, yet another CSP (chiracel-OD). It is noteworthy that these authors were able to achieve not only significant reduction in solvent consumption, but also a better productivity with SMB than with batch chromatography (6.3 times better for formoterol and 2.7 better for guaifenesin).

II-4. Modeling of SMB

The SMB modeling used in this work has been previously and extensively discussed (Zhong and Guiochon, 1996, Zhong et al., 1997). Basically the modeling used consisted of two parts, first, **the column models**, which include a set of mass balance equations for each feed component, a set of kinetic equations and a set of isotherm equations, and second, **the node model** which describes initial and boundary conditions.

II-4-1 Column Models

Mass Balance Equations

The differential mass balance of component i (i=1,2) in a column located in section j (j=I, II, III, IV) is given by:

$$\frac{\delta C_{i,j}}{\delta t} + u_j \frac{\delta C_{i,j}}{\delta z} + F \frac{\delta q_{i,j}}{\delta t} = D_L \frac{\delta^2 C_{i,j}}{\delta z^2} \qquad (2\text{-}1)$$

where $C_{i,j}$ and $q_{i,j}$ are the liquid and solid concentrations of component i in a column in section j, u_j is the liquid phase velocity, D_L is the axial dispersion coefficient, F is the phase ratio which is equal to $(1-\varepsilon)/\varepsilon$, with ε being the total column porosity.

Lumped Kinetic Model (transport-equilibrium)

In this study, the solid film linear driving force model was used to account for the mass transfer kinetics (Guiochon et al., 1994). This model assumes that the rate of variation of the stationary phase concentration, $\delta q/\delta t$, is proportional to the difference between the concentration of the compound in the stationary phase at equilibrium with the concentration C in the mobile phase, q^*, and the actual concentration, q. The proportionality coefficient, k_f (min^{-1}), is the mass transfer rate coefficient. The combination of this rate equation and the mass balance equation constitutes the transport dispersive model (Guiochon et al., 1994). This model still includes an axial dispersion coefficient. Its value was set constant, and the mass transfer coefficient was derived by identification of the experimental profile to a numerical solution of the model. Numerical solutions can be obtained using an appropriate program (Guiochon et al., 1994).

Equilibrium Isotherm

The isotherm is the thermodynamic relationship which characterizes the equilibrium between the solid and the mobile phases (Guiochon et al., 1994):

$$q^*_{i,j} = f(C_{i,j}) \qquad (2\text{-}2)$$

In fact the objective of the study in chapter (V), was precisely to determine the type and nature of this relationship for PP enantiomers.

Initial and Boundary Conditions

Initially the system contains only the liquid and the solid phase in

equilibrium without any feed component. The boundary conditions at the column inlet are the Danckwert type conditions (Zhong and Guiochon, 1998):

$$C_{i,j}(z,0) = 0 \qquad q_{i,j}(z,0) = 0 \tag{2-3a}$$

$$u_j C_{i,j}(0,t) - D_L \frac{\delta C_{i,j}}{\delta z}(0,t) = C_{i,j}^{in} \tag{2-3b}$$

$$\frac{\delta C_{i,j}}{\delta z}(L,t) = 0 \tag{2-3c}$$

where $C_{i,j}^{in}$ is the concentration of component i at the inlet of column j. In SMB the feed and the draw-off nodes are shifted after a pre-determined switching time t^*:

$$t^* = \frac{L}{u_s} = \frac{(1-\varepsilon)LA}{Q_s} \tag{2-4}$$

L being the length of the column, u_s the solid phase velocity, ε the total porosity, Q_s the solid phase flow rate, and A the column cross section area. This switching, along the fluid direction, allows to simulate the backward movement of the solid phase. To account for this mode of operation, the boundary conditions of each column are updated accordingly at the beginning of each new cycle, which can be achieved using the node equations described in the next paragraph (Zhong and Guiochon 1996).

II-4-2 The Node Model

Ruthven and Ching (1989) determined the flow and integral mass balance equations at each node. In the following equations, Q_I, Q_{II}, Q_{III} and Q_{IV} are to the flow rates through the corresponding sections, Q_D is the desorbent flow rate, Q_E the extract flow rate, Q_F the feed flow rate and Q_R the raffinate flow rate.

1. Desorbent node (eluent) :

$$Q_{IV} + Q_D = Q_I \tag{2-5a}$$

$$C_{i,IV}^{ou} Q_{IV} + C_{i,D} Q_D = C_{i,I}^{in} Q_I \tag{2-5b}$$

2. Extract draw-off node :

$$Q_I - Q_E = Q_{II} \tag{2-5c}$$

$$C_{i,I}^{ou} = C_{i,II}^{in} = C_{i,E} \tag{2-5d}$$

3. Feed node :

$$Q_{II} + Q_F = Q_{III} \tag{2-5e}$$

$$C_{i,II}^{ou} Q_{II} + C_{i,F} Q_F = C_{i,III}^{in} Q_{III} \tag{2-5f}$$

4. Raffinate draw-off node:

$$Q_{III} - Q_R = Q_{IV} \tag{2-5g}$$

$$C_{i,III}^{ou} = C_{i,IV}^{in} = C_{i,R} \tag{2-5h}$$

$C_{i,j}^{ou}$ and $C_{i,j}^{in}$ are the concentrations of component *i* at the outlet and inlet of the column in section *j* respectively. The flow rates Q_j are related to the liquid phase velocity u_j by: $Q_j = \varepsilon A u_j$, with A being the column cross section area.

II-4-3 Estimation of Experimental Parameters

Ruthven and Ching (1989) proposed a set of four equations that need to be fulfilled in order to achieve complete separation of a binary mixture (i.e. to have the less retained component moving in the direction of the mobile phase, and the more retained moving "with" the solid phase).

$$Q_S = Q_F / (K_2/\beta - K_1\beta) \quad (2\text{-}6a)$$

$$Q_R = (K_2/\beta - K_1/\beta)\, Q_S \quad (2\text{-}6b)$$

$$Q_E = (K_2\beta - K_1\beta)\, Q_S \quad (2\text{-}6c)$$

$$Q_D = (K_2\beta - K_1/\beta)\, Q_S \quad (2\text{-}6d)$$

Where Q_S is the solid phase flow rate (virtual or simulated)

$$Q_S = (1-\epsilon)\, A\mu_S = (1-\epsilon)\, A \times L/t^* \quad (2\text{-}7)$$

ϵ : total column porosity — L: length of the column

A: column cross section area — t^*: switching time

μ_S: solid phase velocity — F: Phase ratio $[(1-\epsilon)/\epsilon]$

$K_{1,2}$: Henry coefficients ($= k_{1,2}/F$), and — $k_{1,2}$: Retention factors

β: safety factor

The optimal situation in terms of productivity (or eluent consumption) is obtained with $\beta = 1$, however, greater values (typically between 1 and $\sqrt{\alpha = K_2 / K_1}$) are used to avoid instability of the system.

Preliminary experiments are first needed to determine F, K_1 and K_2 for each one of the columns used later in the SMB experiment. Then, It is obvious, from the set of equations above, that once Q_F and the safety factor are chosen (usually arbitrarily) , one can easily derive the other flow rates (solvent, raffinate, and extract) along with the switching time. It is noteworthy that in order to obtain positive flow rates the safety factor need to be smaller than $\sqrt{\alpha}$, ($\alpha = K_2 / K_1$). The different flow rates, and the switch time are, actually, all what is needed to start an SMB run under linear conditions. However, this approach is not as straightforward when a run under nonlinear conditions is considered (Zhong and Guiochon, 1997). For such conditions (non-linear), Mazzotti and co-workers (1997) proposed a different method, based on a theory called the "triangle theory", which can be implemented in order to determine the SMB operational conditions. This approach will be discussed in chapter (VI).

Chapter III

Equipments and Experimental Procedures

III-1 The Column Packing Procedure

The set of columns used in the SMB experiments (and in the PP adsorption behavior study) were packed in house. The hardware (20 x 1.0 cm I.D. empty columns with end fittings) were purchased from Supelco (Bellefonte, PA). The packing material, a gift from Chiral Technologies (Exton, PA), was cellulose tribenzoate, coated on macro-porous silica (commercial name: Chiracel OB) with an average particle size of 20μm. Figure 3-1 shows the major chemical micro-structure of Chiracel OB.

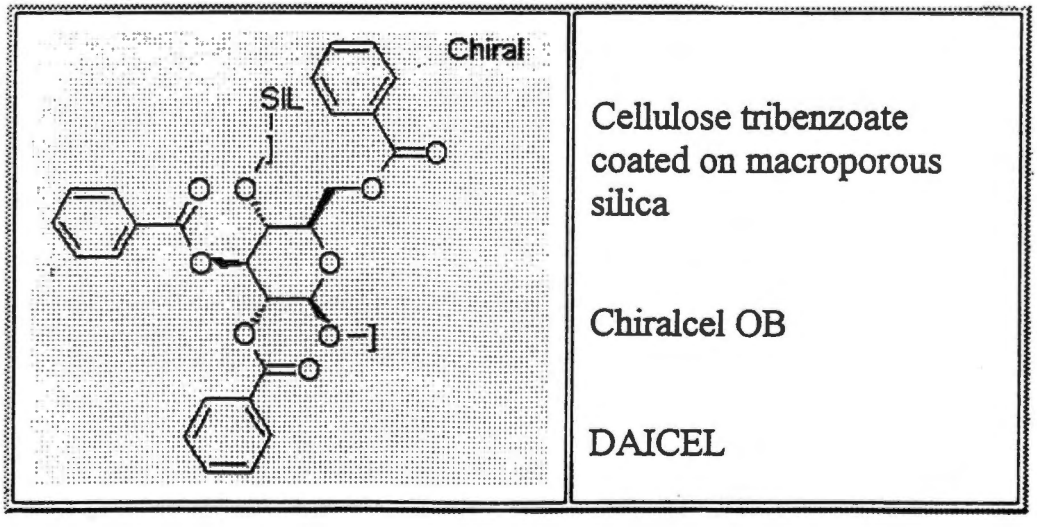
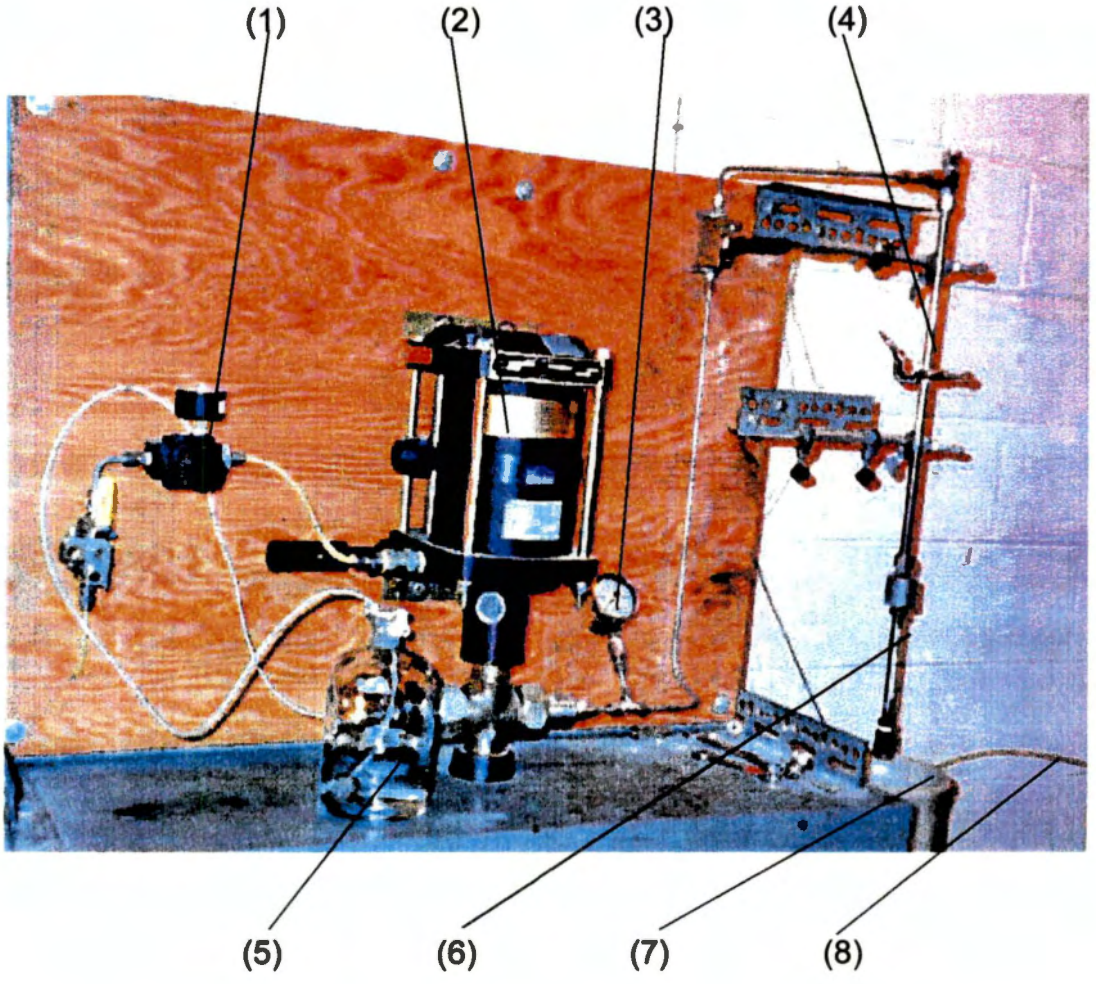


Figure 3-1 : Chemical Structure of Chiracel OB Stationary Phase

The columns were packed using the slurry method : For each column 10.5 to 11 grams of CSP was weighed and suspended in 40 ml of methanol. After thorough stirring, the suspension was transferred to the packing equipment reservoir (item 4, Figure 3-2), which was connected in one end to the column to pack (item 6, Figure 3-2), and in the other end to an air driven fluid pump (Haskel, Burbank, CA) (item 2, Figure 3-2). This type of pump could deliver the pushing solvent (here methanol) under a pressure up to 15,000 psi, supplemented with a powerful compressor (Campbell Hansfeld, Harrison, OH) (not shown in Figure 3-2). For our packing material, given the particle size (20μm), 2000 psi was the maximum pressure allowed; otherwise, the risk of particle breakage became too high. The pressure was adjusted using a control knob (item 1, Figure 3-2), and monitored on a pressure gauge (item 3, Figure 3-2). Once a column was packed, it was flushed, still under pressure, with 400 to 500 ml of the pushing solvent. Finally, the pressure was released, and the column disconnected from the packing equipment. Each column was first, abundantly flushed with pure isopropanol, then with the appropriate mobile phase before any experiment was performed.

III-2 The SMB System

The SMB system we used was a laboratory scale continuous chromatography model ICLC 16-10 from Prochrom (Indianapolis, IN, USA;



(1) Pressure Control Knob

(2) Air Driven Fluid Pump

(3) Pressure Gauge

(4) Reservoir (40ml capacity)

(5) Pushing Solvent Bottle

(6) Column

(7) Waste Container

(8) To The Compressor

Figure 3-2 : The Column Packing Equipment

Champigneulles, France). Figure 3-3 shows a picture of such system. It basically consists of :

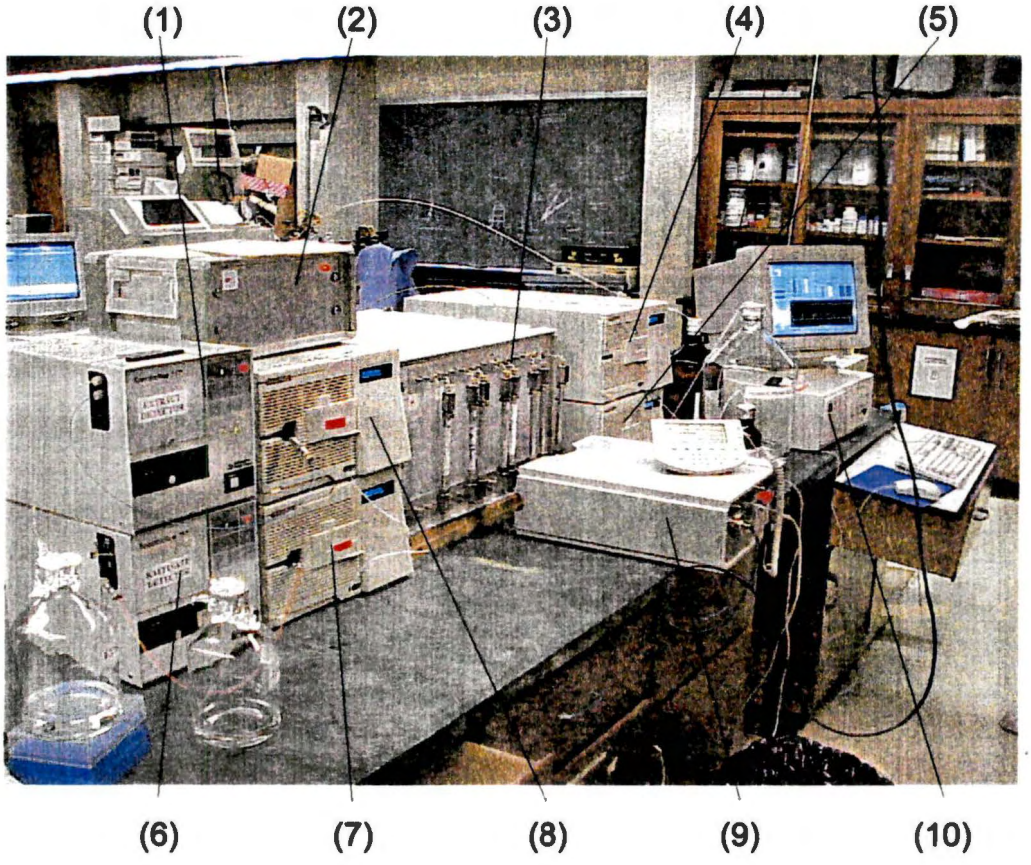
* Four HP 1050 pumps (Hewlett-Packard, Palo Alto, CA), two pumps for the incoming streams; namely the feed (item 4, fig. 3-3), and the solvent (item 5), and two pumps for the outgoing ones (raffinate (item 7), and extract (item 8)).

* Five electro pneumatic 16-port-valves (Valco, Houston, TX): one for each of the four streams mentioned above and a fifth one connected to the recycle (see Figure 3-4).

* Nitrogen "cylinder" delivering a constant flow of N_2 used to activate and move the valves around, at switching time (item not shown).

* A computer (item 10, Figure 3-3), interfaced with the whole system (via an interface box, item 2) to control the flow rates, the switching time, the 5 valve positions and the desired column setting (from 8 columns to a maximum of 16). A software provided by Prochrom was used to establish communication between the computer and the chromatographic system (Chrosoft® , Prochrom, Champineulles, France, 1997).

* Three UV detectors: two of them (Spectroflow 757, variable wave length, Applied Biosystems, Ramsey, NJ) were placed respectively after the raffinate and the extract pumps (raffinate and extract detectors, item 6 and item 1, Figure 3-3, respectively). The third detector (HP1100, variable wavelength Hewlett-Packard, Palo Alto, CA) was equipped with a high pressure flow cell, and was connected to the main stream of the system between the end of one column



(1) Extract Detector

(2) Interface Box

(3) Front Panel with Columns

(4) Feed Pump

(5) Solvent Pump

(6) Raffinate Detector

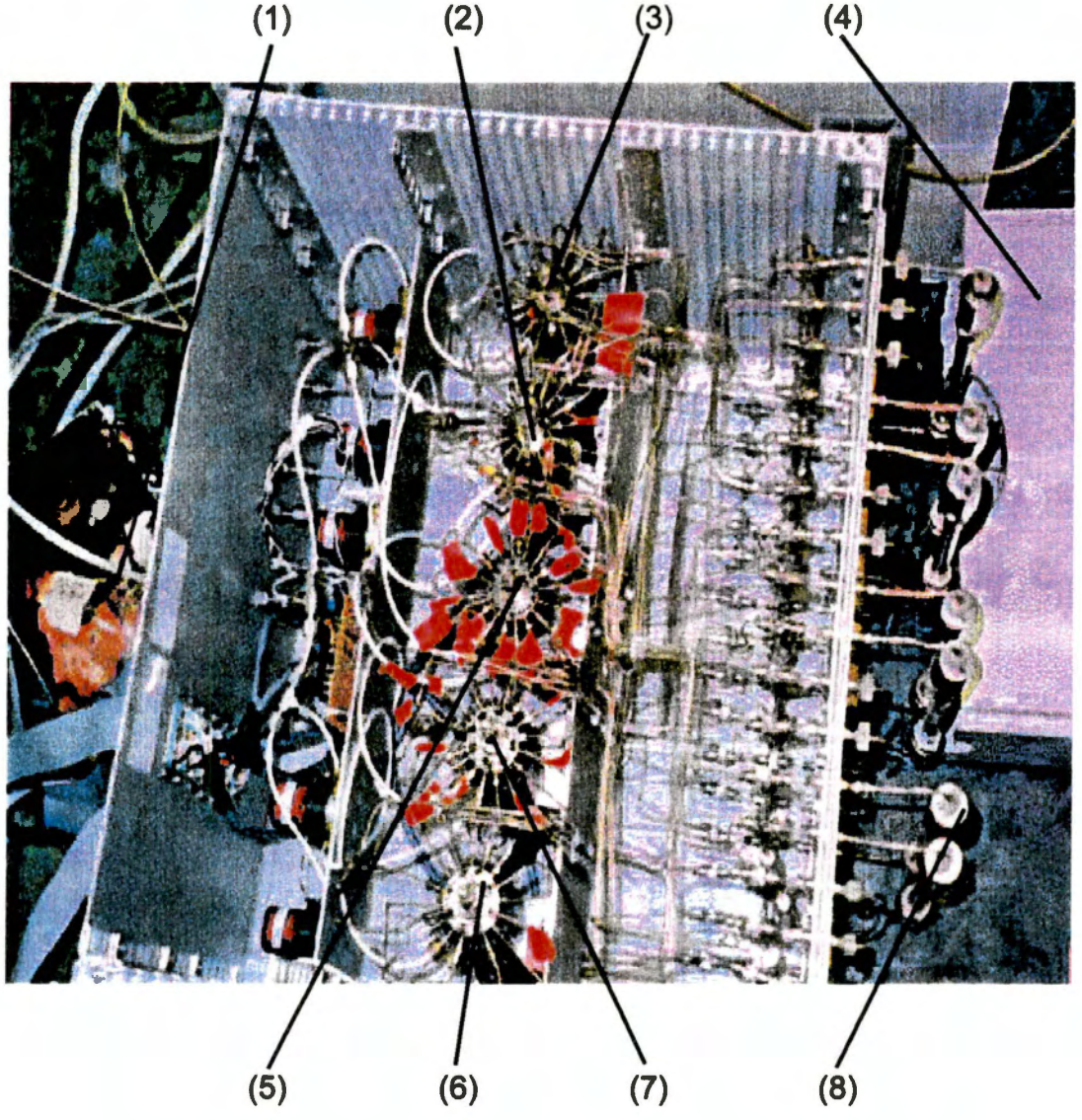
(7) Raffinate Pump

(8) Extract Pump

(9) "On-Line" Detector

(10) Computer and Monitor

Figure 3-3 : A Photograph of The SMB System Used in This Study



(1) From Nitrogen Cylinder

(2) Solvent Valve

(3) Feed Valve

(4) "On-Line" Detector

(5) Recycle Valve

(6) Raffinate Valve

(7) Extract Valve

(8) Front Panel with Columns

Figure 3-4 : Inside of The SMB System Viewed from Above

section and one of the rotary valves (item 9, Figure 3-3). This setup allowed us to investigate in detail the concentration profile of the two components inside the system at any given time during a run. Evidently, the "online" detector could not distinguish between the two components inside the system, instead it gave a global response equivalent to the sum of both component responses (Yun, 1996). The wavelength for the three detectors varied depending on the compound studied.

* A front panel (item 3, Figure 3-3), where the number of connected columns (generally 8, 12 or 16) can be changed to match the desired column-setting. As mentioned earlier we used the eight column setting for our experiments. The columns were isolated from each other by sapphire balls and seat check valves which ensured an unidirectional flow through the set (Prochrom Inc., 1997).

III-3 The High Performance Liquid Chromatography System

The role of high performance liquid chromatography (HPLC) was pivotal throughout this work. First, it was used during the newly packed column testing experiments, when columns needed to be characterized under analytical conditions before they could be included in an SMB experiment. Second, an HPLC system was the single most important equipment used in the PP adsorption behavior study (Chapter V). Finally, HPLC was used for quantitative

and qualitative analysis of the feed and the different streams (raffinate, extract and recycle) collected after each SMB experiment.

Two different HPLC systems were interchangeably used depending on the availability at the time of each experiment. Separate detector calibrations were obtained for the two systems, and the appropriate calibration curve was used to convert the detector signal to concentration. The first system was an HP 1090 liquid chromatograph (Hewlett-Packard, Palo Alto, CA, USA), equipped with a ternary-solvent delivery system, an automatic sample injector with a 250-µl loop, a diode-array UV detector, and a computer data acquisition system using the HP-chem-station software (version A.05.03). The second system was a Gilson modular liquid chromatograph (Gilson, Middleton, WI) composed of a master data module (model 621), an isocratic pump (model 302), and a dynamic mixer (model 811). The sample injection was carried out with a 6-port-VICI-injector (Valco, Houston, TX). For detection, Spectra-Physics variable wavelength detector (Spectra-Physics, San Jose, CA) was used. The whole system was controlled with a PC-based Gilson 715 software (Gilson, Middleton, WI). The acquired data from either system were downloaded to one of the computers at the university of Tennessee computer center for further data processing.

III-4 The PP Antimicrobial Activity Experiment

Antimicrobial activity of racemic PP, R, and S-PP enantiomers were investigated using the filter paper disc diffusion method described previously by Meena and Sethi (1994), and by Elggayar (1999). The technique consists of streaking a (previously tested, and not more than 24 hour old) viable microorganism on the surface of a non-selective medium. Then, a sterile 6 mm diameter filter paper disc (Difco, Detroit, MI) is placed in the center of the petri dish. Finally, a drop of the investigated chemical is deposited on the disc. After the appropriate incubation period and temperature (see chapter VII), the inhibition zone around the paper disc is measured and compared with the control (a drop of sterilized distilled water). For our study, five bacteria and three fungi were used (see later). All tests were done in triplicate. Statistical analysis were easily carried out given the numerical nature of the results (reported in mm). The data were fitted to a completely randomized design (CRD) with factorial treatment arrangement (microorganism, chemical and their combination were the three tested fixed effects).Analysis was performed using PROC MIXED of SAS version 6.12 (SAS Institute, 1996).

Chapter IV

Separations of Selected Flavor Compounds Enantiomers by SMB under Linear Conditions

IV-1 Introduction

Commercially available CSP's have the disadvantage of being fairly selective. It is, indeed, quite rare, if not impossible, to find a "universal" CSP which would have more than a few applications. In other words, if the access to stationary phases is restricted (which was our case, with only one type of CSP available), the number of applications is necessarily limited also. Therefore, the number of flavor compounds that were suiTable for our study was rather limited. We tried various well-known chiral flavor compounds including linalool, limonene, menthol, benzoin, 1-phenyl-1-propanol , and various lactones (hexa-, hepta-, octa-, nona-, and decalactone in both delta (δ) and gamma (γ) forms). Only three of the mentioned racemic compounds were separated on our CSP, with a decent separation factor ($\alpha > 1.1$): benzoin, δ-octalactone and 1-phenyl-1-propanol (PP). In this chapter, the results of enantioseparations of those three compounds by SMB under linear conditions are reported. For SMB experiments under non-linear conditions (see the two next chapters) only PP was used. Benzoin could

not be used because of a very low separation factor (α = 1.15), which did not allow a reasonable degree of overloading, and resulted in complete loss of resolution between the two enantiomers at fairly low concentrations. Furthermore, benzoin crystals displayed an extremely low solubility in our mobile phase, adding another hurdle to its use in non-linear conditions, where highly concentrated solutions are usually used. Delta-octalactone, on the other hand, was not quite stable under the experimental conditions of SMB, characterized by long runs easily exceeding twenty hours. After runs of this magnitude, HPLC analysis of the feed, the raffinate, or the extract, systematically generated new (and unknown) peaks believed to be degradation products. A more detailed stability study for δ-octalactone, which would have included positive identification of those unknown compounds, was abandoned in early stages because of time constraint.

IV-2 Separation of Benzoin Enantiomers

Benzoyl-phenylcarbinol ($C_{14}H_{12}O_2$, Molecular Weight, MW = 212.22), known as 2-Hydroxy-2phenyl-acetophenone, or more commonly as benzoin is a solid, white synthetic flavor compound in the shape of "monoclinic prisms or needles" (Furia and Bellanca, 1971). It is soluble in acetone and boiling alcohol, its melting point is in the range of 132-137°C. It can be synthesized by "treating an alcoholic solution of benzaldehyde with an alkali cyanide" (Furia and Bellanca,

1971). The use of benzoin in foods is regulated in the Code of Federal Regulation (CFR) under Title 21, Part 172 (food additives for direct addition to foods for human consumption), subpart F (flavoring agents and related substances), section 515 (synthetic flavor substances and adjuvants). It is sporadically used in non-alcoholic beverages, ice cream, candy, baked goods, gelatins and puddings, to confer a light balsamic odor and bitter taste reminiscent of almond (Furia and Bellanca, 1971). Commercially, benzoin is only available in the racemic form.

IV-2-1 Conventional HPLC Generated Data

Sixteen columns were packed with chiracel OB according to the procedure outlined in paragraph III-1, although only eight were ultimately used in the SMB experiments. Preliminary experiments showed that a mobile phase made of a mixture of hexane 85 : ethanol 15 (v/v), delivered at a flow rate of 2.5 ml/min, was appropriate, generating adequate retention factors (k's between 1 and 2.5). Lower proportions of ethanol (or smaller flow rates) resulted in longer run times, while higher proportions (or flow rates) resulted in unacceptable losses of resolution.

Before any SMB experiment was carried out, the packed columns were individually tested, in order to determine and compare their characteristics. The Gilson HPLC system (Gilson, Middletown, WI), described in paragraph III-3,

was utilized for the column testing. An 85:15 mixture (v/v) of HPLC grade n-hexane (Fisher scientific, Fair Lawn, NJ) and absolute 200 proof ethanol USP (AAPER Chemicals, Shelbyville, KY) was used as mobile phase (flow rate = 2.5 ml/min). Each column was flushed until a stable baseline was reached (detection wavelength set at 254 nm). Then 20 µl, of a diluted solution of racemic benzoin (Aldrich, Milwaukee, WI), was injected into the column. Table 4-1 displays the characteristics of the eight closest columns chosen for the SMB experiment. In Table 4-1, t_0 represents the time needed for a non-retained compound (here 1,3,5-tri-tert-butyl-benzene, or TTBB, purchased from Aldrich, Milwaukee, WI) to traverse the column, which, when converted to volume units, characterizes the void volume (V_0) inside the column. V_0 can be used to determine the porosity ϵ (which is the ratio of V_0 to V_t, the column total volume) and the phase ratio F (equal to $[1-\epsilon]/\epsilon$). The other parameters (t_i and k'_i) represent retention times and retention factors, respectively. Table 4-1 shows that, except for the phase ratio F(where cumulative errors generated an average RSD>5), the relative standard deviations (or RSD) were relatively small, which indicates ,a rather, excellent reproducibility from one column to the other. These results warrant that this set of columns may be used in an SMB system, without anticipating any significant effect of column to column variations on the overall performance.

Table 4-1 : Characteristics for the 8 Closest Columns Obtained with Benzoin

Experimental Conditions : Mobile Phase = Hexane 85 : EtOH 15 (v/v),
Flow Rate = 2.5 ml/min, Detection at 254 nm, Vinj = 20 ul

Col. #	t_0 (min)	t_1 (min)	k'_1[a]	t_2 (min)	k'_2[a]	Alpha (α)[b]	Porosity (ε)	F[c]
1	4.61	13.61	1.95	14.94	2.24	1.15	0.734	0.363
2	4.61	13.12	1.85	14.89	2.23	1.21	0.734	0.363
3	4.67	13.33	1.85	14.52	2.11	1.14	0.743	0.345
7	4.55	13.30	1.92	14.57	2.20	1.15	0.724	0.381
9	4.67	13.51	1.89	14.60	2.13	1.12	0.743	0.345
12	4.71	13.92	1.96	15.22	2.23	1.14	0.750	0.334
13	4.57	13.33	1.92	14.52	2.18	1.14	0.727	0.375
16	4.74	13.68	1.89	14.77	2.12	1.12	0.754	0.326
Mean	**4.64**	**13.48**	**1.90**	**14.75**	**2.18**	**1.15**	**0.739**	**0.354**
STD[d]	**0.07**	**0.26**	**0.04**	**0.25**	**0.06**	**0.03**	**0.011**	**0.020**
RSD[e](%)	**1.45**	**1.90**	**2.15**	**1.69**	**2.53**	**2.37**	**1.45**	**5.52**

(a) $k'_i = (t_i - t_0) / t_0$

(b) $\alpha = k'_2 / k'_1$

(c) Phase ratio = $(1-\varepsilon) / \varepsilon$

(d) Standard Deviation

(e) Relative Standard Deviation
RSD = (STD / mean)*100

IV-2-2 SMB Operating Conditions

To determine the operating conditions for SMB the mean values of the column characteristics (Table 4-1) were used. Those values were incorporated in the equations discussed in paragraph II-4-3, in order to derive the switching time and the four different flow rates (feed, solvent or desorbent, raffinate and extract). As mentioned earlier, the feed flow rate is chosen arbitrarily. However, that choice is neither unrestricted nor completely random. It is, usually, based on the inherent limitation(s) of the system in terms of maximum flow rates and pressures, which depend, not only on the pumps used, but also on the type (and particle size) of the packing material. Higher flow rate for the feed is obviously preferred from production rate standpoint. However, given the close inter-relations with the other flow rates (equations 2-6a, b, c, and d), higher feed flow rate (Q_F) leads to higher solid phase flow rate (Q_S, see equation 2-6a); thus, to higher raffinate (Q_R) , extract (Q_E), and desorbent (Q_D) flow rates (equations 2-6b, c, and d). It is noteworthy that Q_D (calculated in equation 2-6d) is not the flow rate set for the solvent pump, it is rather the amount of "fresh" solvent that needs to be added to compensate for the solvent withdrawn with the raffinate and the extract streams. The flow rate of the solvent pump is actually the flow rate of section (I), which is the sum of Q_D and the recycle flow rate Q_{IV} (equation 2-5a).

Another parameter, that needed to be chosen "arbitrarily" before determining the SMB operating conditions, was the safety factor β. We have

seen (in paragraph II-4-3) that the range for such parameter was directly linked to the separation factor α, since, in order to achieve positive flow rates, the maximum value allowed for β was $\sqrt{\alpha}$, while the minimum was 1. For benzoin, the mean α was 1.15 leading to a narrow range (between 1 and 1.072) for β.

With the aforementioned restrictions taken into account, with a feed concentration chosen in the linear range (ie. very diluted feed solution), and with the Henry's coefficients (K_i) determined from the retention factors k'_s ($K_i = k'_i / F$), two sets of slightly different conditions were determined through calculations first, then later on, carried out experimentally. In the first set, the feed flow rate(Q_F) was selected to be 0.12 ml/min, and the safety factor β to be 1.034. The first row of Table 4-2 (Set 1) shows the SMB operating parameters, calculated using equations from paragraph II-4-3, with Q_F and β given the chosen values. In the second set, Q_F was increased to 0.15 ml/min, and β decreased to 1.025. The corresponding operating parameters are shown in the second row of Table 4-2 (set 2). Reducing β from 1.034 to 1.025, allowed us to keep virtually the same conditions for SMB when Q_F was increased by 25%. However, care should be taken not to get β too close to one; otherwise the instability of the system, and the risk of collapsing with the slightest deviation(s) -of any given parameter- would outweigh any potential increase in production rate.

Table 4-2: Two Sets of SMB Experimental Conditions for Benzoin Enantiomer Separation

Set	Beta	Q_f	C_{FT} (g/l)	Q_d	Q_r	Q_e	Q_I	Q_{II}	Q_{III}	Q_{IV}	Switch time
Set (1)	1.034	0.12	0.5	0.35	0.23	0.24	2.72	2.48	2.6	2.37	832
Set (2)	1.025	0.15	0.5	0.32	0.23	0.24	2.71	2.47	2.62	2.39	831

Beta: Safety Factor

Q_f: Feed Flow rate (ml / min)

C_{FT} : Total Feed Concentration (C_{F1}+C_{F2})

Q_d: Desorbent Flow rate (ml / min)

Q_r: Raffinate Flow rate (ml / min)

Q_e: Extract Flow rate (ml / min)

Q_j (j = I, II, III, IV): Flow rate (ml / min) in section j

Switch time: in seconds

IV-2-3 Results and Discussion

The parameters displayed in Tables 4-1 and 4-2 were incorporated in computer programs, developed by chemical engineers in our research group, in order to simulate the separation process of benzoin enantiomers by SMB, and try to predict the behavior of the whole system. The basis for such process modeling was outlined in chapter II-4. Computer simulations were run for both sets (1 and 2) of Table 4-2. However, since process modeling and computer simulation are not the focus of this work, simulation results reported are for set (1) only. They are presented here for illustration purposes, to demonstrate how useful (and time saving) computer simulations can be in setting up experimental conditions, especially at the initial stage. Modeling and computer simulation can also be extremely helpful in predicting the effects of altering one or more experimental parameter(s) on the overall behavior of a given system, without experimentally changing the parameter(s). Such benefits are magnified when a process such as SMB (where several hours are typically needed, before steady state is reached) is considered.

Figures 4-1a and b display the predicted and normalized production of the raffinate (a) and the extract (b) versus the cycle rank (or number of switch). These two figures show that both productions were characterized by a start-up period, during which the amount produced, per time unit, increased with the cycle rank before steady state was reached. Conventionally, steady state is considered

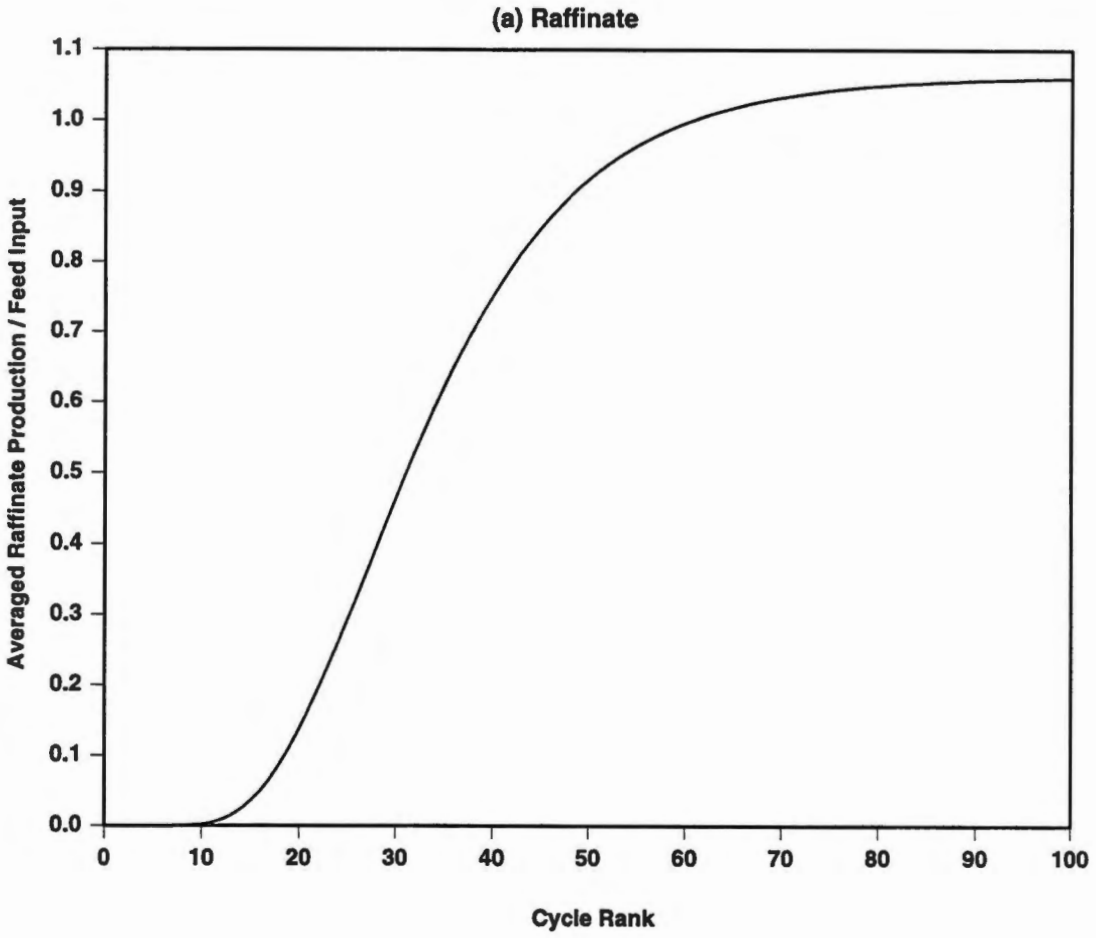


Figure 4-1: Normalized Production of Raffinate and Extract vs Cycle Rank

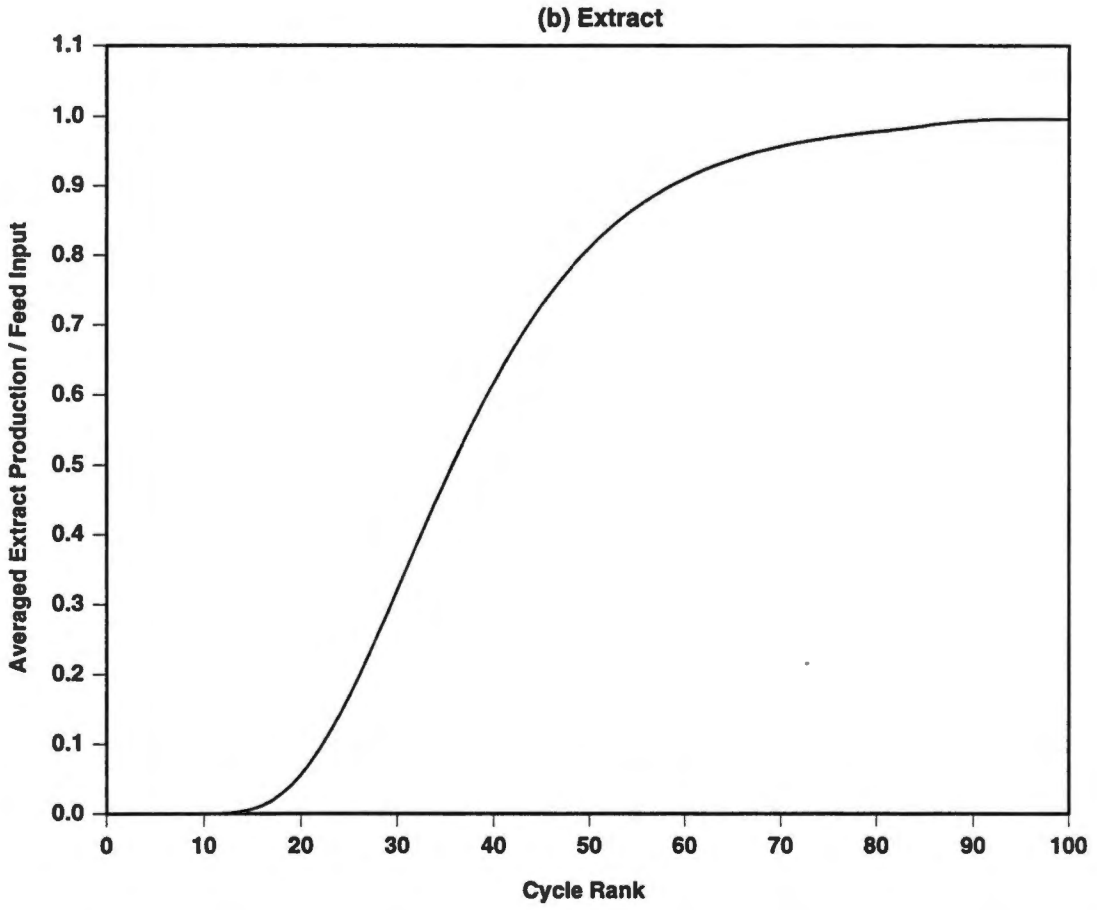
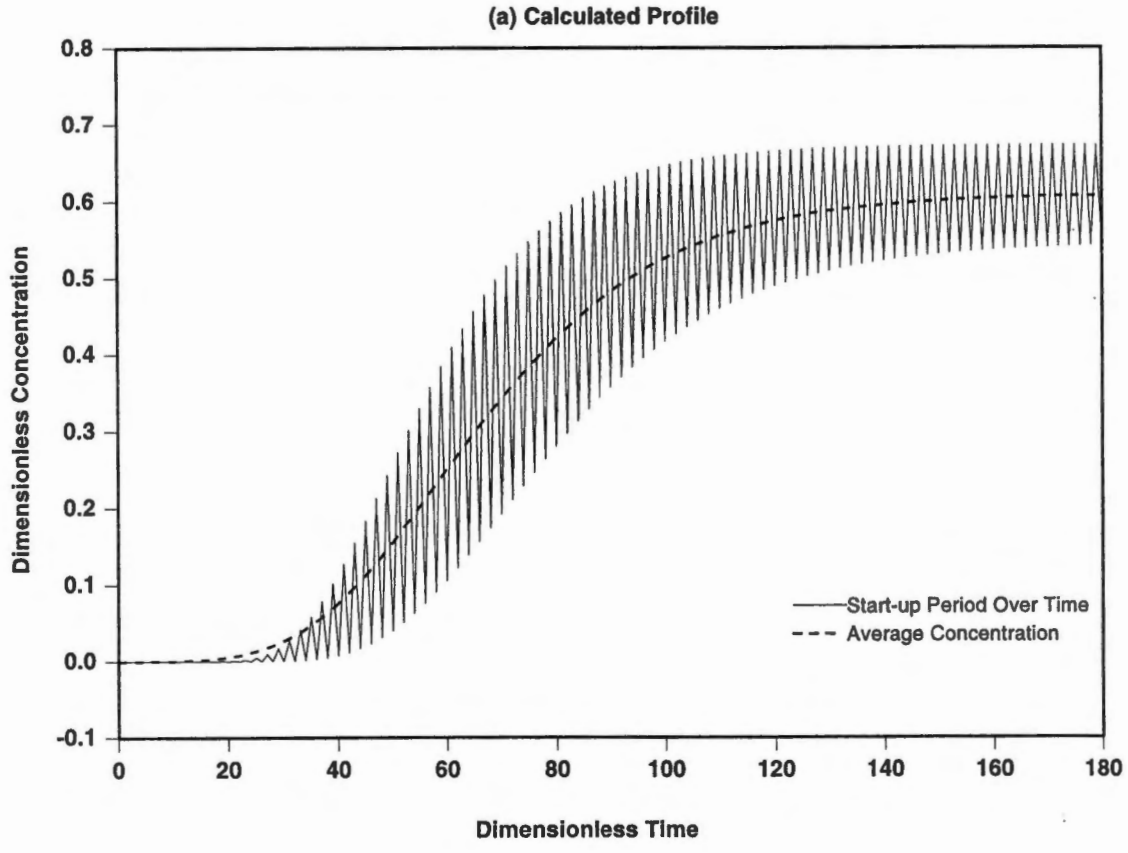


Figure 4-1(Cont.): Normalized Production of Raffinate and Extract vs Cycle Rank

reached when a production of 99% of the asymptotic value is achieved (Yun, 1996). In our case, approximately 80 cycles were estimated to be needed to reach steady state, which amounts to more than 18 hours (given a switch time of 832 seconds), illustrating, again, the role of modeling and computer simulation in time saving. Indeed, in a trial-and-error approach, 18 hours would be the time needed, before the results, for a chosen set of parameters, can be assessed. Furthermore, any parameter adjustment would required another 18 hours, before its effect can be evaluated. Once steady state is reached, the mass balance of SMB requires that, the average amount for each component that enters the system, is equal to the amount that leaves it. However, this requirement does not apply during the start-up period, where lower productions are obtained, compared to the amount of feed going in, due to the initial accumulation of the feed inside the system (Yun, 1996).

Figures 4-2a and 4-3a show the calculated concentration history during the start-up period for the raffinate and the extract, respectively. The oscillations of both profiles, even after the steady state was reached, confirm the periodic aspect of SMB (Yun, 1996). The dotted lines (in both figures) represent the average concentration of each product over a super cycle (corresponding to "n" switching times, "n" being the number of columns used in the experiment, in our case n was equal to 8). Figures 4-2b and 4-3b are the experimental equivalent of the analogous Figures 4-2a and 4-3a. They represent signals, of the raffinate (4-2b), and the extract (4-3b) detectors, recorded on a chart recorder with the



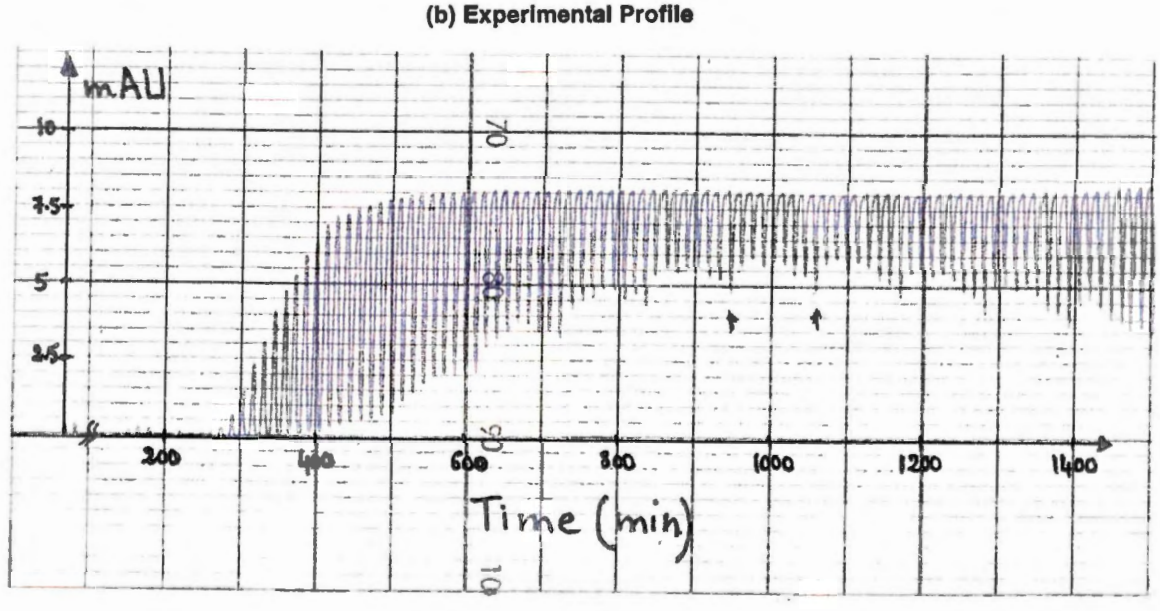
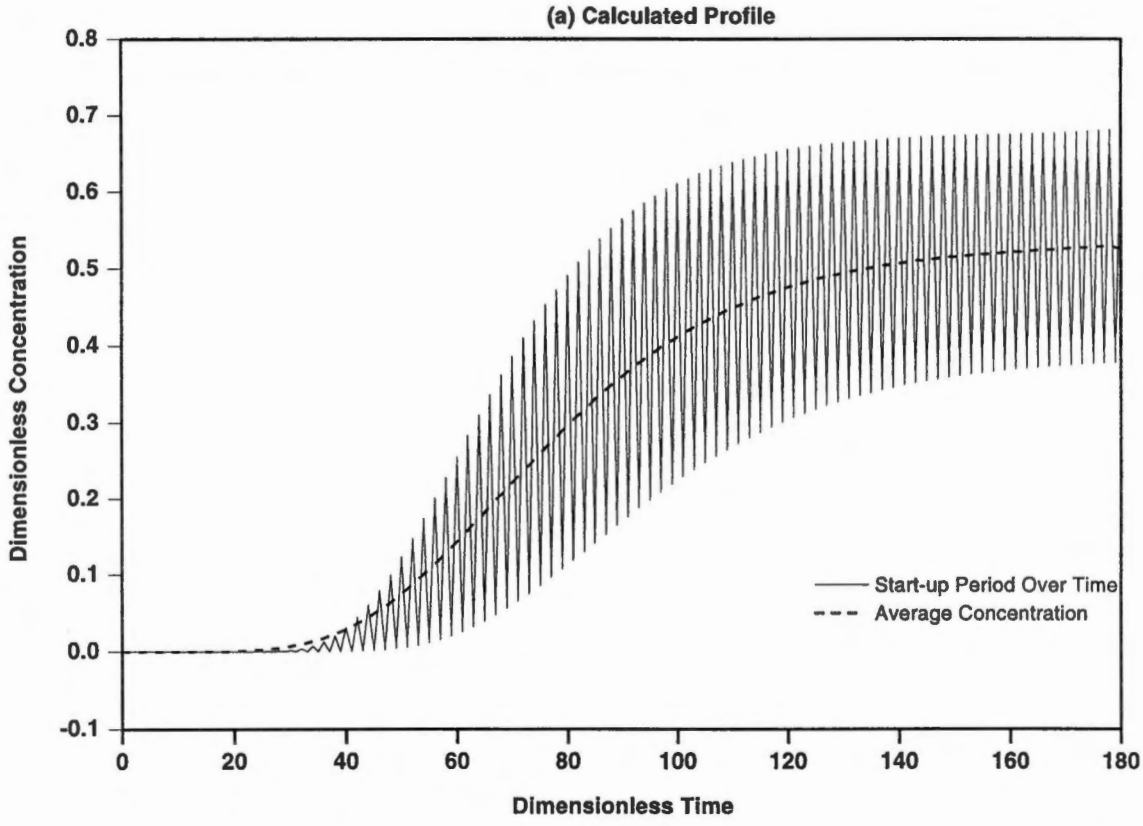


Figure 4-2: Raffinate Start-up Concentration Profile for Benzoin Separated by SMB



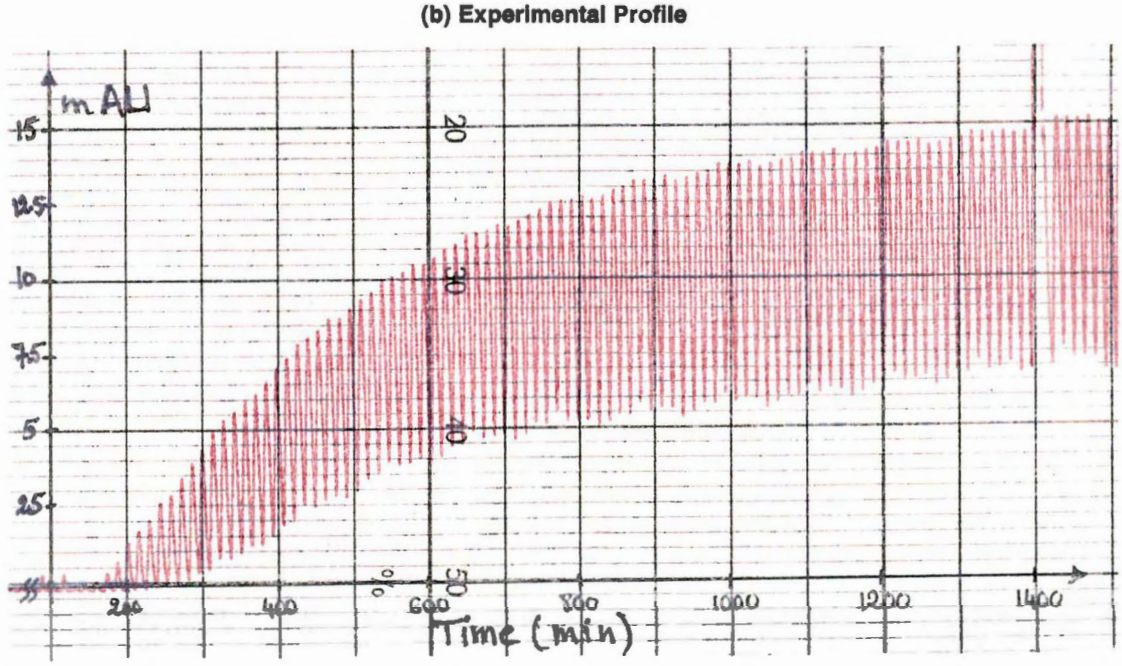


Figure 4-3: Extract Start-up Concentration Profile for Benzoin Separated by SMB

chart speed set at 0.1 mm/min, and an overall recorder range set at 0.5 Volt for both figures. It is interesting to note the quasi-similarity between Figures 4-2a and 4-2b on one hand, and between Figures 4-3a and 4-3b on the other, which confirms the validity of the model used in the computer simulations. Unfortunately, we could not use a more rigorous method of confirmation (where the two figures are super-imposed in a single figure), because, at the time of the benzoin experiments, our data acquisition system was temporarily out of order, and chart recording print outs were the only output data available. It is noteworthy, that the modeling procedure, used here, has been extensively studied, tested and successfully implied with excellent agreements between experimental and calculated results (Yun, 1996; Yun et al., 1997).

Once the correct experimental parameters were determined, adjusted (experimentally the switching time used was 835 seconds for both set 1and 2, instead of 832 and 831 used in calculations) and confirmed, longer runs were carried out. During one of those runs, the signal from the on-line detector (item 9, Figure 3-3) was recorded, after steady state was reached. The signal was then converted to concentration profile and compared to the calculated profile (for set 2, Table 4-2 only). Figures 4-4a and b show the comparison of the two profiles, just before (Figure 4-4a), and after (Figure 4-4b) a switch. Although the match was less than perfect, between experimental and calculated profiles, a decent agreement can be observed, where the overall shape, the location(s) of the fronts, and of the plateaus were fairly predicted by the model. Figures 4-4a & b

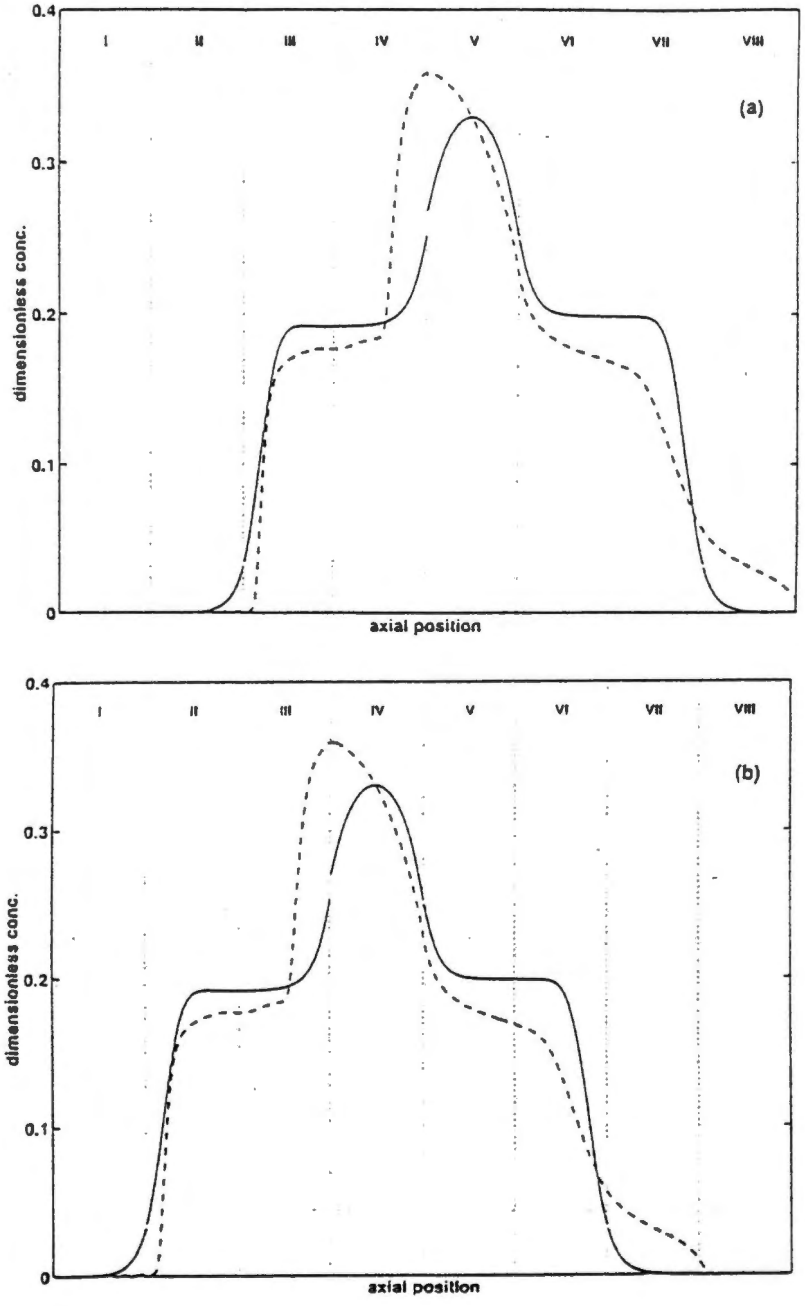


Figure 4-4: Comparison Between Calculated and Experimental Elution Profiles Inside the SMB System

Straight Line: Calculated Profile (according to parameters in set 2, Table 4-2)

Dotted Line: Experimental Profile Recorded from the On-Line Detector (see text)

(a): Just Before the Switch (b): Just After the Switch

show that the raffinate front, of the experimental profile, was more diffused than the calculated one, leading to believe that the dispersion inside the system might have been under-estimated when computer simulation was performed, on the other hand extra column volume may have, in this case, contributed to band broadening. In chromatography, dispersion, or band broadening is a complex phenomenon, which is difficult to account for accurately in modeling, given the number of potential causes (Guiochon et al., 1994).

In order to assess the degree of success of a given separation by SMB, streams coming out of the system (raffinate, extract, and recycle) need to be analyzed, ideally on-line. Such process monitoring is only possible, if one can discriminate between the two components on-line. For chiral separations, this becomes possible, if two polarimeters, or two chiral detectors are used at the raffinate and extract ports respectively. If continuous monitoring is not possible (which was our case), samples from the three streams need to be collected, when steady state is reached, over a period equivalent to a super-cycle (eight consecutive switches in our case, with eight being the number of columns). The samples are, then, analyzed on a separate conventional HPLC system.

The HP 1090 chromatograph, described in paragraph III-3, was used to analyze the raffinate, the extract, and recycle samples, collected at their respective ports during the two SMB runs, corresponding to the conditions summarized in Table 4-2 (with an adjusted switch time of 835 s). For reference purposes, the feed was also analyzed along with the collected samples.

For the HPLC analysis described above, a chiracel OB-H analytical column (25 cm x 0.46 cm), packed with similar CSP as our SMB columns, but with smaller particle size (5 μ versus 20 μ), was used. The use of such column generated a much shorter analysis time, thus a significant saving, not only in time, but more importantly in mobile phase consumption. Furthermore, this type of column usually displays a significantly higher efficiency (over 10,000 plates in this case), which allows an invaluable improvement in the resolution, and an enhancement of the overall separation performance. In our case, the use of the analytical column improved the resolution from a mere valley, between the two benzoin enantiomers (obtained with our large SMB columns), to a complete baseline separation. Such improvement in the resolution enabled us to perform, not only qualitative analysis, but quantitative as well.

Considering the low concentration range for the feed solutions used in our experiments, the collected samples were extremely diluted. Therefore, to improve detection, all samples to be analyzed (except the feed) were first concentrated. The concentration process consisted of completely evaporating the mobile phase, from a known volume of each sample, using a Büchi rotavapor (Brinkmann Instruments, Westbury, NY). The system was under vacuum, and the rotating sample bottle was immersed in a water bath with the temperature set to 45-50°C. Finally, the sample was recovered in a known volume of mobile phase (hexane 85 : ethanol 15, v/v).

The analytical column was first flushed with the mobile phase (at a flow

rate of 1 ml /min), until a stable baseline was reached (detection wavelength was 254 nm). Then, a 20 µl, concentrated, sample volume was injected. The purity of stream i was determined by calculating the simple ratio:

$$P_i = \frac{A_i}{A_i + A_j} \qquad (4\text{-}1)$$

with A_i being the area under the peak of interest (compound i), and A_j the area under the contaminating peak.

Figure 4-5 displays the results of the analysis of samples collected during the first run (set 1, Table 4-2). Excellent results were obtained, with the raffinate and the extract exhibiting a purity of 99.7% and 98.8% respectively. The recycle was basically free of both products, except for, almost undetectable, traces.

The results from the previous run prompted us to increase the feed flow rate by 25% (from 0.12 to 0.15 ml/min), in an attempt to match the conditions shown in Table 4-2, set 2. The SMB system (including the columns) was, first cleaned, and flushed with pure mobile phase, before the second run was started. After steady state was reached, samples from the raffinate, the extract and the recycle, were collected (over a super-cycle), concentrated following the procedure outlined in the previous paragraph, then analyzed on the same HPLC system. Figure 4-6 displays the analytical chromatograms, obtained when the collected samples were analyzed. Once again, the separation was successful, yielding almost pure streams. The purity, for both streams (raffinate and extract),

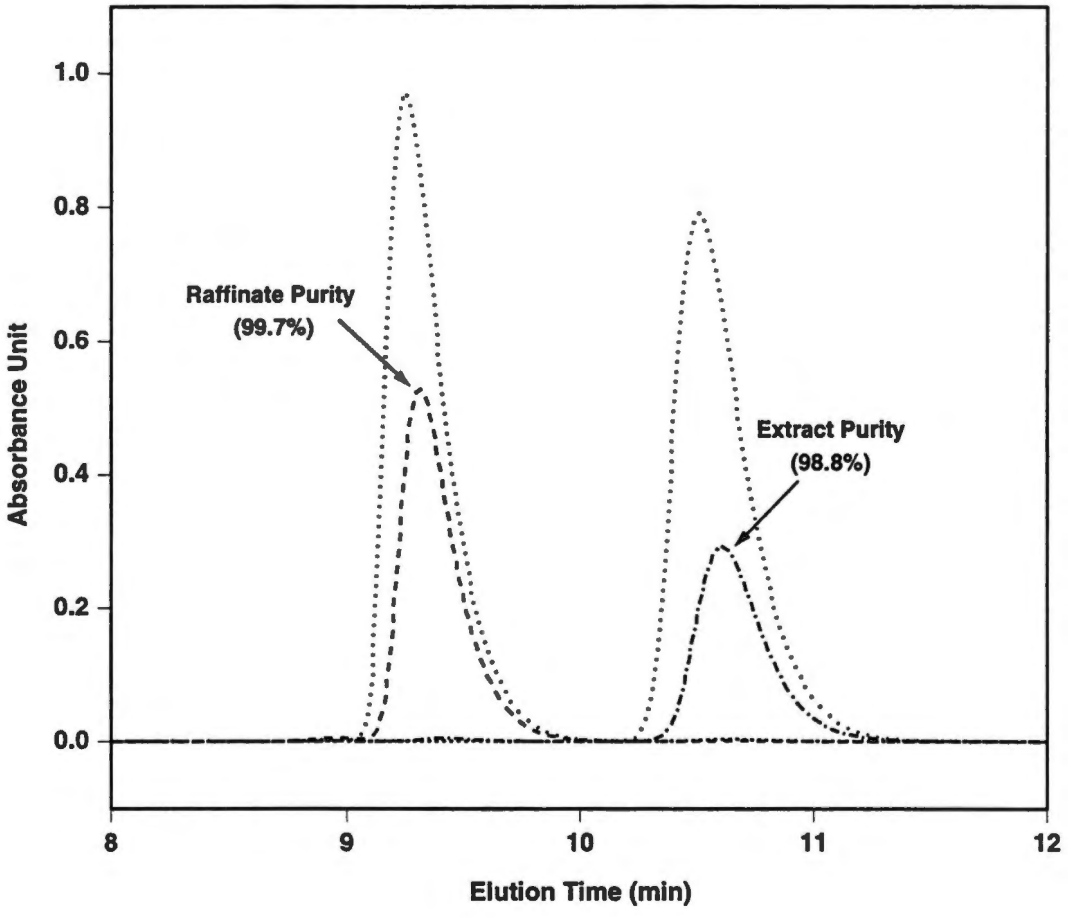


Figure 4-5: Analytical Chromatograms for Samples Collected During Benzoin Enantiomer Separation by SMB (run 1, see SMB Experimental Conditions in set 1, Table 4-2).

Dotted Line: Feed — Dashed Line: Raffinate

Dashed-Dotted Line: Extract — Solid Line: Recycle

Analytical Conditions: Column: 25 x 0.46 cm I.D. Chiracel OB-H

Mobile Phase: Hexane85:EtOH15, FR=1mL/min, Detection at λ = 254 nm

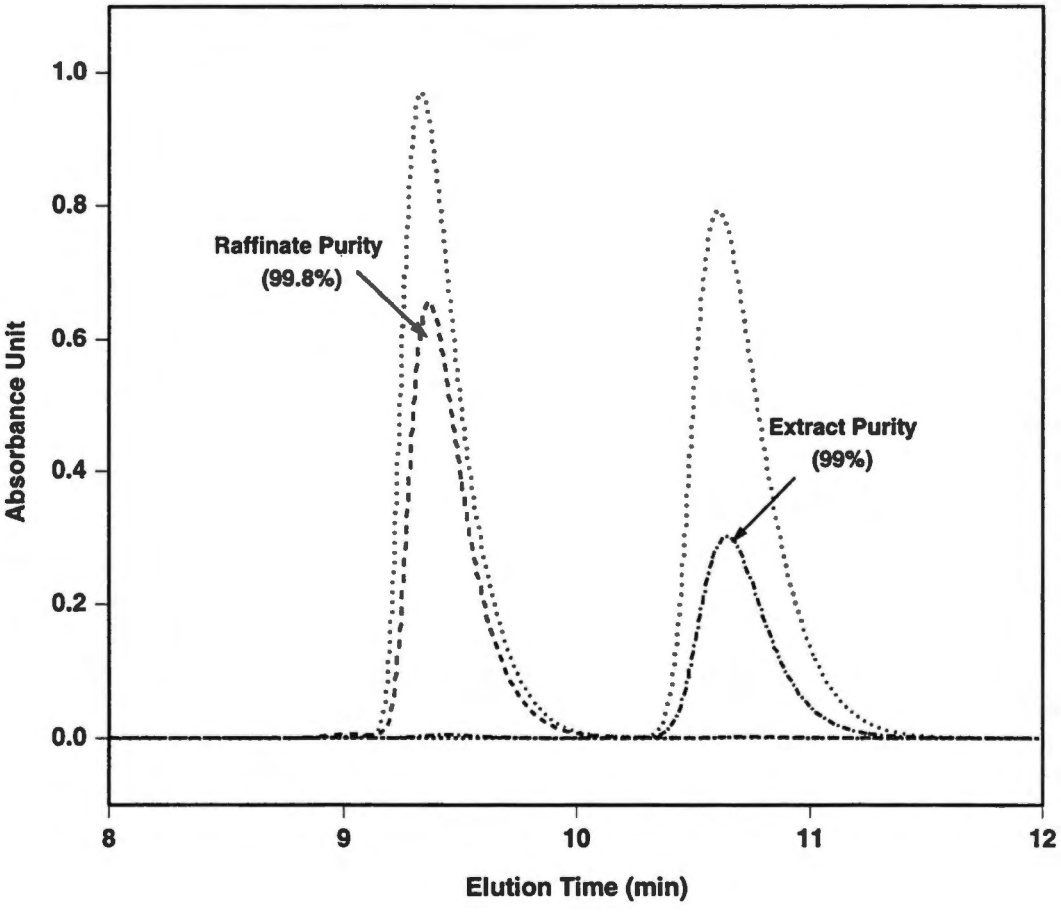


Figure 4-6: Analytical Chromatograms for Samples Collected During Benzoin Enantiomer Separation by SMB (run 2, see SMB Experimental Conditions in set 2, Table 4-2).

Dotted Line: Feed Dashed Line: Raffinate

Dashed-Dotted Line: Extract Solid Line: Recycle

Analytical Conditions: Same as in Figure 4-5

actually improved (by 0.1 to 99.8%, and 0.2% to 99%, respectively). While such improvements might be considered negligible, they, really, are not, if we consider that the feed input was increased by 25%. With such increase, one would expect a drop in both, or either, stream purity. However, we should keep in mind that, in both runs, we were operating under linear conditions (i.e. working with very diluted solutions), which could mean that a slight increase of the feed input (in term of flow rate) may not have a significant effect after all. Nevertheless, we were able (with the help of computer simulations, and calculations using simple equations), to determine, and implement, operational conditions for the separation of benzoin enantiomers using SMB. The degree of success achieved (in term of stream purity) was surprising, given the extremely low separation factor (α) of 1.15, obtained in this case. Unfortunately, such a low factor (along with the poor solubility of benzoin in our mobile phase), was also behind our inability to upgrade this separation to the non-linear conditions.

IV-3 Separation of δ-Octalactone Enantiomers

Delta-octalactone is a member of a large group called "Lactones", which is a generic term that refers to cyclic ester of hydroxyl-acid formed by removing water from the corresponding acid molecules. Gamma (γ) and Delta (δ) lactones are the ones of importance for the flavor and fragrance industry. They occur naturally, contributing to the aroma of a number of fruits (coconut, peach,

apricot, strawberry). They can also be easily obtained through synthesis using acyclic precursors (Baurer and Garbe, 1985). These compounds are chiral, but only racemic mixtures are commercially available, even though several studies have showed that the two enantiomers may differ in their intensity (with the R-isomers generally being more intense) (Guichard et al., 1990; Boelens et al., 1993; Mussinan, 1993; Dufosse, et al., 1994; and Koppenhoefer et al., 1994).

Delta-octalactone ($C_8H_{14}O_2$, Molecular Weight, MW = 142.2) is a yellowish liquid flavor agent with a strong fruity, coconut-like, odor and a very sweet taste. The Center of Food Safety and Applied Nutrition (CFSAN) lists δ-octalactone, as one of the chemicals allowed to be used in food for human consumption, in its document entitled "Everything Added to Food in the United States" or EAFUS for short, available on its homepage (Anonymous, 1999). However, δ-octalactone is not listed in Title 21 of CFR, while its gamma (γ) counter-part is, in the same Part (172), Subpart (F) and Section (515) as benzoin. Therefore, it seems that, while obviously allowed, the use of δ-octalactone has not been fully regulated, and that γ-octalactone seems to be more frequently used to confer similar flavor profiles. Unfortunately, γ-octalactone enantiomers were not separated on our CSP, while δ-octalactone's were, making our choice, of the latter for our study, a forced one.

IV-3-1 Conventional HPLC Generated Data

Preliminary experiments showed that, in order to obtain suitable k's, the appropriate mobile phase to use was a mixture of hexane 90 : ethanol 10 (v/v), delivered at a flow rate of 2.5 ml/min. The same eight columns, used for benzoin, were used here. The columns needed to be, again, individually tested, on the same HPLC system (the Gilson). All the chemicals and solvents used, were the same as the ones used for benzoin, except for the racemic mixture, where benzoin was replaced by δ-octalactone (purchased from TCI America, Portland, OR). Table 4-3 shows the eight column characteristics, determined for δ-octalactone. The parameters presented in Table 4-3, were previously described, except for the efficiencies N_0, N_1, and N_2, which were not determined for benzoin. N_0, N_1, and N_2 were calculated at the half-width for the non-retained compound (TTBB), component 1 (the R (-) - δ-octalactone), and component 2 (the S (+) - δ-octalactone) respectively. The signs for the two enantiomers were determined using a polarimeter.

The RSD's for all parameters reported in Table 4-3, except for the efficiencies, were less than 5%, validating the results obtained with benzoin. This type of results suggests that, while some column parameters may drift, after a long period of use, the direction of such drifts is, usually, the same for most columns, keeping intact their original similarities, and their "eligibility" to be used together in an SMB system. However, occasionally, over an extended period of

Table 4-3 : Characteristics for the 8 Closest Columns Obtained with Delta-octalactone

Experimental Conditions : Mobile Phase = Hexane 90 : EtOH 10 (v/v), Flow Rate = 2.5 ml/min
Detection at 215 nm, Vinj = 20 ul

Col. #	t_0 (min)	t_1 (min)	k'_1[a]	t_2 (min)	k'_2[a]	Alpha (α)[b]	Porosity (ε)	F[c]	N_o[d]	N_1[e]	N_2[f]
1	4.54	12.10	1.67	14.63	2.22	1.33	0.723	0.384	1271	1015	1014
2	4.52	12.12	1.68	15.07	2.33	1.39	0.719	0.390	1009	1309	1191
3	4.60	11.79	1.56	14.21	2.09	1.34	0.732	0.366	1360	1123	1011
7	4.51	11.8	1.62	14.19	2.15	1.33	0.718	0.393	1689	1200	1059
9	4.58	11.91	1.60	14.36	2.14	1.33	0.729	0.372	1411	1113	986
12	4.60	12.06	1.62	14.52	2.16	1.33	0.732	0.366	1267	1117	1013
13	4.63	12.15	1.62	14.67	2.17	1.34	0.737	0.357	1059	931	863
16	4.67	12.22	1.62	14.70	2.15	1.33	0.743	0.345	1142	1174	1159
Mean	**4.58**	**12.02**	**1.62**	**14.54**	**2.18**	**1.34**	**0.729**	**0.372**	**1276**	**1123**	**1037**
STD[g]	**0.06**	**0.16**	**0.04**	**0.29**	**0.07**	**0.02**	**0.009**	**0.017**	**218**	**115**	**103**
RSD[h](%)	**1.21**	**1.36**	**2.25**	**2.01**	**3.41**	**1.49**	**1.21**	**4.46**	**17.07**	**10.20**	**9.90**

(a) $k'_i = (t_r - t_0) / t_0$
(b) $\alpha = k'_2 / k'_1$
(c) Phase ratio = $(1-\varepsilon) / \varepsilon$
(d) Efficiency for non-retained compound
(e) Efficiency for component 1
(f) Efficiency for component 2
(g) Standard Deviation (SD)
(h) Relative SD
RSD = (STD / mean)*100

time, columns may just become defective, thus the importance of, periodically, testing columns used for long runs, to check for defective ones, and eventually replace, or re-pack them.

By comparing Tables 4-1 and 4-3, the only parameter, we can anticipate to be the same is t_0 (and the parameters derived from it ϵ and F), since all the other parameters are dependent on the experimental conditions. In Tables 4-1 and 4-3, we can see that t_0 is slightly different (4.64 versus 4.58 min). This difference can not be attributed to the difference in mobile phase composition, since t_0 is independent of such parameter. In fact t_0, or more accurately V_0, is characteristic of a column, and should not vary with the experimental conditions. To explain the slight shift in t_0 between the two sets of experiments, one should know that, chronologically, the δ-octalactone experiments took place before the benzoin ones. Knowing such fact, it becomes easy to understand the drift, and more importantly, its direction (an increase of 0.06 min or 3.6 s). Indeed, an increase of t_0 means that the non-retained compound "spends" more time inside the column, suggesting a slight increase of the column void volume. Such scenario is conceivable (and more than likely), if we consider that some particles, from the stationary phase, may very well leach out of the column during long runs, creating larger void volume. Furthermore the assumption that TTBB is not adsorbed at all, may not be totally true. In such case, the slightest adsorption of TTBB would result in different t_0 if different mobile phase modifiers are used.

IV-3-2 SMB Operating Conditions

Once the analytical data and the column characteristics are set, the procedure of determining the SMB operating conditions (for linear case) is straightforward. It is identical to the one used for benzoin, where the average column characteristics are incorporated in the paragraph II-4-3 equations. In the case of δ-octalactone, the conditions were slightly easier to determine than for benzoin, mainly because of a larger separation factor (1.34 instead of 1.15). The calculated conditions to be used in the SMB experiments are summarized in Table 4-4. The chosen feed flow rate was 0.4 ml/min, while the safety factor β was chosen to be 1.028. On the other hand, we started, with a more diluted feed solution than for benzoin: 0.2 g/ l total feed concentration versus 0.5 for benzoin.

IV-3-3 Results and Discussion

The experimental conditions displayed in Table 4-4 were implemented in a first SMB run. After steady state was reached, samples from the three streams leaving the system (raffinate, extract, and recycle), were collected over a super-cycle and concentrated according to the method outlined in paragraph IV-2-3. The concentrated samples were then analyzed, along with the feed (0.2 g/l), on the Gilson HPLC system. At the time of these analysis, the analytical column was unavailable, instead, we used one of the spare SMB column (16 columns were

Table 4-4:SMB Experimental Conditions for Delta-octalactone Enantiomer Separation

Beta	Q_f	Q_d	Q_r	Q_e	Q_I	Q_{II}	Q_{III}	Q_{IV}	Switch time
1.028	0.4	0.61	0.49	0.52	3.04	2.52	2.92	2.43	730 s

Beta: Safety Factor

Q_f: Feed Flow rate (ml / min)

Q_d: Desorbent Flow rate (ml / min)

Q_r: Raffinate Flow rate (ml / min)

Q_e: Extract Flow rate (ml / min)

Q_j (j = I, II, III, IV): Flow rate (ml / min) in section j

Switch time: Switching time in seconds

packed, only 8 were used). The column was flushed with the mobile phase (hexane 90 : ethanol 10) at 2.5 ml/min, before injecting 20 µl of each sample. The detection wavelength was set at 215 nm.

Figure 4-7 displays the analytical chromatograms obtained when all the samples collected above were analyzed (total feed concentration of 0.2 g/l). Completely pure streams were obtained, however the feed concentration was extremely low, as shown by the noisy baseline, and the scale on the Y axis. Therefore, we performed several SMB runs, where the experimental conditions were kept the same, while the total feed concentration was gradually increased to 0.4, 0.8 and 1.0 g/l. The corresponding analytical chromatograms, resulting from the sample analysis are shown in Figures 4-8, 4-9, and 4-10, respectively.

A close look to Figures 4-7 through 4-10, reveals that pure raffinate and extract streams were obtained, without altering the experimental conditions, up to a total feed concentration of 0.8 g/l. When the feed concentration was increased to 1.0 g/l, the extract purity was still 100%, while the raffinate purity dropped to 91%, suggesting that a mild overloading of the system might had started to manifest at that point. The fact that the extract was pure, while the raffinate was not, warrants that, the system "switched" too late, i.e. after the extract front had left section III into the raffinate port. Such phenomenon, would normally happen under overloading conditions, where the solutes start moving, inside the columns, faster than their velocity under linear conditions. Since switching time (in linear case) is usually chosen between the two retention times

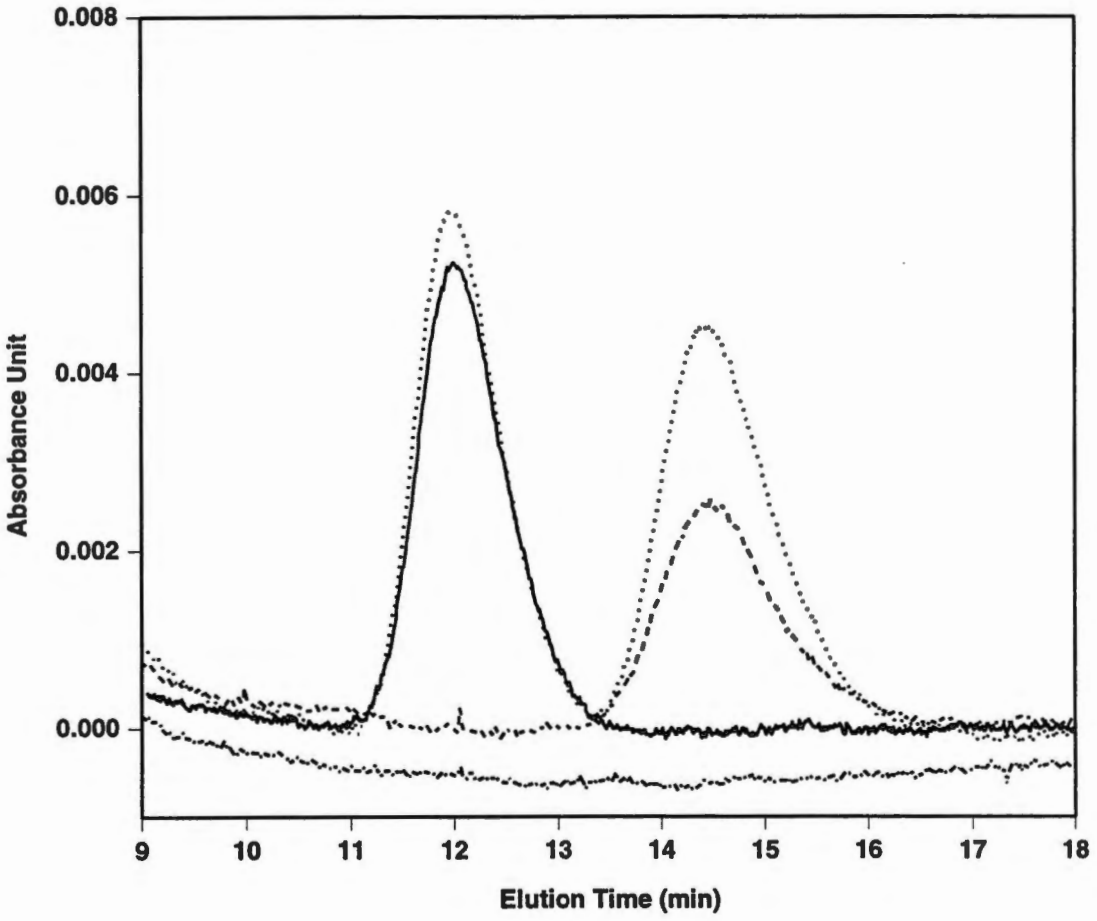


Figure 4-7: Analytical Chromatograms for Samples Collected During δ-Octalactone Enantiomer Separation by SMB (see SMB Experimental Conditions in Table 4-4, Total Feed Concentration = 0.2 g/l).

Dotted Line: Feed — Solid Line: Raffinate

Dashed Line: Extract — Dashed-Dotted Line: Recycle

Analytical Conditions: Column: 20 x 1.0 cm I.D. Chiracel OB, Vinj = 20µl
Mobile Phase: Hexane90:EtOH10, FR=2.5 ml/min, Detection at λ = 215 nm

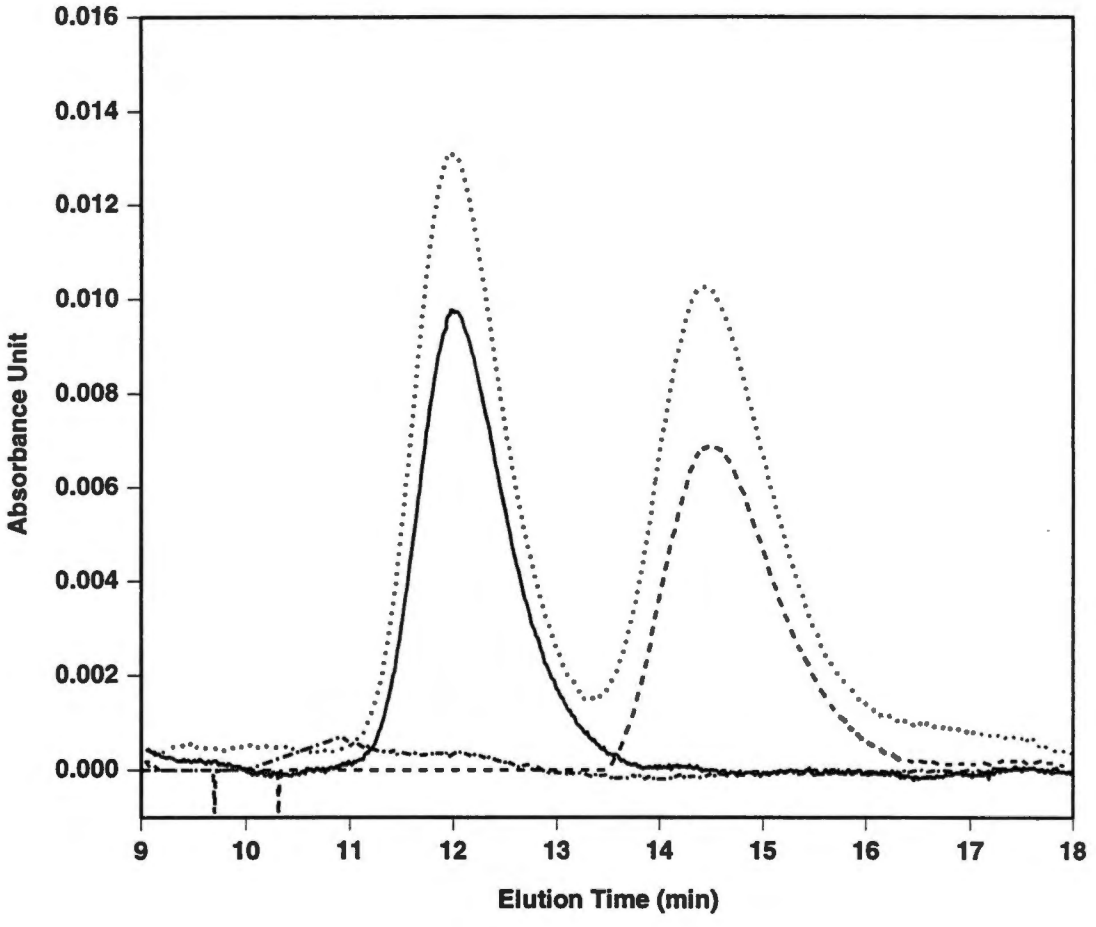


Figure 4-8: Analytical Chromatograms for Samples Collected During δ-Octalactone Enantiomer Separation by SMB (see SMB Experimental Conditions in Table 4-4, Total Feed Concentration = 0.4 g/l).

Dotted Line: Feed — Solid Line: Raffinate

Dashed Line: Extract — Dashed-Dotted Line: Recycle

Analytical Conditions: same as in Figure 4-7

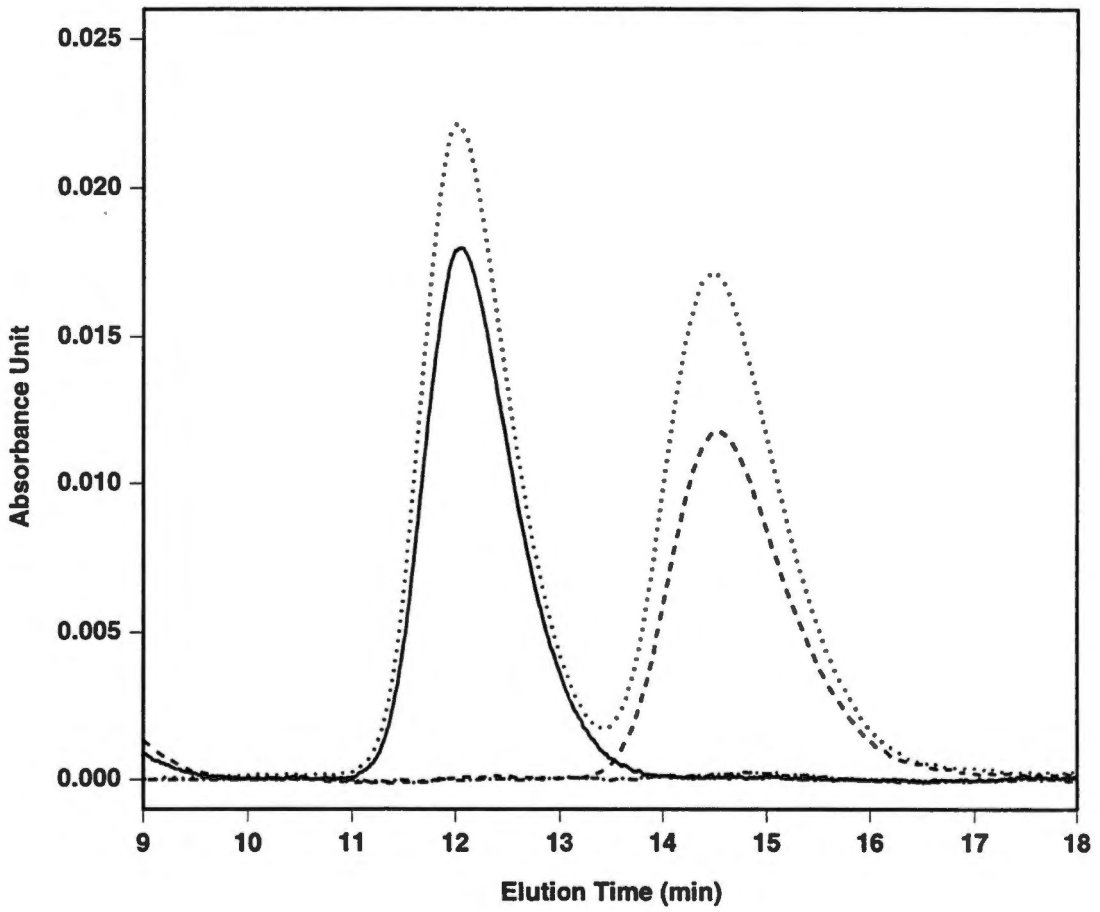


Figure 4-9: Analytical Chromatograms for Samples Collected During δ-Octalactone Enantiomer Separation by SMB (see SMB Experimental Conditions in Table 4-4, Total Feed Concentration = 0.8 g/l).

Dotted Line: Feed
Solid Line: Raffinate
Dashed Line: Extract
Dashed-Dotted Line: Recycle

Analytical Conditions: same as in Figure 4-7

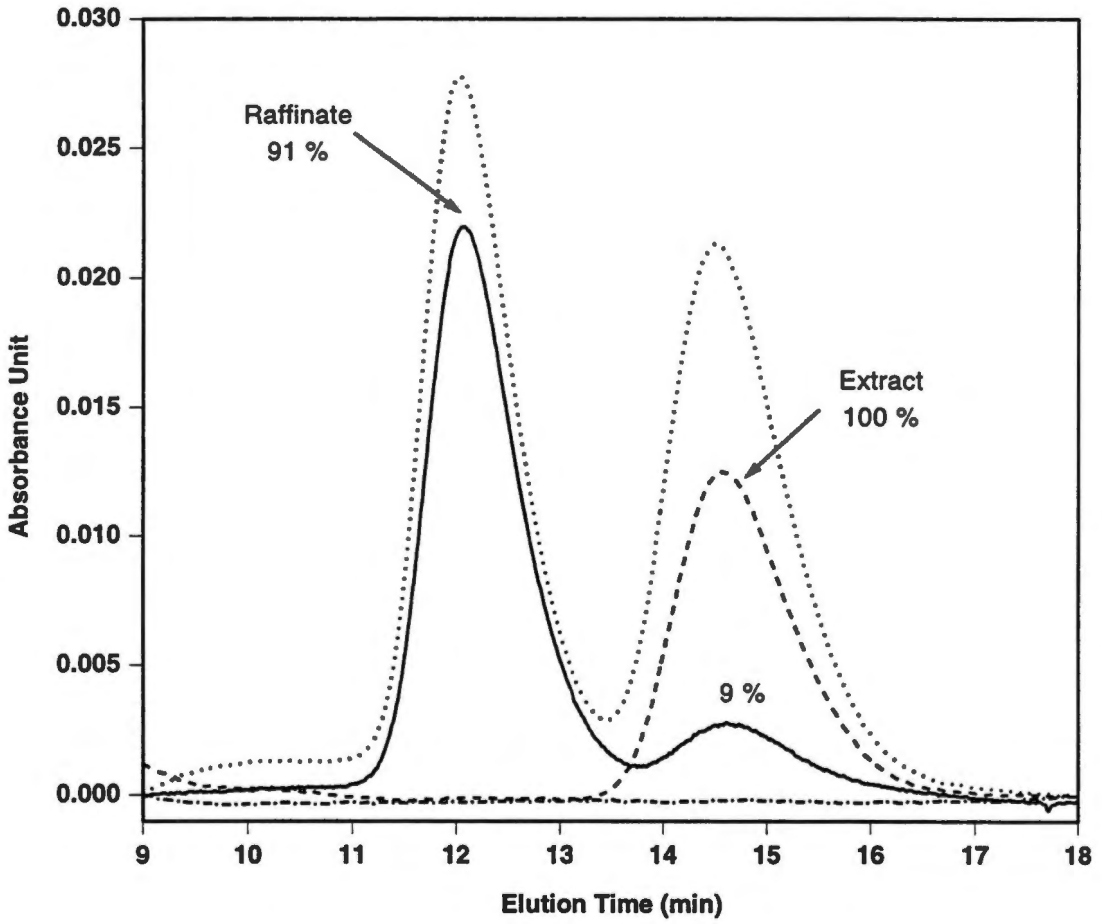


Figure 4-10: Analytical Chromatograms for Samples Collected During δ-Octalactone Enantiomer Separation by SMB (see SMB Experimental Conditions in Table 4-4, Total Feed Concentration = 1.0 g/l).

Dotted Line: Feed
Solid Line: Raffinate
Dashed Line: Extract
Dashed-Dotted Line: Recycle

Analytical Conditions: same as in Figure 4-7

t_1 and t_2 (determined with a flow rate equal to the flow rate in section II), if the solutes start moving faster, and the switch time was not altered, the switch would occur "too late" allowing component 2 to pollute the stream of component 1. The solution, then, would be to reduce the switching time, in order to compensate for the higher velocity of the solute fronts, which means altering the conditions determined for the linear case. Such action was not taken, because of this chapter scope, limited to linear chromatography. Dealing with change of solute velocities with increasing concentrations is in the domain of non-linear chromatography, which will be discussed in the two next chapters.

IV-4 Separation of 1-phenyl-1-propanol (PP) Enantiomers

1-phenyl-1-propanol ($C_9H_{12}O$, Molecular Weight, MW = 136.19) is a colorless synthetic flavor compound with a distinctive balsamic floral fragrance and a sweet honey-like taste, used in numerous food products such as non-alcoholic beverages, ice cream, candy and baked goods (Furia and Bellanca, 1971). the use of PP in food, for human consumption, is regulated in Title 21 of CFR, under the same Part, Subpart and Section (172, F, and 515 respectively), as benzoin. The first carbon with four different groups, confers a chiral attribute to 1-phenyl-1-propanol. Unlike benzoin and δ-octalactone, where only the racemic mixtures are commercially available, for PP, both enantiomers as well as the racemic mixture are available. However, the difference in price between

the racemic product and the two active ones is considerable (less than $0.38/g for racemic mixture, versus over $148/g for the active enantiomers). Thus, the interest in trying to separate and purify the two enantiomers from the cheaper racemic mixture.

IV-4-1 Conventional HPLC Generated Data

Preliminary experiments showed that the appropriate mobile phase , to be used for PP separation, was a mixture of hexane 95 : ethyl-acetate 05 (v/v), delivered at a flow rate of 2.5 ml/min. Ethyl-acetate and hexane, used in the making of the mobile phase, were HPLC grade, purchased from Fisher (Fisher scientific, Fair Lawn, NJ), while racemic PP was purchased from Aldrich (Aldrich, Milwaukee, WI). Preliminary testing also, allowed us to re-use six of the original eight SMB columns (#1, 2, 3, 7, 12 and 16), while columns # 9 and 13 had to be replaced. Table 4-5 summarizes the characteristics of the eight columns, ultimately used in the SMB experiments for PP enantiomer separation. Once again, the relatively low RSD's attest that those columns were suitable for use within an SMB system.

Table 4-5 : Characteristics for the 8 Closest Columns Obtained with PP

Experimental Conditions : Mobile Phase = Hexane 95 : Ethyl-Acetate 05 (v/v), Flow Rate = 2.5 ml/min
Detection at 270 nm, Vinj = 20 ul

Col. #	t_0 (min)	t_1 (min)	k'_1[a]	t_2 (min)	k'_2[a]	Alpha (α)[b]	Porosity (ε)	F[c]
1	4.61	10.64	1.31	12.56	1.72	1.32	0.734	0.363
2	4.57	10.35	1.26	12.61	1.76	1.39	0.727	0.375
3	4.68	10.34	1.21	12.19	1.60	1.33	0.745	0.343
4	4.51	10.37	1.30	12.12	1.69	1.30	0.718	0.393
7	4.50	10.8	1.40	12.63	1.81	1.29	0.716	0.396
12	4.67	10.95	1.34	12.78	1.74	1.29	0.743	0.345
14	4.77	10.91	1.29	12.89	1.70	1.32	0.759	0.317
16	4.74	10.57	1.23	12.44	1.62	1.32	0.754	0.326
Mean	**4.63**	**10.62**	**1.29**	**12.53**	**1.71**	**1.32**	**0.737**	**0.357**
STD[d]	**0.10**	**0.25**	**0.06**	**0.27**	**0.07**	**0.03**	**0.016**	**0.030**
RSD[e](%)	**2.18**	**2.37**	**4.73**	**2.14**	**3.93**	**2.44**	**2.18**	**8.27**

(a) $k'_1 = (t_1-t_0) / t_0$
(b) $\alpha = k'_2 / k'_1$
(c) Phase ratio = $(1-\varepsilon) / \varepsilon$
(d) Standard Deviation
(e) Relative Standard Deviation
RSD = (STD / mean)*100

IV-4-2 SMB Operating Conditions

Following the procedure outlined in the previous paragraphs, SMB conditions can be easily derived by incorporating data from Table 4-5 into the equations from paragraph II-4-3. The average separation factor (α) was determined to be 1.32, which allowed a larger range for the choice of the safety factor (β): from 1 to 1.15 (or $\sqrt{\alpha}$). In our case, we chose β equal to 1.047 and set the feed flow rate to 0.3 ml/min. The calculated parameters (flow rates and switching time) are summarized in Table 4-6. Those conditions were, then experimentally implemented. The feed total concentration was 0.5 g/l.

IV-4-3 Results and Discussion

After the steady state was reached, the raffinate, extract and recycle streams were collected over a super-cycle, and analyzed (along with the feed) on the HP1090 chromatograph. The analytical column (25 x 0.46 cm I.D. chiracel OB-H) was used for th analysis. The mobile phase (hexane 95 : ethyl-acetate 05) was delivered with a 1.0 ml/min flow rate, and the detector wavelength was set to 270 nm. Figure 4-11 shows analytical chromatograms, obtained when the different streams were analyzed. The results were, again, excellent with the raffinate displaying a 100 % purity, and the extract displaying over 97 % purity, while the recycle was, basically, clean allowing its re-use, therefore allowing the

Table 4-6:SMB Experimental Conditions for PP Enantiomer Separation

Beta	Q_f	Q_d	Q_r	Q_e	Q_I	Q_{II}	Q_{III}	Q_{IV}	Switch time
1.047	0.3	0.59	0.43	0.47	2.96	2.49	2.79	2.36	654 s

Beta: Safety Factor

Q_f: Feed Flow rate (ml / min)

Q_d: Desorbent Flow rate (ml / min)

Q_r: Raffinate Flow rate (ml / min)

Q_e: Extract Flow rate (ml / min)

Q_j (j = I, II, III, IV): Flow rate (ml / min) in section j

Switch time: Switching time in seconds

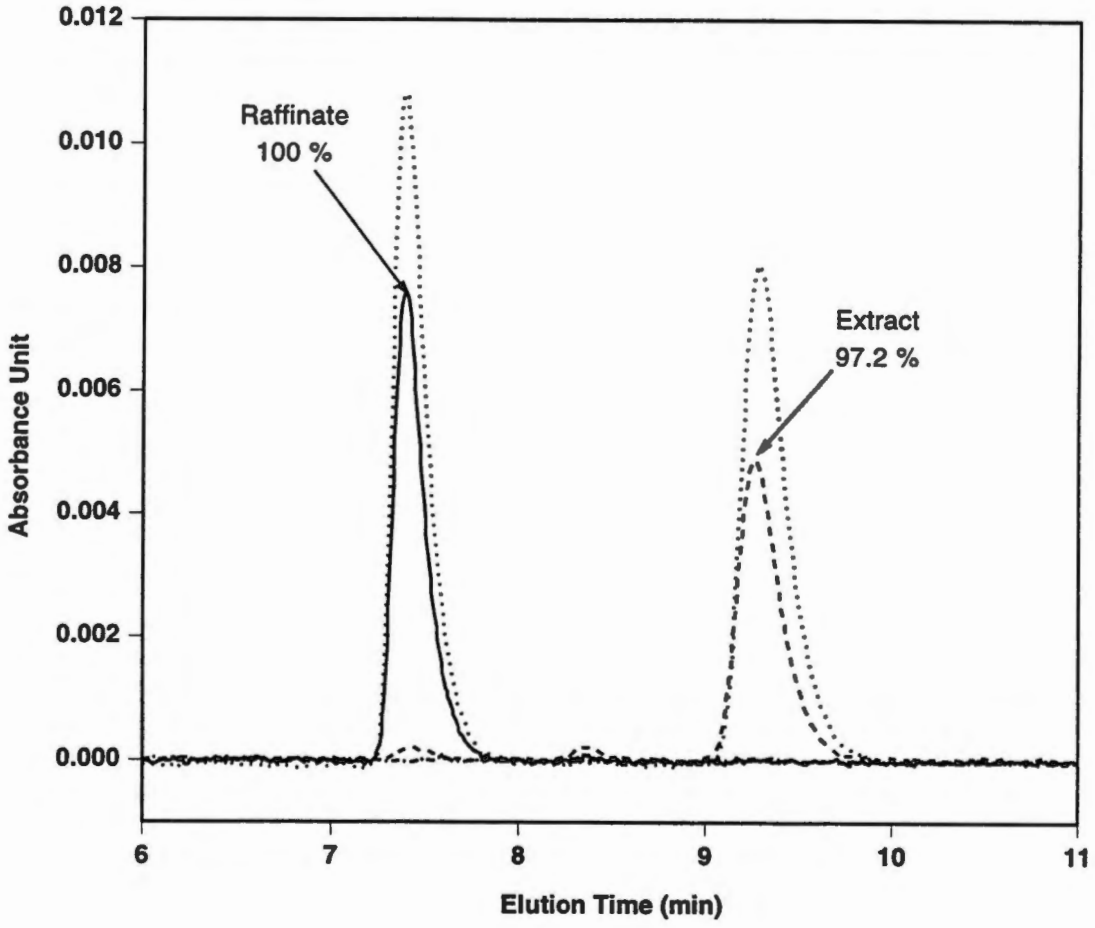


Figure 4-11: Analytical Chromatograms for Samples Collected During PP Enantiomer Separation by SMB (see SMB Experimental Conditions in Table 4-6, Total Feed Concentration = 0.5 g/l).

Dotted Line: Feed — Solid Line: Raffinate

Dashed Line: Extract — Dashed-Dotted Line: Recycle

Analytical Conditions: Column: 25 x 0.46 cm I.D. Chiracel OB-H, Vinj = 20µl
Mobile Phase: Hexane 95 : Ethyl-Acetate 05, FR=1 ml/min,
Detection at λ = 270 nm

biggest advantage of SMB (significant reduction in mobile phase consumption) to show .

IV-5 Summary

We have shown, through this chapter, that determining experimental conditions for SMB, at least for the linear case, is straightforward. Getting a set of columns with fairly close characteristics, seems to be the biggest hurdle. Once this hurdle is cleared, the experimental conditions (mainly flow rates and switch time) can be easily derived using the set of equations presented in chapter II. We showed that, this procedure works well, regardless of the separation factor between the two components to be separated. Finally, we confirmed how advantageous the use of appropriate simulation programs, can be, especially in processes like SMB. Indeed, modeling may be used to predict the behavior of the whole system, and investigate the effect of various parameter changes, without having to actually perform the experiment, resulting in tremendous saving of time and money.

The challenge we faced, after showing confirming that SMB works under linear conditions, was to investigate its behavior under non-linear conditions. However, before we could do that, we had to determine the nature of the thermodynamic relationship between the solid and mobile phase, i.e. to determine equilibrium isotherms for the selected compound and its enantiomers:

1-phenyl-1-propanol, chosen for the reasons cited in the beginning of this chapter. Therefore, in the next chapter we will address the aspect of studying the adsorption behavior of PP enantiomers on our CSP (chiracel OB). Then, in the chapter following next (Chapter VI) we will focus on the behavior of SMB under non-linear conditions.

Chapter V

1-phenyl-1-propanol Enantiomer Separation by SMB under Non-linear Conditions : Adsorption Behavior Study

V-1 Introduction

Enantioseparations using preparative liquid chromatography techniques can be cost effective when compared to enantioselective synthesis. However, to uphold this advantage, chromatographic separations need to be optimized from both production rate and purity standpoints. Effective and rapid optimization procedures may be easily carried out through modeling and computer simulation, resulting in considerable savings of time and money (Guiochon et al., 1994). This theoretical approach is yet more critical when a sophisticated process such as simulated moving bed (SMB) is considered. As shown in previous chapters, reaching steady-state in SMB after any parameter change takes typically several hours. This renders optimization through the conventional trial-and-error method a very expensive proposition. However, the modeling of any chromatographic process relies heavily on the preliminary determination of accurate adsorption isotherms (Guiochon et al., 1994). In other words, the degree of accuracy of the modeling, and of the predictions of the band profiles calculated from this model

is directly related to the accuracy of the isotherm model itself, and to that of its parameters. This illustrates the extreme care and attention that need to be given to the determination of the isotherm data. Modeling and computer simulations can also be used (as we have seen) in linear chromatography. In such case, however, only the Henry's coefficients K_i (k_i '/F, which is in fact the original slope in the relationship between the concentration of component i in the solid phase q_i and its concentration in the mobile phase C_i) are needed .

The mechanism of enantioseparations on chiral stationary phases is not well understood. This is, in part due, to the paucity of thermodynamic data available. For chiral phases, on which the density of selective sites is low and these sites are isolated, the most widely accepted assumption is that the adsorbent surface is heterogeneous and contains two types of sites (Guiochon et al., 1994; Fornstedt et al., 1997). The first type are low-energy, non-selective sites. They are the most abundant ones and are characterized by fast mass transfer kinetics. They contribute significantly to the adsorption of both enantiomers, but have no role in their separation. The second type of sites, essentially bonded ligands, are selective and responsible for chiral recognition, therefore, for the separation of the enantiomers. Those sites are characterized by a high adsorption energy and slow mass transfer kinetics, which may cause important band broadening in some cases (Fornstedt et al., 1997). Cellulose-based phases are more complex, with a much higher density of enantioselective sites and conversely, a lower interaction energy. There are reasons to suspect

that a more complex isotherm model is required for such phases (Seidel-Morgenstern and Guiochon, 1993).

The objective of this study was to determine, accurately, the quantitative isotherm behavior of 1-phenyl-1-propanol (PP) enantiomers on Chiracel OB (cellulose tribenzoate coated on silica gel), to use this result to predict the band profiles of single components and binary mixtures, and to investigate the mass transfer kinetics effect on the elution profiles.

V-2 Experimental Set-up

V-2-1 Equipment and Materials

Equipment

All the experiments, for the isotherm determination, were carried out on the HP 1090 liquid chromatograph described in paragraph III-3. For the purification of the racemic mixture (see next sub-paragraph) , an LC-50 dynamic axial compression system skid (Prochrom, Champineulles, France) was used. The 50 mm I.D. column was operated with a Dynamax SD-1 dual-piston pump (Rainin, Woburn, MA, USA). The whole system was previously described (Sarker and Guiochon, 1995a; 1995b).

Materials

In all the experiments, we used a 20 x 1.0 cm I.D. column, packed in-house with Chiracel OB (cellulose tribenzoate coated on a silica gel substrate, 20μm particles) from Daicel (Tokyo, Japan). The choice of this relatively large column diameter was dictated by our need to pack, use, and characterize accurately a set of eight closely similar columns for experiments to be made with an SMB separator. The column characteristics were determined under similar experimental conditions as the ones outlined in Table 4-5. The total porosity (ϵ_T = 0.721) was determined by injecting a non-retained compound (*1,3,5*-tri-*tert*-butyl benzene, t_0 = 4.61 min at a flow rate of 2.5ml/min). The efficiency of the column (N = 1000 plates) was determined for non-retained TTBB, from the width of the peak at half height. At infinite dilution, k' was 1.19 for S-PP and 1.61 for R-PP, and the selectivity factor was α = 1.35. The mobile phase used, in all experiments, was a mixture (v/v) of HPLC grade hexane 95 : ethyl-acetate 5 delivered at a flow rate of 2.5 ml/min.

HPLC grade n-hexane and ethyl acetate were purchased from Fisher Scientific (Fair Lawn, NJ, USA). 1,3,5-tri-tert-butyl benzene (TTBB), S-PP, R-PP, and the racemic mixture of PP were obtained from ALDRICH (Milwaukee, WI, USA). Although the PP products (S-, R-, and the racemic mixture) were more than 99% pure, the products received from the manufacturer contained an impurity that absorbed significantly at the chosen wavelengths (254 and 270 nm), and needed to be removed.

V-2-2 Purification of PP Products

The axial compression column was packed with a slurry of 250g of C18-bonded silica Impaq (BTR separation, Wilmington, DE, USA) in isopropanol. A compression pressure of 20 bars was applied to the piston to consolidate the bed (a low compression pressure is recommended for materials with irregular particles (Sarker and Guiochon, 1995a; 1995b; Sarker et al., 1996)). This pressure was maintained over the weekend, before the purification started. The resulting bed had a length of approximately 28.5 cm. The efficiency of the chromatographic bed was determined to be equal to 3700 theoretical plates. Toluene was used as the non-retained tracer, and eluted after $t_0 = 3.77$ min, with a flow rate of 118 ml/min; therefore the porosity was computed to be equal to 0.795. Each time 5ml of undiluted racemic PP was injected into the column, for a total of 100 ml. The pure PP was collected between minute 9 and minute 25. The period between two consecutive injections was 30 minutes.

The choice of the stationary phase was based on preliminary experiments showing the good separation between the two PP enantiomers and the impurity. The product obtained was free from the UV-absorbing impurity.

For the two enantiomers, small amounts (1ml each) were purified by preparative HPLC using a semi-preparative column (25 × 1cm), packed with the same stationary phase(C18-bonded silica Impaq).

V-2-3 Determination of Adsorption Isotherm for Single Component

The adsorption isotherm data for the PP enantiomers were measured using single-step frontal analysis. Two compartments of the solvent delivery system were used. One (reservoir A) was filled with the pure mobile phase. The other compartment (reservoir B) was filled with a solution of one enantiomer. In all experiments, the column was first equilibrated with pure mobile phase, prior to injecting a large volume sample (*ca.* 15ml). This injection resulted into the elution of a breakthrough, curve followed by a concentration plateau corresponding to the elution of the injected mixture, after equilibrium was reached. Then the sample pulse was washed off the column. Before the next injection, the column was flushed with pure mobile phase, until equilibrium was reached again. This procedure is tedious and time consuming, but has the advantage, over the conventional staircase method, of avoiding cumulative errors in isotherm calculation. Each successive pulse injected contained 5%, up to 20%, and then 10% more solution B than the previous one. The last one was obtained with 100% solution B (5.6g/l for S-PP and 5.43g/l for R-PP).

The UV detector was calibrated at 270nm. The UV-absorbance data were transformed into concentrations by averaging the measurements made on each plateau. The slightly nonlinear calibration curve was fitted to a second-degree polynomial. Due to the non-chiral nature of the UV response, the same

calibration curve was used for both enantiomers.

The amount of each compound adsorbed by the stationary phase at equilibrium were determined from the elution time of the inflection point of the breakthrough curve through the classical equation (Jacobson et al., 1987):

$$q = \frac{C(V_F - V_0)}{V_a} \qquad (5\text{-}1)$$

where q is the amount adsorbed on the solid phase in equilibrium with the concentration C in the mobile phase, V_F is the retention volume of the inflection point of the breakthrough curve, V_0 is the column void volume, and V_a is the volume of adsorbent in the column.

V-2-4 Determination of Competitive Adsorption Isotherms

The competitive adsorption isotherms were measured using the single-step binary frontal analysis method (Jacobson et al. 1987). The two compartments of the pump were filled, one (A) with the pure mobile phase, and the other (B) with a solution of racemic PP (total concentration 6.6 g/l). In all experiments, the column was equilibrated with pure mobile phase prior to injecting a large volume plug (ca. 15ml) of diluted solution B. The elution signal

has two successive steps, one of pure less retained compound (S enantiomer), the other of injected solution. There was no need to analyze the relative concentration of the two enantiomers in the intermediate plateau, since it contained exclusively the first enantiomer (Jacobson et al. 1987). The concentration of S-PP at the intermediate plateau was derived from the calibration curve at 270nm and the plateau height. The adsorbed amount of each enantiomer in the mixture, q_x, was derived from the retention volumes of the two breakthrough curves and their corresponding concentrations, C_x, using the equation given by Jacobson et al. (1987).

$$q_x = \frac{C_x(V_{S+R}-V_0) - C_{x,ip}(V_{S+R} - V_S)}{V_a} \qquad (5\text{-}2)$$

where V_0, V_{S+R}, V_S, and V_a are the column holdup volume, the elution volumes of the two breakthrough fronts, and the volume of adsorbent in the column, respectively. $C_{x,ip}$ is the concentration of the S enantiomer at the intermediate plateau.

V-2-5 Fitting the Isotherm Data to the Isotherm Model.

The experimental adsorption data were fitted to the *Langmuir* and the *bi-Langmuir* isotherm models, the latter with eight, six, and four parameters (see later).The best values of the coefficients of these models were calculated using

a nonlinear regression program (Sigma Plot 4.00, SPSS Inc., San Rafael, CA, USA). The best coefficients for the isotherm parameters were obtained by minimizing the following function :

$$\sigma^2 = \sum_{i=1}^{N_d} \frac{q_i^{exp} - q_i^{th}}{q_i^{th}} \qquad (5\text{-}3)$$

where N_d *is* the number of data points, and q_i^{exp} and q_i^{th} are the experimental and the calculated data points, respectively. In the regression, the experimental data were given a weight equal to $1/q_{experimental}$ to account for the nearly constant relative error made in the measurement of the amounts adsorbed at equilibrium.

V-3 Theory : Band Profile Calculations

The band profiles were calculated using two models of nonlinear chromatography, the equilibrium-dispersive model and the lumped kinetic model.

V-3-1 Equilibrium-dispersive Model

This model assumes instantaneous equilibrium between the stationary and the mobile phase, and integrates the differential mass balance equation for the two components of the mixture, taking the isotherm equations into account. To account for the finite column efficiency, an apparent dispersion coefficient, D_a,

is used instead of the axial dispersion coefficient which would account for axial and eddy dispersion. The axial dispersion coefficient is assumed constant and equal to its value under linear conditions.

$$D_a = \frac{u_o L}{2N} \qquad (5\text{-}4)$$

where u_o is the mobile phase velocity, L the column length, and N the number of theoretical plates. This model is valid when the band profile is more influenced by the nonlinear behavior of the equilibrium isotherm than by kinetic effects. this is so, because all contributions to band broadening are lumped together into the single apparent axial dispersion coefficient, D_a (Guiochon et al., 1994).

V-3-2 Lumped Kinetic Model (transport-equilibrium)

In this study, the solid film linear driving force model was used to account for the mass transfer kinetics (Guiochon et al., 1994). This model assumes that the rate of variation of the stationary phase concentration, $\partial q/\partial t$, is proportional to the difference between the concentration of the compound in the stationary phase at equilibrium with the concentration C in the mobile phase, q^*, and the actual concentration, q. The proportionality coefficient, k_f (min^{-1}), is the mass transfer rate coefficient. The combination of this rate equation and the mass balance equation constitutes the transport-dispersive model (Guiochon et al., 1994). This model still includes an axial dispersion coefficient. Its value was set

constant and equal to half the value of the apparent axial dispersion coefficient used for the equilibrium dispersive model (corresponding to an efficiency of 1000 theoretical plates). The mass transfer coefficient was derived by identification of the experimental profile to a numerical solution of the model. Numerical solutions can be obtained using an appropriate program (Guiochon et al., 1994).

V-3-3 Boundary Conditions

These conditions characterize the experiment performed. Initially the column was free of sample, containing only the stationary phase in equilibrium with pure mobile phase. We used the classical boundary conditions of elution chromatography corresponding to the injection of a rectangular pulse of known width and maximum concentration. Injection profiles obtained for three different volumes (0.5, 1, and 2 ml) are shown in Figure 5-1. They validate the assumption of a rectangular pulse injection.

V-4 Results and Discussion

V-4-1 Modeling of Single Component Equilibrium Isotherms

The single component isotherm data obtained for each enantiomer were fitted to the Langmuir and the bi-Langmuir models. Figure 5-2 compares these

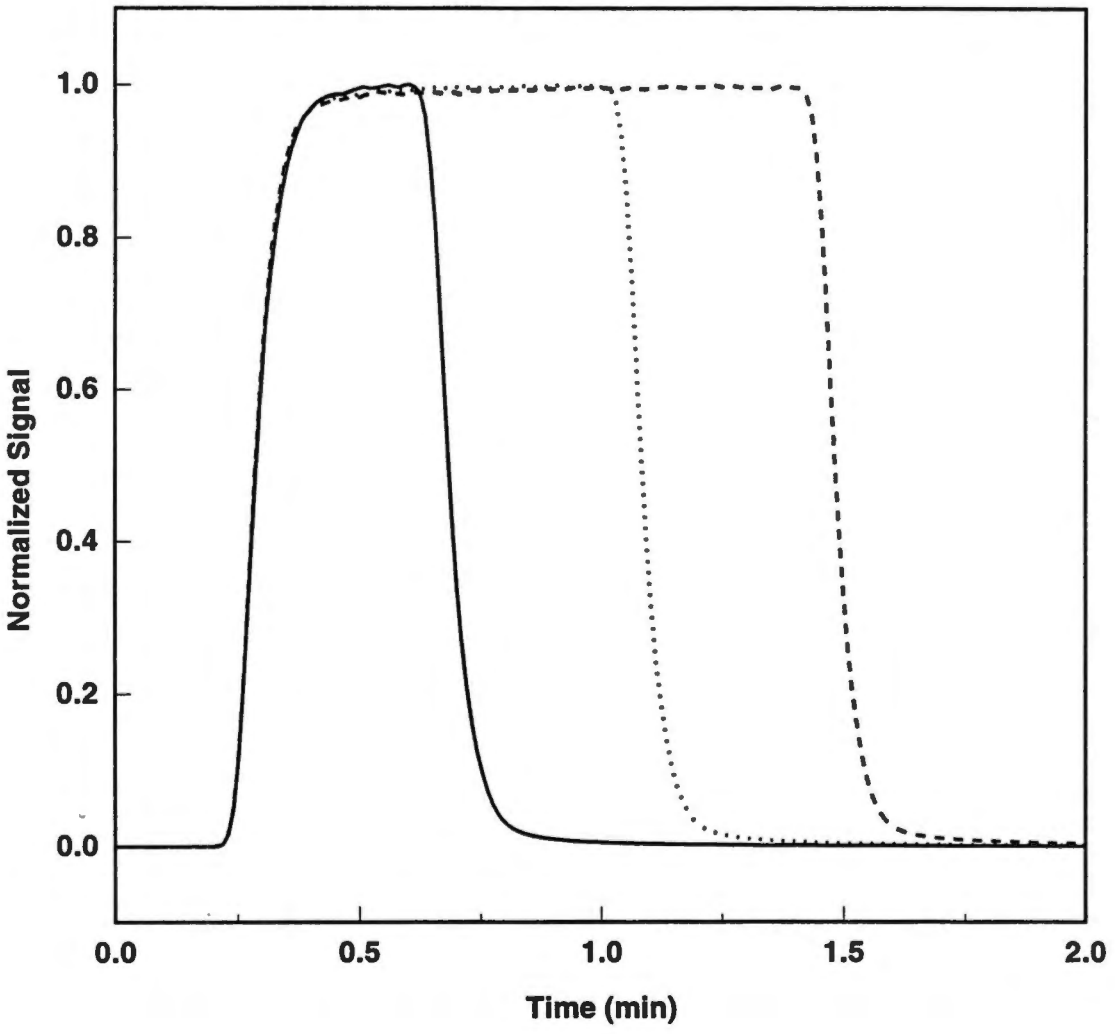


Figure 5-1: Injection Profiles of Increasing Volumes of a Racemic PP Solution, without Column.

Solid Line: 0.5 ml, Dashed Line: 1.0 ml, Dotted Line: 2.0 ml

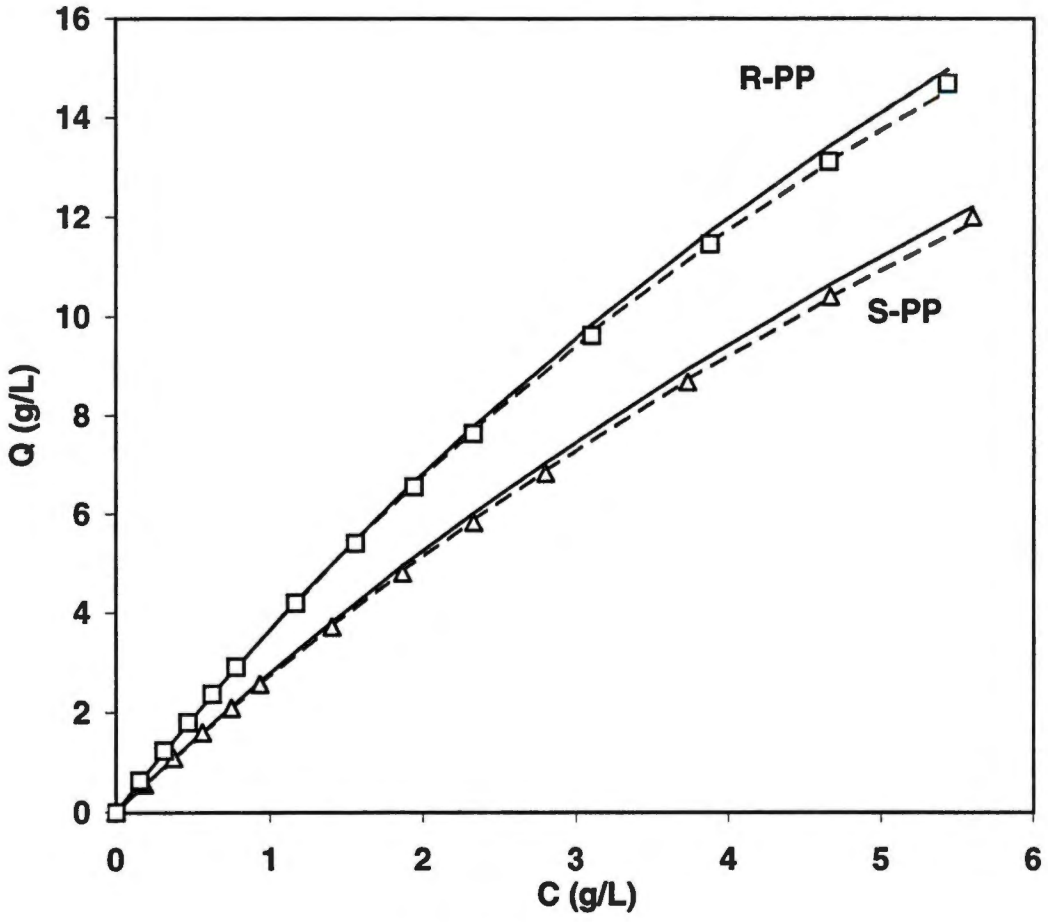


Figure 5-2: Comparison of Single Component Experimental Data (symbols: △ = S-PP, □ = R-PP) for 1-Phenyl-1-Propanol Enantiomers on Chiracel OB, to the Best Fitted Langmuir Model

Dashed Line: Regression of Experimental Data (single) to the Langmuir Model
Solid Line: Regression of Combined Competitive and Single Component Data

Experimental conditions: 20x1.0 cm column, Mobile phase: Hexane 95 / Ethyl-acetate 5 (v/v), Flow rate = 2.5 ml/min. Mobile phase concentration ranges: 0.18 to 5.6 g/l for S-PP, and 0.15 to 5.4 g/l for R-PP.

data (symbols), and the best fitted Langmuir model (dashed line).This model fits the data better than the bi-Langmuir model (results not shown). The Scatchard plots of the data is shown in Figure 5-3 (symbols for experimental data, dashed lines for the best Langmuir model). It exhibits a near linear relationship, consistent with a Langmuir model (Andrade, 1985; Jacobson et al., 1990). So, the Langmuir model appears to be preferable for the sake of simplicity. The best values of the parameters for each model are reported in Table 5-1, with the absolute (STD) and the relative standard deviations (RSD) for each parameter. The RSD's are lower with the Langmuir model than with the bi-Langmuir one. A further discussion of the results obtained in attempting to fit the competitive isotherm data to the bilangmuir model is given later.

The solid line in Figure 5-2 shows the single component isotherms calculated from the set of coefficients obtained by fitting together the experimental data obtained in both the single-component and the competitive adsorption measurements to the competitive Langmuir model. Although the agreement is not perfect, it still remains very good. This result suggests that it is possible, at least in some cases, to predict reasonably well the single component isotherm from the measurements of competitive isotherm data using only the racemic mixture. If this result is verified, the whole set of competitive isotherms for any mixture of the two enantiomers could be obtained from racemic mixture only.

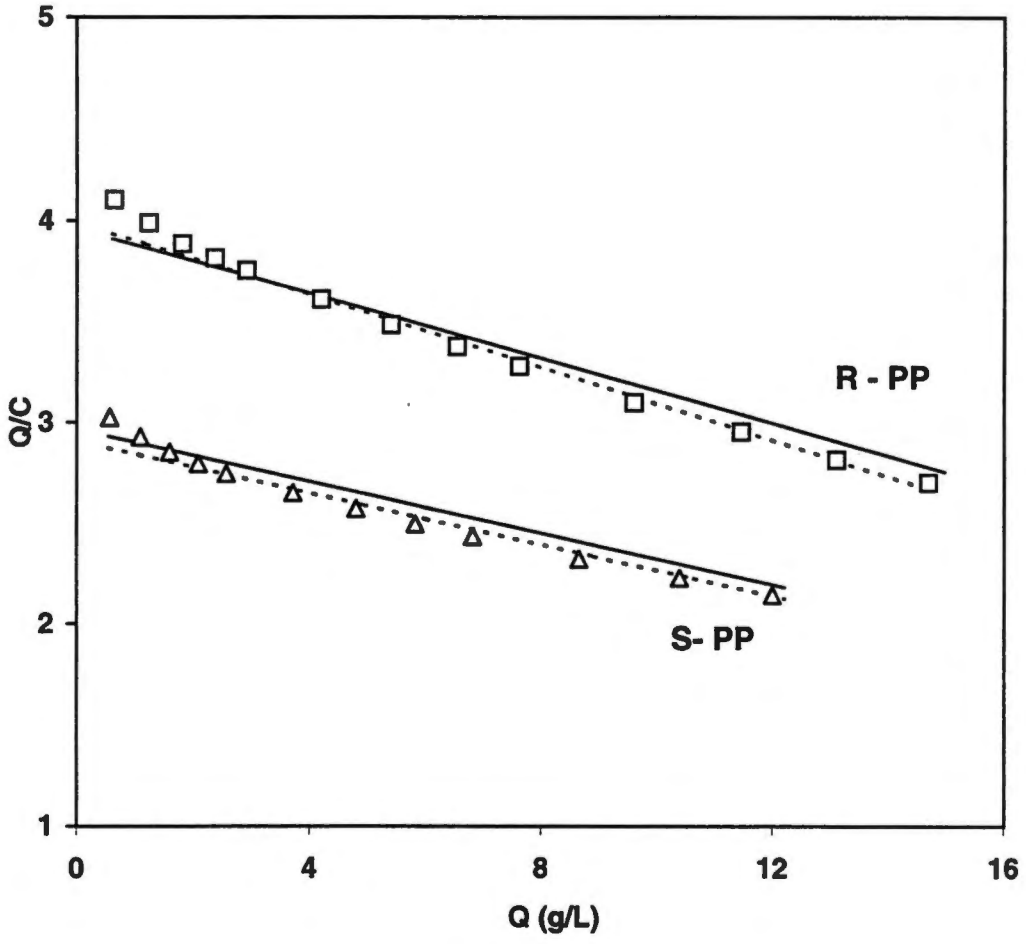


Figure 5-3: Scatchard plots of the Experimental Adsorption Data (symbols:△=S-PP, □=R-PP) of 1-Phenyl-1-Propanol Enantiomers.

Dashed Line: Regression of Experimental Data (single) to the Langmuir Model
Solid Line: Regression of Combined Competitive and Single Component Data
Experimental Conditions: Same as Figure 5-2

Table 5-1 : Single Component Isotherm Coefficients for PP Enantiomers

Experimental Conditions: Mobile Phase = Hexane 95 : Ethyl-Acetate 5 (v/v), Flow rate = 2.5ml/min
20 * 1.0 cm Chiracel OB Column, Detection at 270 nm

Experimental data were fitted to Langmuir and Bi-Langmuir models

# para[a]	site	Isomer	a[b]	STD[c]	RSD(%)[d]	b[e], l/g	STD	RSD(%)	qs[f], g/l
Bilang[g]	ns[j]	S	2.65	0.03	1.0	0.049	0.001	2.9	54.7
		R	3.57	0.09	2.4	0.069	0.003	4.5	51.8
	s[j]	S	0.49	0.02	3.5	1.397	0.238	17.1	0.4
		R	0.63	0.07	10.7	0.975	0.253	25.9	0.6
Lang[h]		S	2.91	0.02	0.7	0.066	0.003	3.8	44.2
		R	3.99	0.02	0.6	0.090	0.002	2.4	44.4

a: Number of Parameters
b: Capacity Factor
c: Standard Deviation
d: Relative Standard Deviation
e: Henry' Coefficient
f: Saturation Capacity
g: Bi-Langmuir Model
h: Langmuir Model
i: Non-Selective
j: Selective

V-4-2 Modeling of the Competitive Equilibrium Isotherms

Even though the fit of single-component data suggested the Langmuir model to be more appropriate, the competitive and the single-component data were fitted together to several models. The competitive bi-Langmuir models with eight, six, five, and four parameters were investigated. The eight parameter model allows both selective and non-selective types of sites to differ for the two enantiomers, an unlikely situation. The six parameter model assumes the non-selective sites to be the same for both enantiomers, while the five parameter model assumes further that the saturation capacity of the chiral sites are the same for both enantiomers ($q_{chiral} = a_s / b_s = a_r / b_r$). This is often the case for stationary phases made of bonded proteins (Jacobson et al., 1990; Jacobson et al. 1991; Fornstedt et al., 1996). Finally, the four parameter model assumes that one of the two enantiomers does not interact with the selective sites. In this case, the model simplifies to Langmuir for this enantiomer, and is bi-Langmuir for the other one. This last model was successfully used to describe the adsorption behavior of phenyl-alanine anilide enantiomers on imprinted polymeric stationary phases (Chen et al., 1999).

The results obtained by fitting all adsorption data to these models are summarized in Table 5- 2. The eight parameter model is the least appropriate, not only generating large RSD's but also estimating the selective site capacity factor to zero for both enantiomers (Table 5-2). All three other bi-Langmuir

Table 5-2 : Competitive Isotherm Coefficients for PP Enantiomers

# para[a]	site	Isomer	a[b]	STD[c]	RSD(%)[d]	b[e], l/g	STD	RSD(%)	qs[f], g/l
8p	ns[j]	S	2.14	1.55	72.4	0.122	0.068	55.1	17.5
		R	2.89	2.10	72.6	0.176	0.109	62.2	16.5
	s[j]	S	0.86	1.56	182.3	0	0.075	*	*
		R	1.23	2.11	172.2	0	0.090	*	*
6p	ns[j]	S or R	2.94	*		0.065	0.002	3.4	45.4
	s[j]	S	0	*		0	0.014	*	*
		R	1.16	*		0.237	0.021		4.9
5p	ns[j]	S or R	2.94	*		0.065	0.002	3.4	45.4
	s[j]	S	0	*		0	0.008	*	*
		R	1.16	*		0.237	0.022	9.3	4.9
4p S (lang[h]) R (Bi-lang[g])	ns[j]	S or R	2.93	0.02	0.6	0.065	0.002	2.9	45.3
	s[j]	S	*	*		*	*		
		R	1.16	*		0.237	0.020	8.6	4.9
Langmuir		S	2.97	0.03	0.9	0.064	0.003	5.1	46.1
		R	3.96	0.04	0.9	0.080	0.003	4.2	49.2

For footnotes a through j and for experimental conditions, see table 5-1

models generated almost exactly the same estimates for the non-selective site parameters (2.935 for a_{ns}, 0.0647 for b_{ns}), and for the selective site parameters for the R enantiomer (a_r = 1.162 and b_r = 0.237). Finally, all three models estimate the selective site capacity factor for the S enantiomer to be zero, making all these models equivalent to the simpler four parameter bi-Langmuir model. As expected, the saturation capacity was found to be much larger (10-fold) for the non-selective than for the selective sites.

The data fitted well to a simple competitive Langmuir model (Table 5-2). The errors, either SE's or RSD's, were not much larger than for the last three bi-Langmuir models. Given the greater simplicity of this model, it seems to be the best choice. Note that the saturation capacities for the two enantiomers (46.05 for S-PP and 49.23 for R-PP) are very close which makes the model nearly thermodynamically consistent. Figure 5-4 compares the experimental data points (symbols: (□) R-PP, (△) S-PP) and the isotherms calculated with the Langmuir model and two sets of coefficients. The first set was derived from the competitive data only (dashed line). The second set was obtained by fitting together the competitive and the single-component data (solid line). There is an excellent agreement between the experimental data and the two sets of isotherms, similar to the one observed in Figure 5-2.

Table 5-3 displays the isotherm coefficients derived from the single component data, the competitive data, and the combined set of data. The three sets of best coefficients afforded by the regression are very close. This

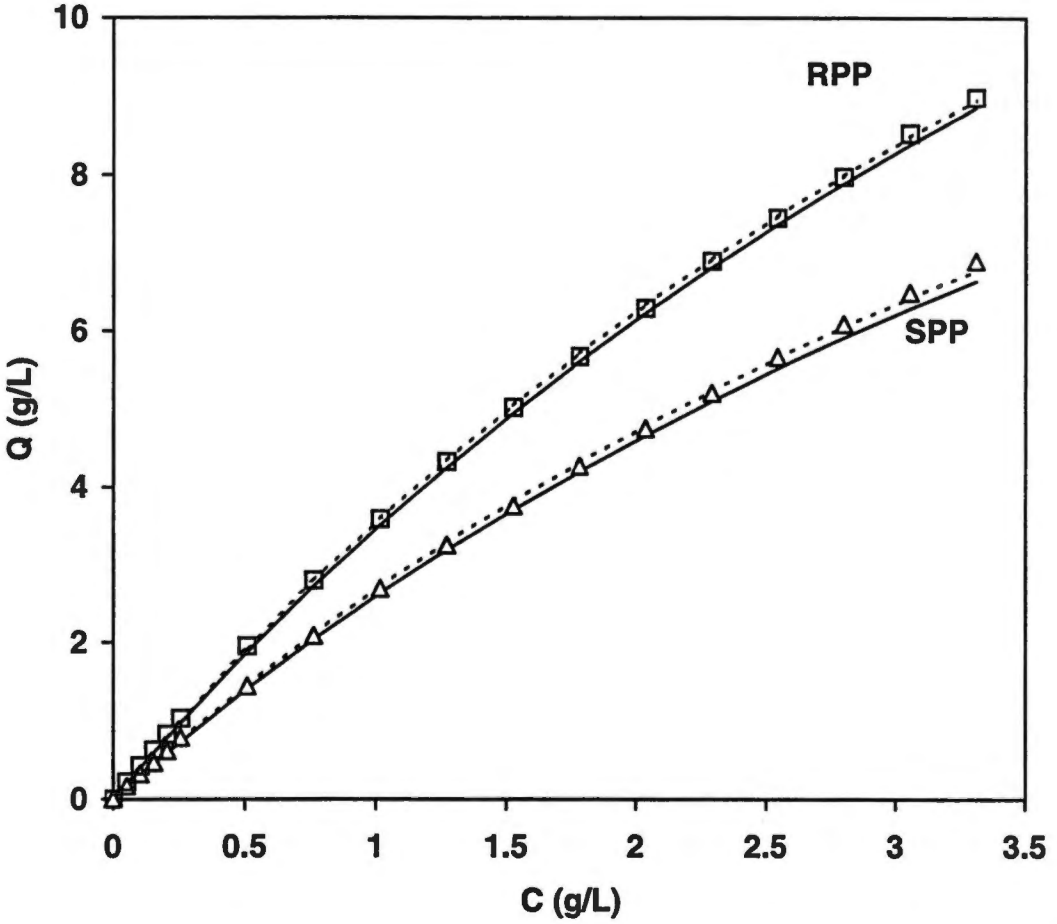


Figure 5-4: Comparison of Experimental Competitive Adsorption Data (symbols: △ = S-PP, □ = R-PP) for 1-Phenyl-1-Propanol Enantiomers on Chiracel OB, to the Best Fitted Langmuir Model

Dashed Line: Regression of Competitive Data (alone) to the Langmuir Model
Solid Line: Regression of Combined Competitive and Single Component Data

Experimental Conditions: Same as Figure 5-2, except for mobile phase concentration range (here from 0 to 6.6 g/l total concentration)

Table 5-3: Comparison of Simple Competitive Langmuir Isotherm Coefficients Determined from Single Component Data, Competitive Data and the Combination of both for PP Products

Experimental Conditions: Mobile Phase = Hexane 95 : Ethyl-Acetate 5 (v/v), Flow rate = 2.5ml/min
20 * 1.0 cm Chiracel OB Column, Detection at 270 nm

	a^d (S)	b^d (S), l/g	a^d (R)	b^e(R), l/g
SCD[a]	2.91	0.066	3.99	0.090
CD[b]	3.09	0.067	4.09	0.088
(SCD & CD)[c]	2.97	0.064	3.96	0.080

a: Single Component Data (SCD)
b: Competitive Data (CD)
c: Combined SCD & CD
d: Henry'Coefficient
e: Capacity Factor

agreement, which is also illustrated in Figures 5-2 and 5-4, is an important result. If confirmed for other racemic mixtures and phase systems, it would be very valuable, allowing major savings in time and money for the determination of the competitive isotherm data required for the successful modeling of enantiomeric separations.

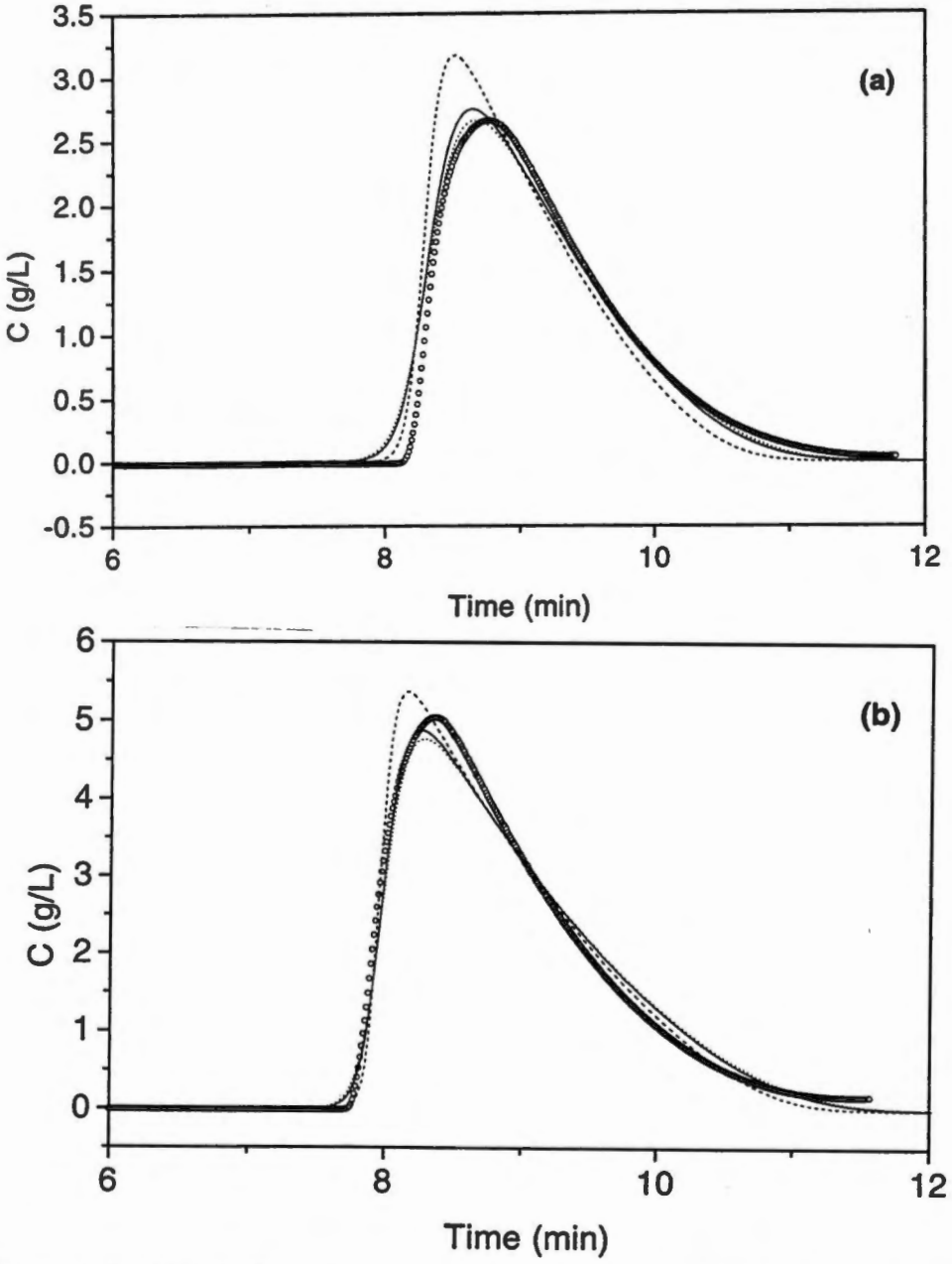
Similar results, with the Langmuir model accounting best for the adsorption behavior of the two enantiomers of 3-chloro-1-phenyl-1-propanol on the same chiral stationary phase, were recently obtained by Cherrak et al. (1999). These results contrast with other previously reported studies in which the bi-Langmuir model was shown to be the model of choice (Jacobson et al., 1990; 1991; Charton et al., 1993; 1994, Fornstedt et al., 1996). Jacobson et al. (1990) measured the equilibrium isotherms of four pairs of enantiomers (mandelic acid, tryptophan, phenyl-butyric acid , and N benzoyl-alanine) on bovine serum albumin bonded to silica. Charton et al. (1993) examined the behavior of methyl-mandelate and of ketoprofene on immobilized cellulose tribenzoate. Fornstedt et al. (1996) investigated the adsorption behavior of the enantiomers of propranolol on the protein CBH I immobilized on silica. More recently, Pais et al. (1998) proposed a model simpler than the bi-Langmuir model, with the sum of a linear and a Langmuir term, to account for the behavior of epoxide enantiomers on microcrystalline cellulose tri-acetate. Finally, Chen et al. (1999) were able to use the four parameter bi-Langmuir model to explain the adsorption of the enantiomers of phenyl-anilide on an imprinted polymeric stationary phase.

V-4-3 Validation of the Isotherm Model

In the modeling of chromatographic processes, an isotherm model is only as good as its ability to predict band profiles, not only for the single components but, most importantly, for binary mixtures, regardless of their absolute or relative concentrations. Finding a suitable model that fits well the experimental data is relatively easy, but a model is valid only if it can be used adequately to predict band profiles. This is why it must be validated.

Single component band profiles

Band profiles were calculated using the best values of the parameters of the competitive Langmuir model (Table 5-2). Figures 5-5a and 5-5b compare the experimental band profiles (symbols) obtained for two samples of different volumes (1 and 2 ml, respectively) of an S-PP solution (9.34g/l), and the profiles calculated with different models and conditions. A fair agreement was observed between the experimental profile, and the profiles given by the equilibrium-dispersive model (dashed line). The main differences are more diffuse front and rear parts of the experimental profile which is also shorter. This suggests that the assumption of a fast mass transfer kinetics may not hold entirely true. The diffuse rear part of the profile exhibits a degree of tailing which might be due to a relatively slow mass transfer kinetics (Guiochon et al., 1994; Fornstedt et al., 1996). The other two profiles in Figures 5-5a and 5-5b were calculated with the transport-dispersive model. In the application of this model, it was assumed that



Figures 5-5: Experimental (symbols [∘]) and Calculated Elution Profiles for 2 Injection Volumes for S-PP Solution (C = 9.34g/l): (a) 1.0ml (b) 2.0 ml.

Dashed Line: Equilibrium-dispersive model

Solid Line: Transport-dispersive model (k_f = 150 min^{-1})

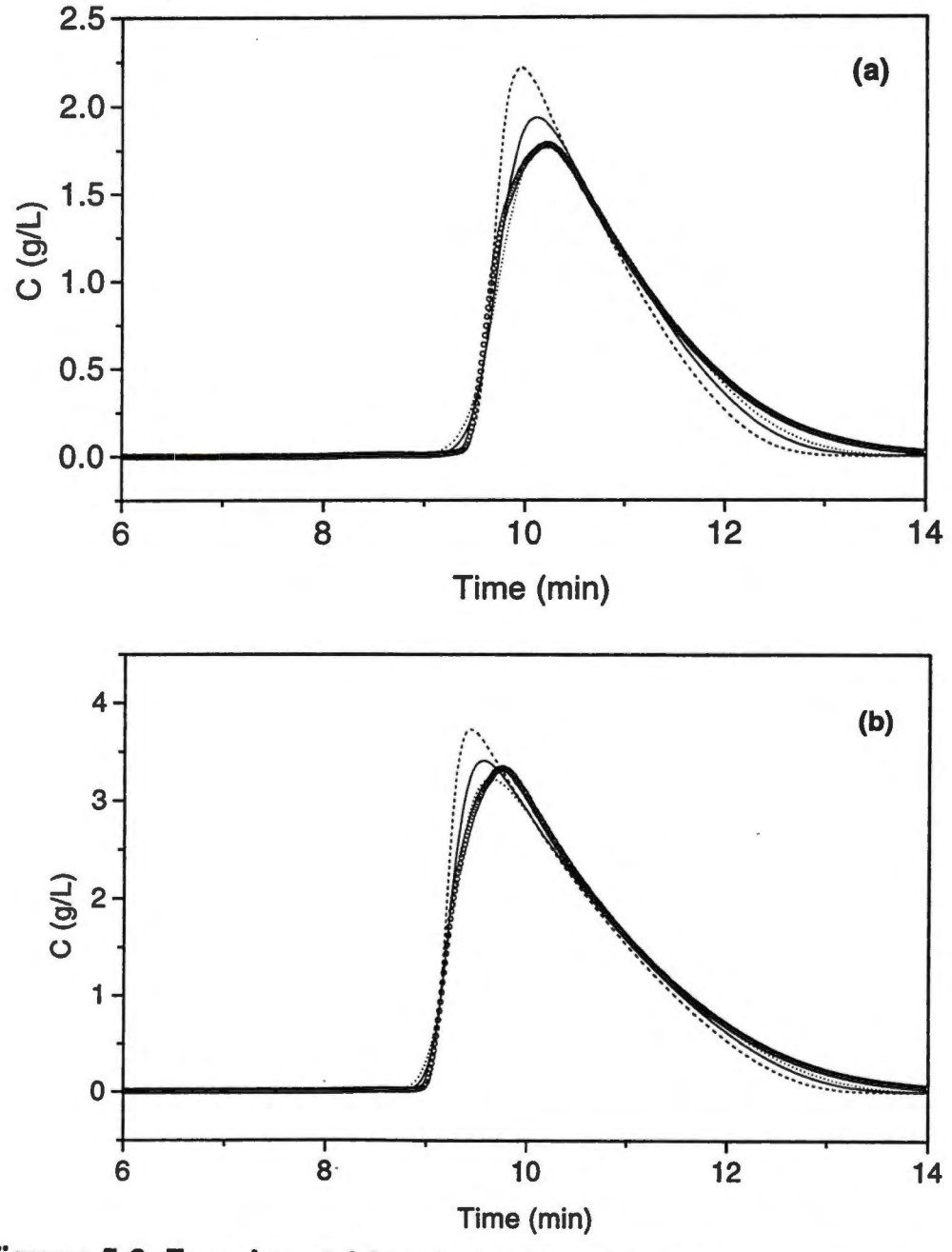
Dotted Line: Transport-dispersive model (k_f = 80 min^{-1})

the axial dispersion coefficient was equal to half the value of the apparent axial dispersion coefficient used for the equilibrium-dispersive model (and corresponding to an efficiency of 1000 theoretical plates). The profiles shown in the Figures were obtained for values of the rate coefficient of 80 (dotted lines), and 150 (solid lines) min^{-1}. The best agreement was obtained with $k_f = 80\ min^{-1}$.

Similar results were obtained for the R enantiomer (7.76 g/l solution). Figures 5-6a and 5-6b compare experimental and calculated profiles. The profiles given by the equilibrium-dispersive model (dashed line) agree only fairly well with the corresponding experimental profiles (symbols). On the other hand, an excellent agreement can be observed with the profiles given by the transport-dispersive model. The best agreement was obtained for $k_f = 60\ min^{-1}$ (dotted line) in both cases. As expected, k_f was found to be lower for the more retained enantiomer (R-PP), albeit only slightly so.

Band Profiles for Binary Mixtures

To further validate the selected model, the band profiles of samples of the racemic mixture of increasing sizes were calculated with the isotherm parameters of the Langmuir model and compared to experimental results. Figures 5-7a to 5-7d illustrate such comparisons for 0.25, 0.5, 1 and 2 ml samples of a 10.62 g/l solution of the racemic mixture. The dotted lines show the profiles calculated with the transport-dispersive model and a rate coefficient $k_f = 10000\ min^{-1}$ for both enantiomers. The dashed lines are the profiles calculated with the same values of k_f's as optimized for the single component profiles (Figures 5-5 & 5-6),

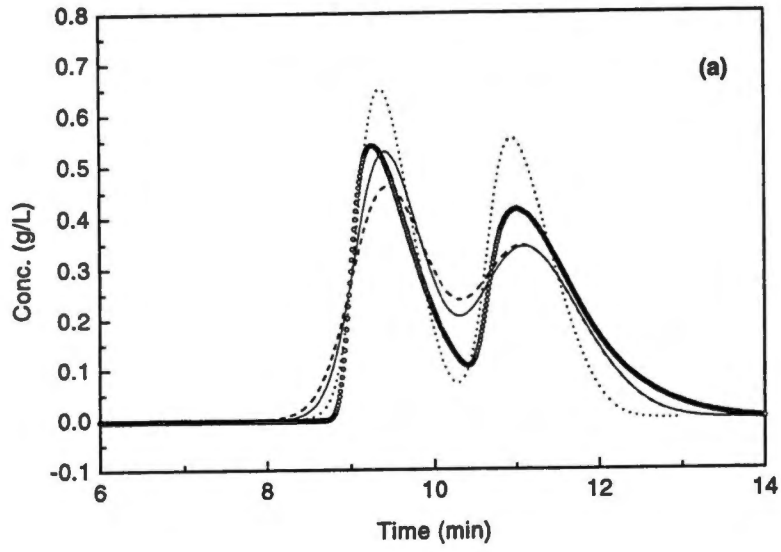


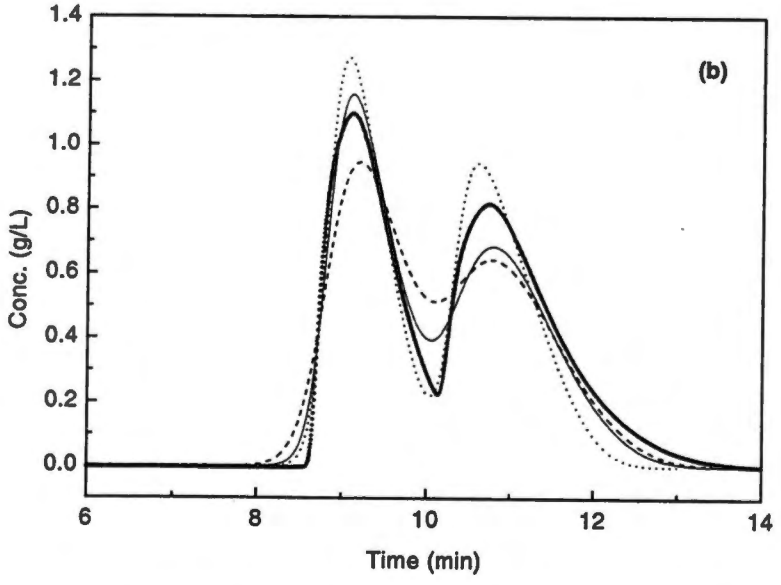
Figures 5-6: Experimental (symbols [◦]) and Calculated Elution Profiles for 2 Injection Volumes for R-PP Solution (C = 7.76 g/l): (a) 1.0 ml (b) 2.0 ml.

Dashed Line: Equilibrium-dispersive model

Solid Line: Transport-dispersive model (k_f = 150 min^{-1})

Dotted Line: Transport-dispersive model (k_f = 60 min^{-1})





Figures 5-7: Experimental (symbols [◦]) and Calculated Elution Profiles for 4 Injection Volumes for Racemic PP

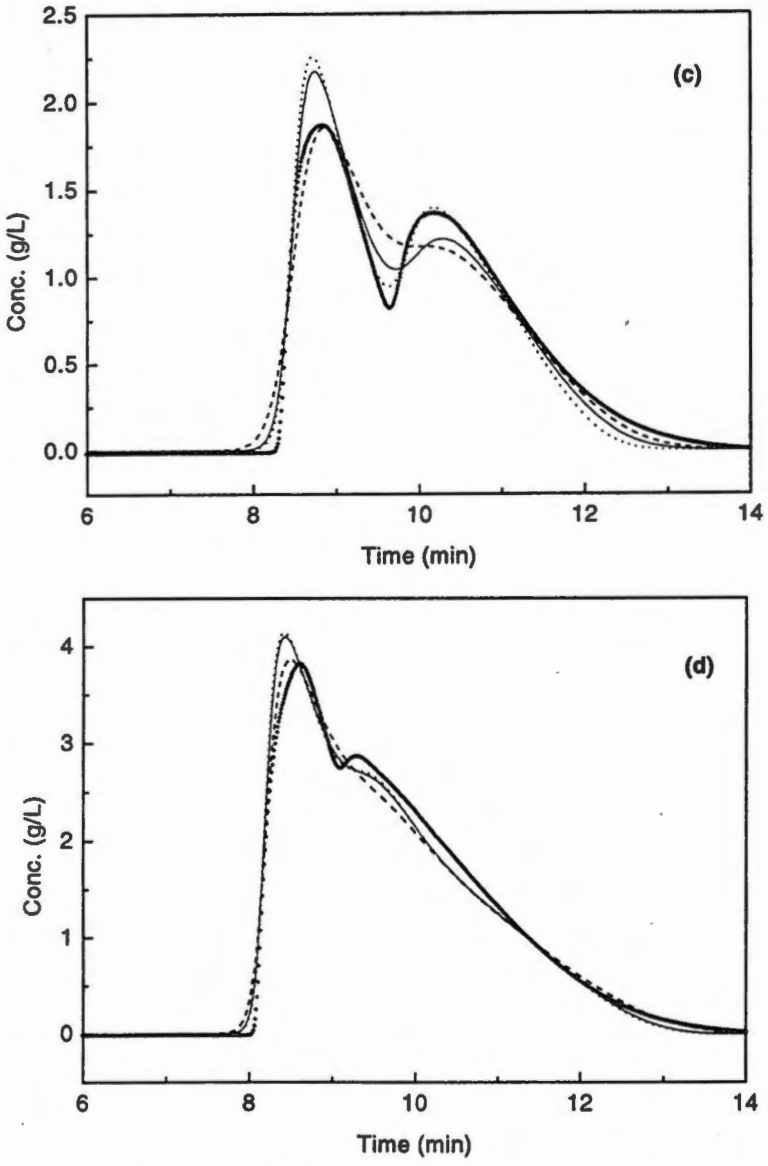
(Total Concentration = 10.62 g/l): (a) 0.25 ml (b) 0.5 ml

Dotted Line: Transport-dispersive model with $k_{f1} = k_{f2} = 10000$ min^{-1}

Dashed Line: Transport-dispersive model with $k_{f1} = 80$ min^{-1}, $k_{f2} = 60$ min^{-1}

Solid Line: Transport-dispersive model a) $k_{f1} = 150$ min^{-1}, $k_{f2} = 60$ min^{-1}

b) $k_{f1} = 300$ min^{-1}, $k_{f2} = 80$ min^{-1}



Figures 5-7 (Continued): Experimental (symbols [∘]) and Calculated Elution Profiles for 4 Injection Volumes for Racemic PP (Total Concentration = 10.62 g/l): (c) 1.0 ml (d) 2.0 ml

Dotted Line: Transport-dispersive model with $k_{f1} = k_{f2} = 10000\ min^{-1}$

Dashed Line: Transport-dispersive model with $k_{f1} = 80\ min^{-1}$, $k_{f2} = 60\ min^{-1}$

Solid Line: Transport-dispersive model c) $k_{f1} = 500\ min^{-1}$, $k_{f2} = 120\ min^{-1}$

d) $k_{f1} = 1000\ min^{-1}$, $k_{f2} = 300\ min^{-1}$

namely 80 min^{-1} for S-PP and 60 min^{-1} for R-PP. Finally the rate coefficients were adjusted in each case to obtain the best possible agreement between calculated and experimental profiles (solid lines). The profiles calculated with high values of the rate coefficients (10000 min^{-1}) do not agree well with the experimental profiles at low concentrations (Figures 5-7a and 5-7b). They agree better at higher concentrations (Figures 5-7c and 5-7d). This confirms the concentration dependence of the mass transfer rate coefficient previously reported (Guiochon et al., 1994; Sajonz et al., 1996; Chen et al., 1999; Miyabi and Guiochon, 1999).

This conclusion is confirmed by the comparison between the solid line profiles which were calculated with values of k_f's different for each sample size, in an effort to match as well as possible each experimental profile with a numerical solution of the transport-dispersive model. This best agreement was obtained with values of k_f's increasing with increasing injection volume (k_{f1} = 150, 300, 500 and 1000 min^{-1}; k_{f2} =60, 80, 120 and 300 min^{-1}, for Vinj = 0.25, 0.5, 1 and 2 ml, respectively). This agreement between calculated and experimental profiles was much better than when values of k_f's, equal to those used to optimize the agreement between experimental and calculated profiles of single components, were used (dashed lines). This suggests a possibility that the rate coefficients could be competitive under certain circumstances.

V-5 Conclusion

The results of this study show that, even though simple isotherm models may lack accuracy under certain conditions (Charton et al., 1993), there are cases in which they can be used satisfactorily, to account for the adsorption behavior of enantiomers. In the case in point, a simple competitive Langmuir model was able to describe well the single-component and competitive behavior of the enantiomers of PP on cellulose tribenzoate. This confirms that the thermodynamics of the interactions between enantiomers and cellulose-based phases are different from those observed on other chiral phases, as shown in recent studies (Pais et al., 1998; Chen et al., 1999; Cherrak et al., 1999). This illustrates the great difficulty encountered in reaching general conclusions regarding the mechanisms of enantioseparations. The task becomes still harder when more complex phenomena, such as mass transfer kinetics, enter into play. Obviously, more research is needed, involving different enantiomeric pairs and different types of CSP's.

Chapter VI

1-phenyl-1-propanol Enantiomer Separation by SMB under Non-linear Conditions

VI-1 Introduction

Operating SMB under linear conditions is of academic usefulness only, (except in the sugar industry, where the isotherms remain linear for a wide range of concentrations). It allows the understanding of the process basics, and the investigation of several of its aspects, without having to deal with complicated issues, such as the ones inherent to non-linear chromatography (Zhong and Guiochon, 1998). However, SMB applications are usually geared toward production, and are seldom carried out in the linear case. Therefore, the overloading conditions, which lead to non-linear competitive adsorption behavior, need to be taken into account, when choosing experimental parameters, ie flow rates and switching time, for an SMB run performed under non-linear conditions (Mazzotti et al., 1996).

The pivotal role, played by modeling and computer simulation, in determining operating conditions for an SMB run, has been emphasized in previous chapters. That role becomes more critical when non-linear conditions

are considered. In general, modeling of a chromatographic process requires three different groups of parameters (Storti et al., 1993): 1) geometrical and physical characteristics (column section and length, particle size, void volume, number of columns per section), 2) Adsorption equilibrium isotherms, and 3) Parameters accounting for mass transport and axial mixing. The usefulness of modeling is, evidently, contingent on how accurately, those parameters are determined. Once the parameters are derived, and the system successfully modeled, it becomes imperative, especially in an industrial setting, to optimize the whole separation process, in order to make it economically feasible (Pynonnen, 1998).

VI-2 Optimization of a Chromatographic Process

VI-2-1 Optimization Procedures

There are three different approaches available for the optimization of a given chromatographic system: the theoretical approach, based on the solution of the various mathematical models, the numerical approach, which uses classical computational methods, and finally the empirical approach (Guiochon et al., 1994). When preparative chromatography (including SMB) is used as a manufacturing step, the single most important objective function that needs to be minimized is **COST** (Pynonnen, 1998). Therefore, any optimization procedure

should be targeted at such objective. According to Felinger and Guiochon (1994), the two major cost components, in preparative chromatography, are solvent consumption and capital costs. In general, production cost (PC) can be divided into three different components (Charton et al., 1994, Guiochon et al., 1994): 1) Fixed costs (FC), which include the investment capital and labor cost, 2) Operating costs (OC), which include solvent, packing material, recycling and energy costs, and 3) Cost of crude material (CC), lost during the process (which remains negligible in SMB).

At the early stages of a process design, before packing material purchase, the most critical factor that needs to be considered is the particle size (Guiochon et al., 1994; Pynnonen, 1998). Smaller particle size leads to higher efficiency, and undoubtedly improves the separation performance. However, small particle size also means higher pressure drop, leading to higher cost, since operating equipments under high pressure, costs markedly more (Pynnonen, 1998). Therefore, whenever possible, larger bead size stationary phase should be selected. Large particle size generates low pressure drop, which allows the use of higher flow rates, and ultimately leads to higher throughput; thus, higher production rates (Guiochon et al., 1994; Pynnonen, 1998). This approach is particularly advantageous with processes which performances are slightly, if at all, affected by low efficiencies. This is the case of SMB, reported to be, questionably, quasi-insensitive to poor efficiencies by several authors (Zhong and Guiochon, 1998; Pynnonen, 1998; Pedeferri et al., 1999).

Generally, because a system may be already in place, it is not always possible to start an optimization procedure at the packing material particle size stage. Instead, optimization has to start downstream from such a step, and be carried out not for the whole system, but rather for new application(s).

VI-2-2 Optimization Parameters

In a chromatographic process, there are numerous parameters that can be optimized. Guiochon et al. (1994) listed and defined several ones, from which we relate a few that are of specific interest to SMB, and refer the interested reader to the cited reference for a more detailed discussion. Among the parameters that can be optimized in an SMB setting, are the recovery yield, the desorbent requirement, the production rate, and the purity. The recovery yield (Y_i) is the ratio between the amount of a given component collected at its port (extract or raffinate) and the amount of the same component introduced with the feed (Guiochon et al., 1994). According to Storti et al. (1995) Y_i can be derived from the following equations (6-1a and b):

$$Y_{ext} = \frac{C_{ext}^{ext} * Q_{ext}}{C_{ext}^{feed} * Q_{feed}} \qquad \text{(6-1a)} \qquad Y_{raf} = \frac{C_{raf}^{raf} * Q_{raf}}{C_{raf}^{feed} * Q_{feed}} \qquad \text{(6-1b)}$$

C_i^j being concentration of component i in stream j, and Q_j flow rate of stream j.

The second parameter considered is the desorbent requirement (DR), which can be defined as the mass of desorbent needed to recover a unit mass of pure product(s) (Storti et al., 1995). It corresponds to the amount of the desorbent make- up, continuously fed into the system with a flow rate (Q_D) equal to (Q_1 - Q_4) (Q_1 and Q_4 being flow rate of section I and IV respectively), in order to compensate for the solvent collected with the raffinate and the extract. Storti et al. (1995) gave a simple equation (6-2) that can be used to estimate DR:

$$DR = \frac{Q_D}{Q_F} \qquad (6\text{-}2)$$

It is already obvious that the Y_i and the DR can not be simultaneously optimized, since maximizing Y_i requires larger solvent consumption (ie larger DR). Therefore, a compromise between those two parameters has to be found. Such trade-offs, usually involving more than just two parameters, are common in optimization procedures. The third optimization parameter of interest is the production rate (PR), defined as the amount of product(s) generated per unit of time (Guiochon et al., 1994). It is often computed with regard to the unit mass of stationary phase, and reported as such to account for adsorbent requirement. Guiochon et al., (1994) proposed to combine PR and DR, and derive another parameter : the specific production (SP), which takes into consideration the amount produced per unit of time, as well as the amount of solvent consumed. SP is simply equal to the ratio of PR over DR. Finally, the parameter that is, most

often, used in optimization is the purity of one, or both streams leaving the system. The extract (raffinate) purity can be derived from equations 6-3a and b:

$$P_{ext} = \frac{C_{ext}^{ext}}{C_{ext}^{ext} + C_{raf}^{ext}} * 100 \quad \text{(6-3a)} \qquad P_{raf} = \frac{C_{raf}^{raf}}{C_{raf}^{raf} + C_{ext}^{raf}} * 100 \quad \text{(6-3b)}$$

In fact the purity is "a constraint of the separation" (Guiochon et al., 1994). It is one of the first parameters that is usually set in advance. Generally, fulfilling the requirement of such constraint, sets the tone for the recovery yield, the production rate, and ultimately the economics of the whole process (Guiochon et al., 1994).

VI-2-3 "The Triangle Theory" as Optimization Tool for SMB

In chapter IV, it was shown that the determination of operating conditions for SMB, in the linear range, can be, rather, simple. However, the same procedure is not as straightforward in the non-linear range (Zhong and Guiochon, 1997). An alternative approach, called "the triangle theory", was first proposed by Storti et al. (1993). Since then, it has been extensively studied, and successfully applied to numerous SMB applications (Storti et al., 1995; Mazzotti et al., 1996; Mazzotti et al., 1997; Migliorini et al., 1998; Francotte et al., 1998; Migliorini et al., 1999; Pedeferri et al., 1999). The "triangle theory" approach was developed in the framework of the equilibrium theory, where axial mixing and

mass transfer resistance were (are) neglected (Storti et al., 1993). Until recently, (Migliorini et al., 1999), this approach was limited to the ideal case (ie assuming infinite efficiency), and to systems exhibiting Langmuirian type adsorption behavior. The key parameters, used in such approach, are the ratios (m_j, with j=1, 2, 3, or 4) between the net fluid flow rate and the adsorbed phase flow rate in each section j (Storti et al., 1995). m_j can be calculated using equation (6-4):

$$m_j = \frac{Q_j t^* - V\varepsilon}{V(1-\varepsilon)} \qquad (6\text{-}4)$$

with Q_j being the volumetric flow rate inside section j, t^* the switching time, ϵ the overall porosity and V the total column volume.

Mazzotti and co-workers (Mazzotti et al., 1996; 1997) rewrote the conditions initially proposed by Ruthven and Ching (1989),and showed that in order to achieve complete separation of a binary mixture, a set of inequalities, involving the flow rates ratios (m_j), have to be fulfilled. First, to assure proper regeneration of the adsorbent, a lower limit is imposed on m_1. Such limit coincides with the Henry coefficient (a_2) of the more retained component. In other words m_1 has to satisfy the inequality: $a_2 < m_1 < \infty$. Likewise, m_4 has an upper limit, that needs to be satisfied, in order to obtain totally regenerated eluent. The expression of such limit is slightly more complicated, compared to the constraint on m_1. The equation (6-5), which allows us to determine the upper limit for m_4 (m_{4cr}), was given by

Mazzotti et al., (1996):

$$m_{4,cr} = \frac{1}{2}\left\{a_1 + m_3 + b_1 C_1^F (m_3 - m_2) - \sqrt{[a_1 + m_3 + b_1 C_1^F (m_3 - m_2)]^2 - 4 a_1 m_3}\right\} \quad (6\text{-}5)$$

with a_1 being the Henry coefficient for component 1 (the less retained), b_1 the capacity factor (component 1), C_1^F the concentration of component 1 in the feed, and m_j the flow rate ratio in section j, calculated according to equation 6-4. The other two flow rate ratios (m_2, and m_3), correspond to the two sections where the separation actually takes place. In the linear case, to reach complete separation (ie to get pure raffinate and pure extract), both m_2 and m_3 have to be larger than a_1, and smaller than a_2 (with a_i being Henry coefficient for component i). In addition, to achieve a positive feed flow rate, m_3 has to be larger than m_2 (since, as we have seen in chapter II, $Q_f = Q_{III} - Q_{II}$). Most of these constraints (except for $m_2 < a_1$) hold true in the non-linear case.

To determine operating conditions for an SMB run, Mazzotti and his co-workers (Mazzotti et al., 1996; 1997) proposed to keep m_1 and m_4 constant (while still satisfying the constraints above), and explore the (m_3 , m_2) plane to determine the region of separation. In the linear case, those authors showed that the overall region, where the separation (not necessarily complete) can take place, is constrained by $m_2 < a_2$, and $m_3 > a_1$. When these two restrictions are combined with the condition needed for positive feed flow rate ($m_3 > m_2$), the separation zone is well defined. Figure 6-1 illustrates such a zone, which is

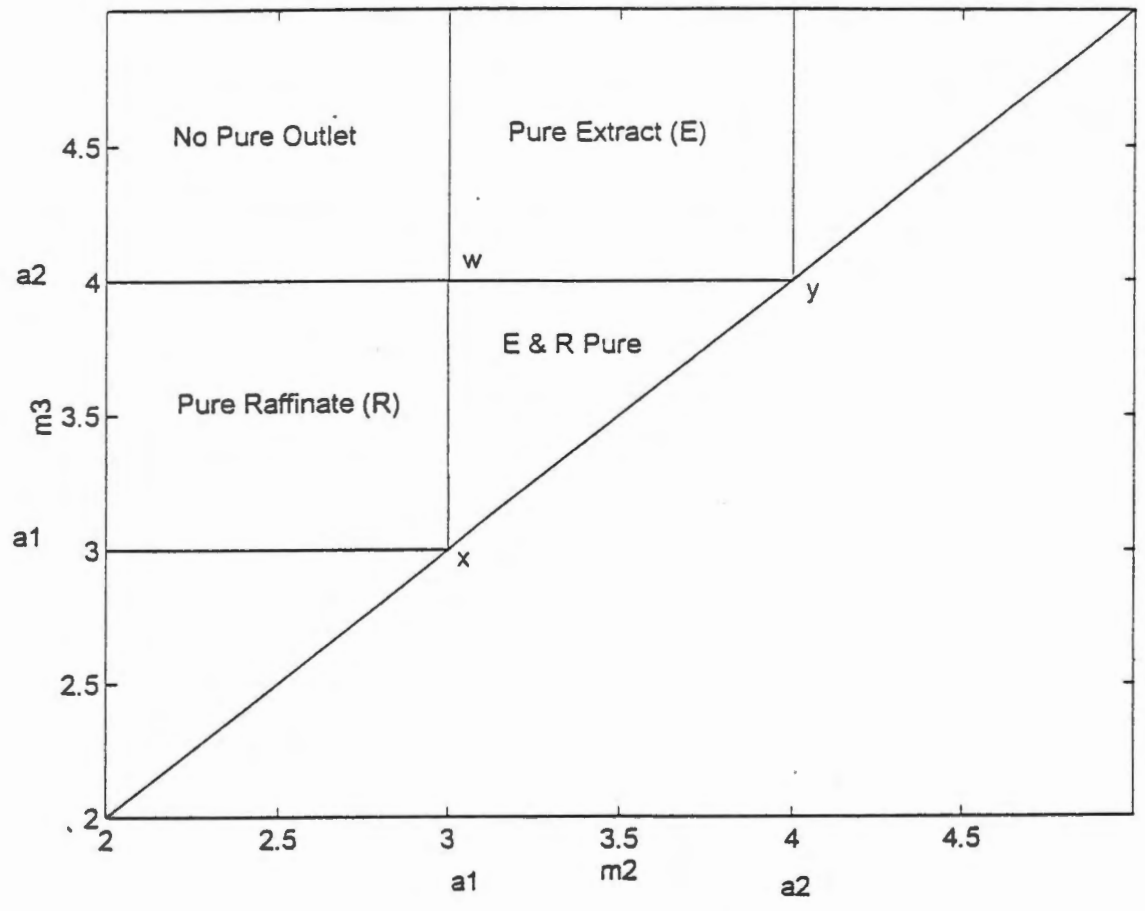


Figure 6-1: The (m_2 , m_3) Plane with the 4 Different Regions for a System Characterized by a Linear Isotherm : Total Feed C. = 0.02g/l, a1 = 3 and a2 = 4

located above the diagonal (where $m_2 = m_3$), for a system with a_1=3, a_2=4 and total feed concentration of 0.02 g/l. The separation zone can further be divided into four regions, among which the most important is the one defined by the triangle wxy, and corresponding to complete separation (Mazzotti et al., 1997). Provided that constraints on m_1 and m_4 are fulfilled, any operating conditions chosen inside the triangle should generate pure products at both the raffinate and the extract ports (Mazzotti et al., 1997). The vertex (w) of the triangle represents the optimal conditions (in terms of PR), with the best compromise for the performance parameters defined earlier. However, "w" also corresponds to the least robust of all operating conditions (Mazzotti et al., 1996). Indeed the vertex "w" is common to all four zones of the general separation region , making it very sensitive to the smallest disturbance that can be due to flow rate fluctuations, to adsorption isotherm inaccuracy, to non-ideal behavior, and / or, to errors in determining the column geometrical characteristics. For "the pure extract" zone (located just above the triangle), where m_3 is $> a_2$, and $a_1 < m_2 < a_2$, the more retained component is carried toward the raffinate port, polluting that stream, while the extract stream is still 100% pure (Storti et al., 1995). Conversely, for "the pure raffinate" zone (situated to the left of wxy triangle), it is the less retained component that pollutes the extract stream (since constraint about $m_2 > a_1$, is no longer satisfied), while the raffinate stream is still pure. Finally, operating conditions in the fourth zone (where $m_3 > a_2$ and $m_2 < a_1$) would generate no pure outlet, since all the constraints about m_2 and m_3 would be

violated.

To generate similar figure (as Figure 6-1) for the non-linear case, accurate adsorption isotherms are needed, along with the exact feed concentration. The need, for such parameters, rises from the fact that, under overloading conditions, the separation triangle boundaries become dependent on the concentration of the feed. Furthermore, the constraints on the flow rate ratios become inter-dependent (Mazzotti et al., 1997). Figure 6-2 shows the effect of increasing feed concentration (while all the other parameters are kept constant), on the shape, size, and location of the separation triangle in the (m_2,m_3) diagram. It is clear from Figure 6-2 that the separation zone shrinks markedly, as the feed concentration increases. We can see, in Figure 6-2, that the different separation zones share a common area around the diagonal, where the feed flow rate tends toward zero (the diagonal corresponds to $m_2 = m_3$, ie to $Q_f = 0$). In such cases, regardless of the feed concentration, Q_f is so small that the amount injected is diluted in the system, matching the linear conditions, rather quickly (Mazzotti et al., 1997)

In summary, the "triangle theory" approach can first be a very useful tool for selecting experimental conditions for an SMB run, under both linear and non-linear conditions. Then, it can be used to determine the "safest" most robust optimal conditions. Optimization using such an approach can, indeed, be quick and efficient. Generally, an optimization procedure based on the"triangle theory" would include the following steps: First, the adsorption isotherms need to be

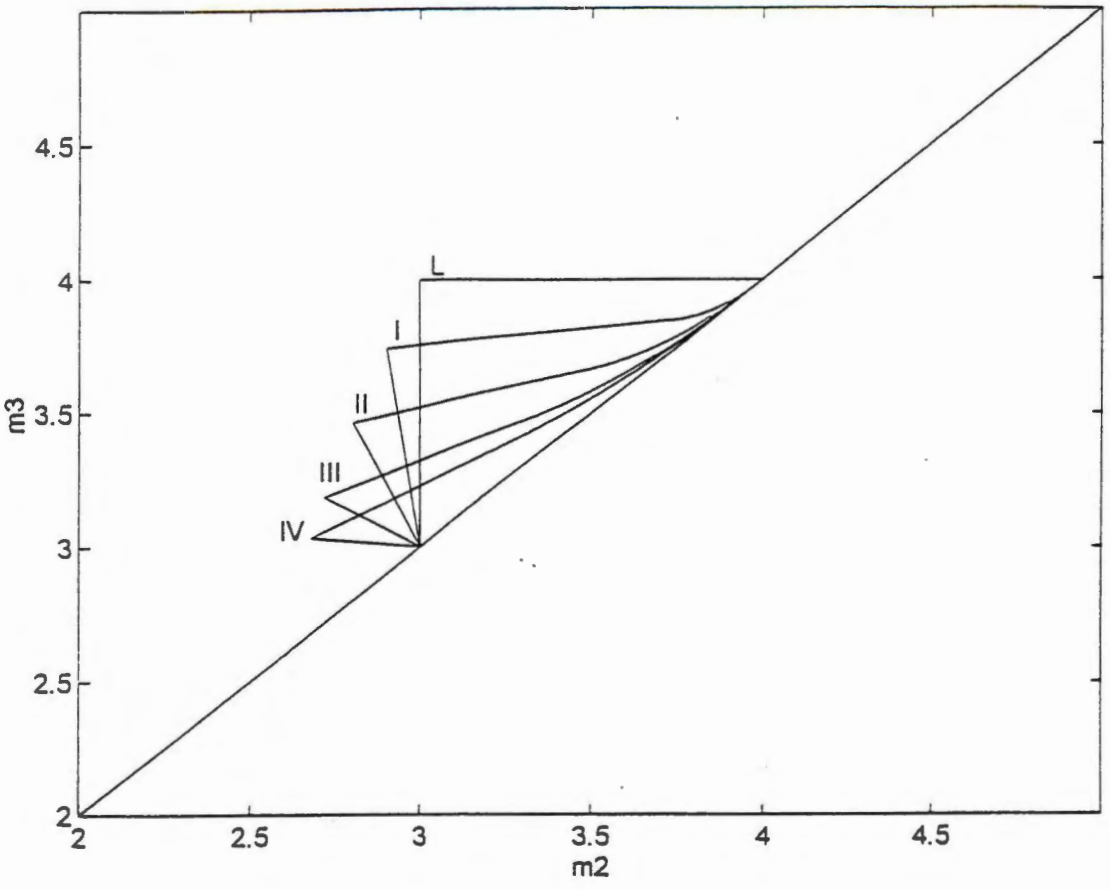


Figure 6-2: Effect of Increasing Feed Concentration on the Complete Separation Zone in the (m_2 , m_3) Plane. qs_1 = 46.58 g/l, qs_2 = 49.75 g/l, b_1 = 0.0644 l/g, b_2 = 0.0804 l/g, $c_{f1} = c_{f2} = c_{ftot}$ / 2. (L): c_{ftot} = 0.02 g/l, (I) :c_{ftot} = 1 g/l, (II): c_{ftot} = 2.5 g/l, (III): c_{ftot} = 5 g/l, (IV): c_{ftot} = 7.5 g/l

qs_i, b_i being the saturation capacity and the capacity factor respectively for component i

determined accurately for a concentration range which includes the anticipated feed concentration. Second, the feed concentration and an "arbitrary" switching time (t^*), have to be carefully chosen. Regarding the switching time selection, it is noteworthy that for better production rate, small values are preferred, however small t^* leads to higher flow rates. Therefore, there is a lower limit for t^*, set according to the maximum pressure, and / or, the maximum flow rate allowed. Furthermore, short t^* would, usually, increase "the wear and tear" on the electro-valves, increasing, by the same token, the cost for maintenance over time. On the other hand time needed to reach steady state is proportional to t^*. Accordingly, the "arbitrary" choice of t^* has to take all these factors into account. The next step involves the selection of m_1 and m_4 which need to fulfill the inequalities mentioned above. Finally, the (m_2 , m_3) diagram is plotted, then m_2 and m_3 are selected so that the operating condition point lays inside the separation triangle. That point need to be as close as possible to the vertex, yet far enough to assure robustness, which can be achieved, only at the expense of separation performance (Mazzotti et al., 1997).

VI-3 Experimental Results

Following the procedure outlined above, we attempted to optimize PP enantiomer separation using our SMB system, with the eight column setting. Except for column # 16, which became defective, and was replaced by column

15, all the columns used were from the run under linear conditions (see Table 4-5, chapter IV). However, as suggested in paragraph IV-3-1, the columns needed to be retested before the SMB run, so to assess any drift in their characteristics, and take such drifts into account when determining SMB operating conditions. Table 6-1 shows the characteristics of the eight retested columns, which were used in the SMB run. By comparing the column characteristics in Table 6-1, with the same characteristics in Table 4-5 (showing basically the same columns, see above), we can see why it is of critical importance to check, periodically, the SMB columns. Such comparison generated some expected, and some unexpected results. For example, we expect that, after six months of use (elapsed period between the two tests), retention times would decrease. Such expectation may be based on the likelihood that the chromatographic bed inside the column, under constant pressure during the runs, would shrink over time. Moreover, it is conceivable that some packing material may leach out during repetitive runs. Such phenomena might be behind the decrease in both t_1 and t_2 by more than 0.6 min (36 s) (compare t_1 and t_2 in Tables 4-5, and 6-1). On the other hand, those same phenomena, if true, would cause t_0 (and the porosity ϵ) to increase, since the shrinkage of the chromatographic bed would result in an increase of the void volume; thus, of t_0. Surprisingly, while our t_1 and t_2 decreased, so did t_0, and this was the unexpected result. In any case, the characteristics exhibited in Table 6-1 were the ones considered, when determining the SMB operational conditions.

Table 6-1 : Characteristics for the 8 Closest Columns Obtained with PP

Experimental Conditions : : Mobile Phase = Hexane 95 : Ethyl-Acetate 05 (v/v), Flow Rate = 2.5 ml/min
Detection at 270 nm, Vinj = 20 ul

Col. #	t_0 (min)	t_1 (min)	k'_1 [a]	t_2 (min)	k'_2 [a]	Alpha (α) [b]	Porosity (ε)	F [c]
1	4.56	10.10	1.21	12.04	1.64	1.35	0.726	0.378
2	4.56	9.84	1.16	12.02	1.64	1.41	0.725	0.379
3	4.59	9.77	1.13	11.68	1.55	1.37	0.730	0.370
4	4.42	9.71	1.20	11.55	1.61	1.35	0.703	0.423
7	4.49	10.28	1.29	12.13	1.70	1.32	0.715	0.399
12	4.59	10.33	1.25	12.19	1.66	1.32	0.730	0.370
14	4.65	10.08	1.17	12.01	1.58	1.36	0.740	0.351
15	4.62	9.88	1.14	11.72	1.54	1.35	0.734	0.361
Mean	**4.56**	**10.00**	**1.19**	**11.92**	**1.62**	**1.35**	**0.725**	**0.379**
STD [d]	**0.07**	**0.23**	**0.06**	**0.23**	**0.06**	**0.03**	**0.012**	**0.023**
RSD [e] (%)	**1.62**	**2.34**	**4.68**	**1.96**	**3.44**	**2.15**	**1.62**	**5.97**

(a) $k'_1 = (t_1 - t_0) / t_0$
(b) $\alpha = k'_2 / k'_1$
(c) Phase ratio = $(1-\varepsilon) / \varepsilon$
(d) Standard Deviation
(e) Relative Standard Deviation
RSD = (STD / mean)*100

For the adsorption isotherms the results obtained in chapter V were used. In that chapter, we showed that the simple competitive Langmuir model accounted well for the adsorption behavior of PP enantiomers on our CSP (Chiracel OB). Such results allowed us to fully take advantage of the "triangle theory" approach, which, as mentioned earlier, has been mainly developed for systems exhibiting Langmuirian type adsorption behavior. Among the results of chapter V, the ones of interest to the current section are summarized in Table 5-3 (adsorption isotherm parameters). We opted for the parameters derived from the combined single component and competitive data (third row of Table 5-3): a_1 = 2.97, b_1 = 0.0644 l/g, a_2 = 3.96, b_2 = 0.0804 l/g (a_i being the Henry'coefficient, and b_i the capacity factor of component i).

Preliminary experiments showed that 5 g/l was an appropriate total feed concentration (ie Cf1 = Cf2 = 2.5 g/l), well within the concentration range of the adsorption isotherm study. The switching time was first assigned a value of 580 seconds. With the feed concentration and the switch time set, we needed to select values for m_1 and m_4 which would fulfill their respective requirement : lower limit for m_1 and upper limit for m_4 . The lower limit for m_1, if one recalls, was simply a_2 (here equal to 3.96), therefore a value of 4 was assigned to m_1, and kept constant, while the (m_2 , m_3) plane was exploited for optimal conditions. For m_4, the upper limit could be computed using equation (6-5). In the present case, m_{4cr} was determined to be equal to 2.686, consequently a value (kept constant) of 2.5 was assigned to m_4. After trying various operating conditions, using the (m_2

, m_3) plane, we decided to carry out an SMB run with conditions corresponding to $m_2 = 2.85$ and $m_3 = 3.15$. Such conditions correspond to the "point-circle" inside triangle A (representing the predicted complete separation zone for our experiment), shown in Figure 6-3. Triangle L, corresponding to the linear case, was added to the figure for comparison sake, and for illustration of the non-linear nature of our experiment. The position of the "point-circle" seems to be an adequate compromise between performance parameters (here mainly purity and PR), and robustness. The SMB experimental conditions, derived from the above procedure, are summarized in Table 6-2.

After steady state was reached, outgoing streams (raffinate, extract, and recycle) were collected over a super-cycle (ie eight switching times), then analyzed on the HP1090 chromatograph. The analytical column (25cm x 0.46 cm Chiracel OB-H, 5μ) was used. The flow rate was set to 1.0 ml/min, the mobile phase was a 95:5 (v/v) mixture of HPLC-grade hexane and ethyl-acetate. The results of the analytical analysis are shown in Figure 6-4. A very good separation was obtained. The raffinate stream displayed a purity >98% , while the extract stream exhibited a purity > 95%. Such purity values may be considered as satisfactory, especially, if the aim is to work with optimal PR. Trying to improve those values will, indeed drastically reduce the PR and the recovery yield of one, or both products.

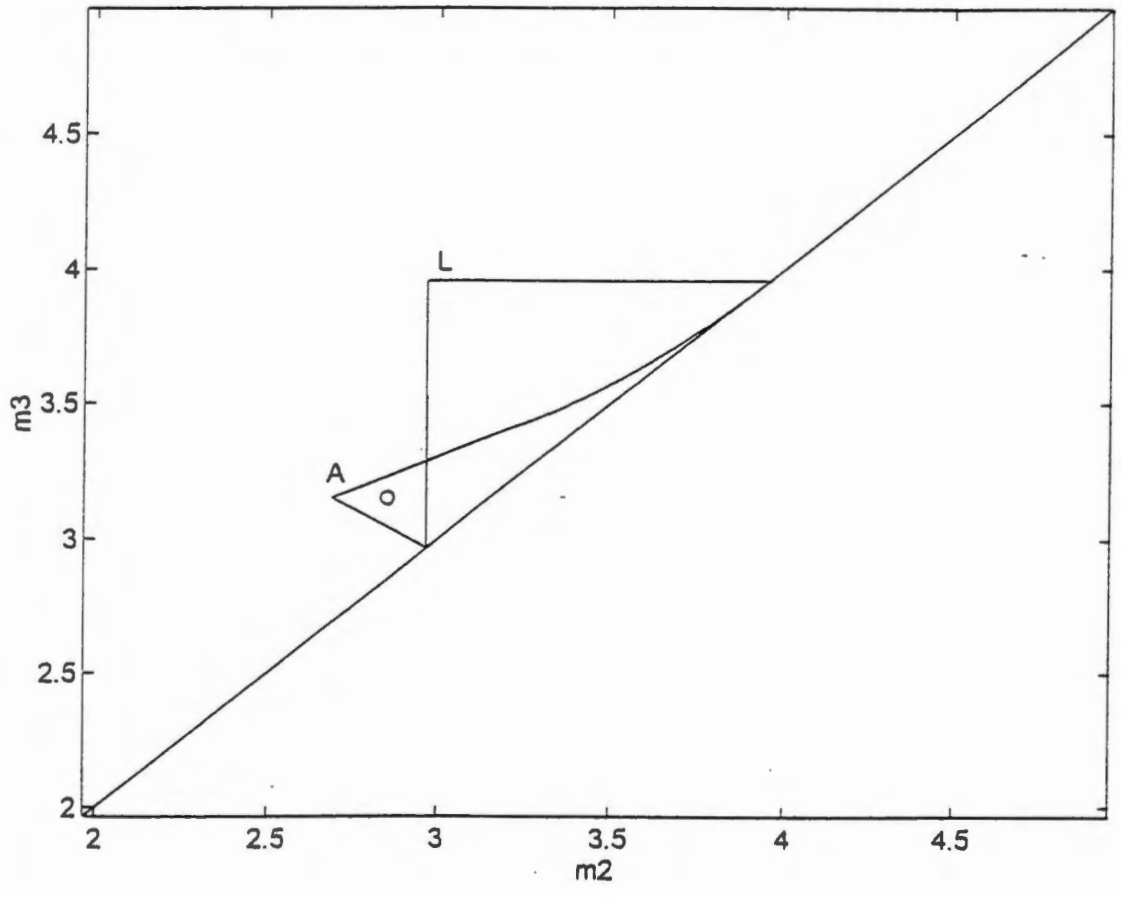


Figure 6-3 : Separation Zone for PP Enantiomers in the (m_2 , m_3) Plane.
qs_1 = 46.05 g/l, qs_2 = 49.23 g/l, b_1 = 0.0644 l/g, b_2 = 0.0804 l/g, C_{ftot} = 5 g/l.
m_1 = 4, m_2 = 2.85, m_3 = 3.15, m_4 = 2.5

Triangle A: Separation zone for our experiment

Triangle L: Separation zone for the linear case

Table 6-2:SMB Experimental Conditions for PP Enantiomer Separation under Non-linear Conditions

Total Feed Concentration = 5 g/l

Q_f	Q_d	Q_r	Q_e	Q_I	Q_{II}	Q_{III}	Q_{IV}	Switch time
0.14	0.71	0.31	0.54	3.11	2.56	2.7	2.4	558 then 580s

Q_f: Feed Flow rate (ml / min)

Q_d: Desorbent Flow rate (ml / min)

Switch time: Switching time in seconds

Q_r: Raffinate Flow rate (ml / min)

Q_e: Extract Flow rate (ml / min)

Q_j (j = I, II, III, IV): Flow rate (ml / min) in section j

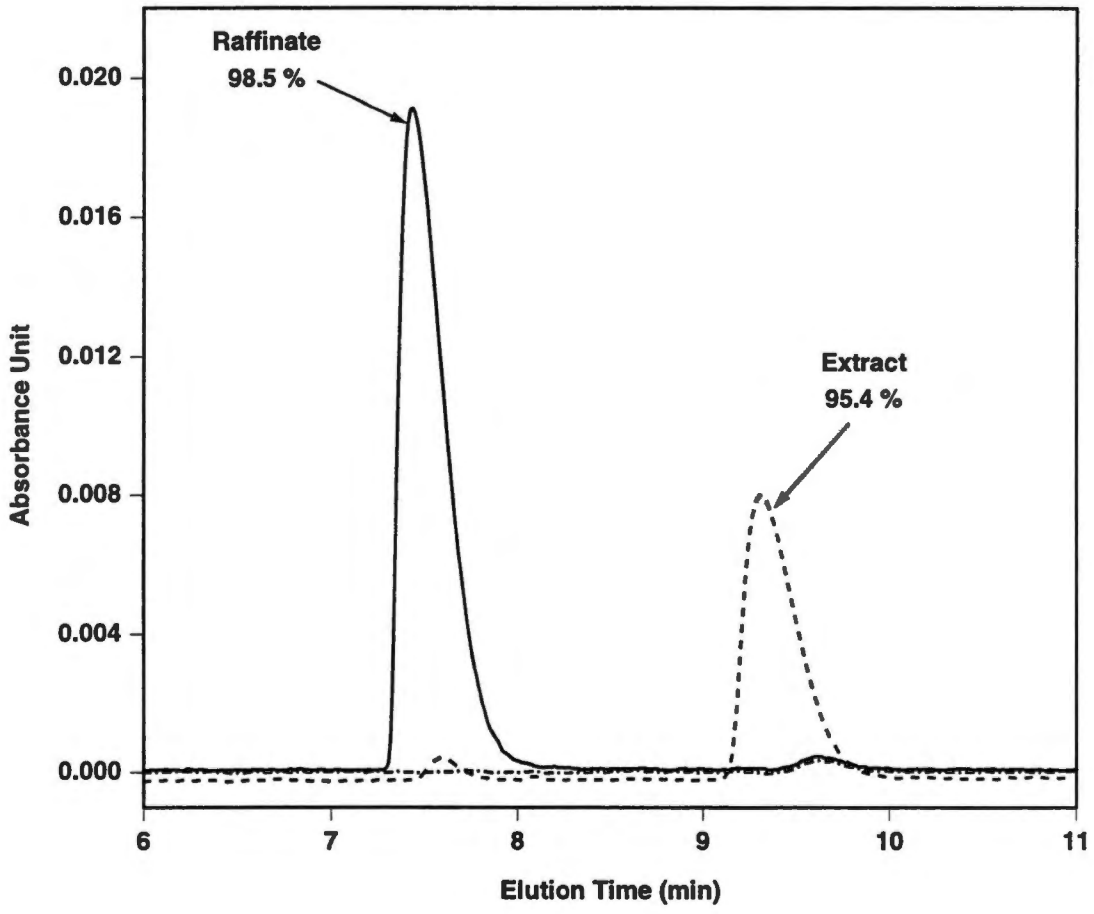


Figure 6-4: Analytical Chromatograms for Samples Collected During PP Enantiomer Separation by SMB under Non-linear Conditions (see Experimental Conditions in Table 6-2, Total Feed Concentration = 5 g/l).

Solid Line: Raffinate Dashed Line: Extract

Dashed-Dotted Line: Recycle

Analytical Conditions: Column: 25 x 0.46 cm I.D. Chiracel OB-H, V_{inj} = 50µl
Mobile Phase: Hexane 95 : Ethyl-Acetate 05, FR=1 ml/min,
Detection at λ = 270 nm

Given the choice of our operating conditions, well within the separation zone (triangle A, Figure 6-3), these results seem discordant with the expected total separation. This may be related to some inaccuracy in the adsorption isotherm determination, to the non-ideal behavior of the chromatographic system, and / or, to some flow rate fluctuations. Such parameters, have a significant influence on the shape and position of the separation triangle, especially under overloading conditions (Mazzotti et al.,1997).

Finally, the daily production rates, of both the raffinate and the extract, were computed. The concentration of each stream was determined using a calibration curve at the 270 nm wavelength, then the concentrations were converted to amounts produced per day, and per day per kilogram of stationary phase. The results are reported in Table 6-3. Overall, a PR of more than 11.6g of PP products/day/kg of CSP was achieved, which might be considered as respectable, given the size of our SMB unit. A slight difference can be observed between the raffinate and the extract PR (6.27 g/day/Kg of CSP versus 5.42 respectively). This difference can be explained by the fact that the raffinate purity was higher, yielding a higher PR (which was calculated only for the pure fraction of the stream, and did not include the other polluting component).

In conclusion, it seems possible to determine rather quickly, operating parameters for an SMB run under non-linear conditions, using the triangle theory approach. However, such method required accurate adsorption isotherm parameters, and well characterized columns. The biggest shortcoming of this

Table 6-3: Production Rate of Raffinate and Extract Produced During PP Enantiomer Separation by SMB under Non-linear Conditions (Total Cf = 5 g/l)

	Flow rate		Concentration	Production rate[2]	
Product	**ml/min**	**ml/day**	**C[1](g/L)**	**g/day**	**g/day/kg of CSP[3]**
Raffinate	0.31	446.4	1.237	0.552	6.27
Extract	0.54	777.6	0.614	0.477	5.42
Total	*	*	*	1.029	11.69

(1) Determined from calibration curve at 270 nm
(2) PR calculated without including impurities
(3) Chiral Stationary Phase

approach, seems to be its limitation to systems exhibiting Langmuirian type adsorption behavior. It will be interesting to see how, this technique can be altered, to allow its use with other systems. Using this technique, we were able to separate PP enantiomers under "severe" overloading conditions, generating satisfactory purity, and more than decent daily PR.

Chapter VII

Investigation of Antimicrobial Activity of 1-phenyl-1-propanol Enantiomers

VII-1 Introduction

Flavor compounds are added to food, primarily for their flavor profile, and for their ability to confer the desired flavor to the supplemented product. Any other benefit, such as antimicrobial activity, would; in fact, be nothing but a welcomed bonus. Indeed, if a compound can exhibit antimicrobial activity, while it is added as flavoring agent, it will surely help in preserving the food product, and may even increase its shelf life. Therefore, the use of food preservative(s) might be reduced, or even eliminated through dual use of flavoring compounds.

Several food flavoring compounds, both natural and synthetic, have been reported to exhibit antimicrobial activity. Jay and Rivers (1984) tested twenty one flavor compounds, and found that eleven were effective antimicrobials, at various degrees, against forty different organisms, gathered in four different groups (lactic bacteria, Gram positive non-lactic bacteria, Gram negative bacteria, and fungi). Diacetyl (2,3-butanedione), and eugenol were among the most effective compounds. Others included carvone, ethyl-vanillin, maltol, menthol, phenyl-

acetic acid, phenyl-acetaldehyde, 2-3-pentanedione and vanillin. Cuong et al.(1994) investigated the antimicrobial activity of various constituents of Vietnamese cajuput oil, among which, several are actual flavor compounds. They reported that S-(+)-linalool displayed the most effective antimicrobial activity. Other components displayed such activity, but are less effective, among them were R-(-)-1-terpinen-4-ol, 1,8-cineole and (±)-α-terpineol. Similar results were obtained by Carson and Riley (1995), when they studied the effects of tea tree oil components on a wide range of microorganisms. Those authors reported that, terpinen-4-ol was active against all assayed microorganisms, while linalool, α-terpineol, and terpinolene inhibited all organisms, except *Pseudomonas aeruginosa*. Finally, two other components of tea tree oil (ρ-cymene and γ-terpinene) did not exhibit any antimicrobial activity.

Several methods are available for the screening of antimicrobial activity. According to Rios et al. (1988), screening methods can be classified into three groups: diffusion, dilution and bioautographic methods. Diffusion methods include agar-overlay technique, where a disk (a hole, or a cylinder), used as reservoir which contains the tested chemical, is brought to contact with a medium inoculated with the assayed microorganism (Rios et al., 1988). After the incubation period, the inhibition diameter (clear zone around the reservoir) is measured. Evidently, the larger the inhibition diameter, the more effective the chemical would be. This technique has the advantage of not requiring homogeneous dispersion in water (Rios et al., 1988). Dilution techniques, on the

other hand, require homogenous dispersion in water (often facilitated with the use of surface-active agents), and are mostly used to determine the minimum inhibitory concentration (MIC). The turbidity of the solution is measured over time, and is taken as indication of bacterial growth (Rios et al., 1988). An increase in the turbidity value, over time, is a sign of ineffectiveness (relative or total) of the chemical to inhibit growth. This type of techniques can also be used in combination with the first type, to determine the MIC for chemicals, already proven to be effective with the first method. Finally, the biautographic methods are, typically, based on agar-diffusion technique, where the tested chemical is transferred from a chromatographic layer (either paper, or thin layer) to an agar plate inoculated with the assayed microorganism (Rios et al., 1988).

Diffusion methods are the most widely used in screening for antimicrobial activity. Such technique was used in all three studies previously cited (Jay and Rivers, 1984; Cuong et al., 1994; Carson and Riley, 1995). We used the paper disc diffusion version of this same technique, to screen for 1-phenyl-1propanol (PP) antimicrobial activity, and to investigate any potential difference among the three forms (S, R, and racemic). To our knowledge, PP has not been screened for such activity, nor has a comparative study of antimicrobial activity, among all three forms, been systematically conducted.

VII-2 Experimental Set-up

VII-2-1 Chemicals, Microorganisms and Culture Media

Chemicals

Before screening for their antimicrobial activity, the two PP enantiomers, produced by SMB, were completely freed from the solvent. The concentration process was carried through evaporation, following the procedure described in paragraph IV-2-3. The concentrated products were, then, transferred to screw-cap vials and kept, along with an equivalent amount of the purified racemic, under refrigeration until needed.

Microorganisms

Five bacteria (among the most common pathogenic bacteria) and three fungi (two molds and one yeast) were selected for this study. The bacteria were *Escherichia coli O157:H7* (ATCC 35150, isolated form apple cider), *Listeria monocytogenes* (ATCC 0398), *Pseudomonas aeruginosa* (ATCC 9027), *Salmonella enteritidis* (unknown origin) and *Staphylococcus aureus* (ATCC 12600). The two molds used were *Aspergillus niger* (UT stock culture) and *Geotrichum candidum* (ATCC 34614), while the only assayed yeast was *Rhodotorula glutinus* (ATCC 32765).

Culture Media

For all five bacteria, the standard method agar (SMA) (Difco, Detroit, MI),

a non-selective medium, was used. SMA was supplemented, after autoclaving (and cooling), with 100 ppm of 2,3,5,triphenyl tetrazolium chloride (TTC) (J.T. Baker, Philipsburg, NJ), to differentiate the colonies better, and clarify the inhibition zone (Elggayar, 1999). For the three fungi, two media were used: SMA and potato dextrose agar (PDA) (Difco, Detroit, MI).

VII-2-2 Procedure

Prior to the screening tests, the assayed bacteria were checked for viability, then transferred twice (each time after 24 hour growth) to brain heart infusion (BHI) tubes for revival and recovery. None of the bacterial culture, used to streak the SMA plates, was more than 24 hour old. Similar viability tests were performed for the fungi, however, the transfer period was of three days each time, instead of only one day.

Once the cultures were revived, they were used to streak SMA plates (and the PDA plates for fungal culture), until their whole surfaces were covered. Then a sterile 6 mm diameter filter paper disc (Difco, Detroit, MI) was placed in the center of each inoculated plate. A drop (20 µl), of one of the three investigated chemicals, or the control (S-PP, R-PP, racemic PP, or sterilized water for control), was deposited on that disc. After waiting 30 minutes, to allow the chemicals to diffuse, the plates were inverted and incubated at the appropriate temperature (35^{0}C for *Escherichia coli* and *Salmonella*, 32^{0}C for the

other bacteria and 30°C for fungal cultures). After the incubation period (24 hours for bacteria and 72 hours for fungi), the diameter of inhibition, around the paper disc, was measured in millimeters (mm). All tests were done in triplicate. Statistically, the data were fitted to a completely randomized design (CRD) with factorial treatment arrangement. The type of microorganism, the nature of the chemical, and their combination were the tested fixed effects. Analysis was performed using PROC MIXED of SAS version 6.12 (SAS Institute,1996).

VII-3 Results and Discussion

VII-3-1 Effect of PP Products on Bacteria

Illustrations showing inhibition diameter of the five investigated bacteria, around PP products on , is shown in Table 7-1. For comparison, each row displays values reflecting the effectiveness of a given chemical on each bacterium. On the other hand, columns, show the differences, if any, in sensitivity of a given microorganism to the three PP products. The inhibition diameter (in mm) for control (sterilized water), for all five bacteria, were equal to zero. Table 7-1 shows clearly that all PP products exhibit a relatively strong antimicrobial activity against all assayed bacteria. However, the degree of effectiveness varied depending on the microorganism. Among the studied bacteria, *Pseudomonas aeruginosa (PA)* was the least sensitive, regardless of the chemical. Cuong et

Table 7-1: Effect of PP Products on 5 Different Bacteria

Chemical	Microorganism				
	E. C.	*L. M.*	*P. A.*	*S. E.*	*S. A.*
Control	NI[(a)]	NI[(a)]	NI[(a)]	NI[(a)]	NI[(a)]
RACEMIC	28.3[(b)] β[(c)]	24 δ	20.3 ε	25.7 χδ	38 α
S-PP[(d)]	25 χδ	25.3 χδ	20 ε	27 βχ	40 α
R-PP[(d)]	24.7 δ	24.7 δ	19.7 ε	26 χδ	40 α

(a) No Inhibition

(d) S & R-1-phenyl-1-propanol

(b) Inhibition Diameter in mm, including the paper disc. Reported values are the average of 3 measurements.

(c) Values followed by different greek letters were significantly different ($P < 0.05$)

E. C.: Echerichia coli O157:H7 *L. M.: Listeria monocytogenes* *P. A.: Pseudomonas aeruginosa*

S. E.: Salmonella enteritidis *S. A.: Staphylococcus aureus*

Note: for each inhibition zone the smallest value that could be measured was 1 mm, the numbers behind the decimal point reported above were the results of averaging 3 measurements each time.

al.(1994), and Carson and Riley(1995), while working with completely different chemicals, reported similar results, where *PA* was also the least sensitive. This type of results suggests that *PA* might have developed a more elaborated defense mechanism, or resistance system than the other investigated bacteria. On the other hand, *Staphylococcus aureus (SA)* was the most sensitive of all bacteria, regardless of the chemical type. The effectiveness of the two active forms (R-PP and S-PP) did not significantly differ (P>0.05) among the remaining three bacteria (*Escherichia coli O157:H7, Listeria monocytogenes (LM),* and *Salmonella enteritidis (SE)*); however, for the racemic mixture *Escherichia coli O157:H7* (*EC*) was significantly more sensitive (P<0.05) than both *LM* and *SE* (Table 7-1, first row).

Vertical, or intra-column comparisons in Table 7-1, (where effectiveness can be compared among the three chemicals for a given bacterium) did not reveal significant difference (P>0.05) for the enantiomers, for any of the assayed bacteria, except for *EC*, where the racemic mixture was found to be significantly more effective (P>0.05) than the two active forms. Although statistically significant (24 versus 28 mm), this small difference has little practical meaning. Such results suggest that, in general, the mechanism of bacteria inhibition by PP may be independent of optical activity.

Figure 7-1 shows a photograph illustrating the effect of PP on the five bacteria used in this study. For simplicity, only one plate per microorganism is shown (and one plate for the control) regardless of the type of chemical, since



Figure 7-1: Illustration of the Effect of PP Products on 5 Bacteria

The clear zones around the plate centers represent the inhibition zones.

the results were not significantly different ($P>0.05$) within a given microorganism.

VII-3-2 Effect of PP Products on Fungi

The results generated from the investigation of PP on the growth of three fungi are summarized in Table 7-2. As in Table 7-1, the effectiveness of a given chemical can be compared among the organisms by comparing numbers of a same row. Likewise, the effects of the three chemicals on a given fungus can be compared by comparing numbers in the same column.

Table 7-2 shows that for both SMA and PDA, the three fungi differed significantly ($P<0.05$) in their sensitivity to PP products, regardless of the chemical type. The yeast (*Rhodotorula glutinus*) was the least sensitive among the three investigated fungi with either media. In fact, *Rhodotorula glutinus* (*RG*) was not inhibited when grown on PDA. For the two molds (*Aspergillus niger* and *Geotrichum candidum*), the order of sensitivity was, somehow, reversed when the growth medium was changed. As shown in Table 7-2, *Geotrichum candidum* (*GC*) was more sensitive on SMA, generating larger inhibition diameters for all three chemicals, while *Aspergillus niger* (*AN*) was more sensitive when PDA was used. For every combination "microorganism / chemical" (except for AN / racemic and AN / S-PP), the zone of inhibition was significantly ($P<0.05$) smaller when PDA was used as growth medium. However, even with such a highly nutritive medium, the inhibition zones were sizeable for the two molds, suggesting a very

Table 7-2: Effect of PP Products on the Growth of 3 known Fungi

Medium	Chemical	Microorganism		
		Aspergillus niger	*Geotrichum candidum*	*Rhodotorula glutinus*
SMA [e]	Control	NI[a]	NI[a]	NI[a]
	RACEMIC	40[b] $\beta\chi$ [d]	56 α	18 γ
	S-PP[c]	40 $\beta\chi$	54 α	20.3 $\phi\gamma$
	R-PP[c]	42.3 β	53.7 α	19.3 γ
PDA [f]	Control	NI[a]	NI[a]	NI[a]
	RACEMIC	37 χ	27.3 $\delta\varepsilon$	NI[a]
	S-PP[c]	37.7 χ	24.3 $\varepsilon\phi$	NI[a]
	R-PP[c]	36.3 χ	29.7 δ	NI[a]

(a) No Inhibition
(b) Inhibition Diameter in mm, including the paper disc. Reported values are the average of 3 measureme
(c) S & R-1-phenyl-1-propanol
(d) Values followed by different greek letters were significantly different ($P < 0.05$)
(e) Standard Method Agar
(f) Potato Dextrose Agar

Note: for each inhibition zone the smallest value that could be measured was 1 mm, the numbers behind the decimal point reported above were the results of averaging 3 measurements each time.

strong antifungal activity for PP in all three forms. These findings suggest that several culture media should be assayed, when evaluating inhibition zones of chemicals which may be antimicrobial.

Table 7-2 shows that, except for *GC* grown on PDA, there was no significant difference(s) ($P>0.05$) in effectiveness among the three forms of PP, regardless of the microorganism and / or the culture medium (intra-column comparisons). For *GC* a slight, but significant difference ($P<0.05$), was detected between R-PP (ID = 29.67 mm) and S-PP (ID = 24.33 mm), while the racemic was not significantly different ($P>0.05$) from either.

The results discussed above can also be illustrated by Figure 7-2, and Figure 7-3. Figure 7-2 is a photograph that shows the three fungi growing without inhibition, where the paper disc was covered with sterilized water only. Such figure was incorporated here to allow an easy comparison with plates exhibiting inhibition zones, such as the ones in Figure 7-3. As in Figure 7-1, only one plate per microorganism is shown in Figure 7-3 since no difference was detected among the three chemicals (except for R-PP and SPP effect on *GC*). In Figure 7-3, it is interesting to note that, for both *AN* plates (SMA and PDA), and for *GC*, PDA plate, one can distinguish between two different inhibition zones. The first zone (CIZ, or complete inhibition zone) is a clear one, reflecting total inhibition, and a second one, slightly bigger (SIZ, or sporulation inhibition zone), placed around the first zone. In this second zone the microorganisms were able to grow, but not to sporulate, suggesting that PP products can at least inhibit sporulation,

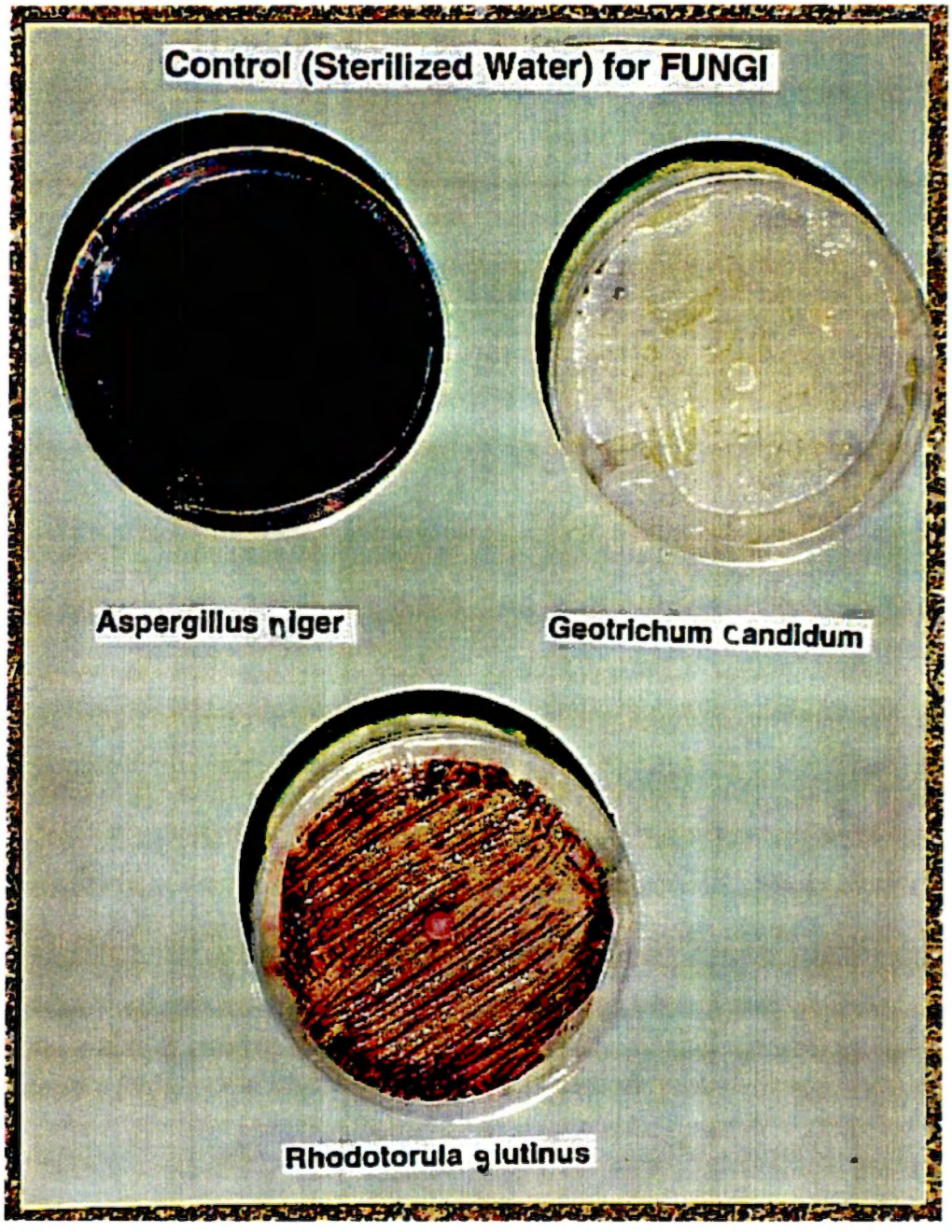


Figure 7-2: Controls (Sterilized Water) for the 3 Fungi

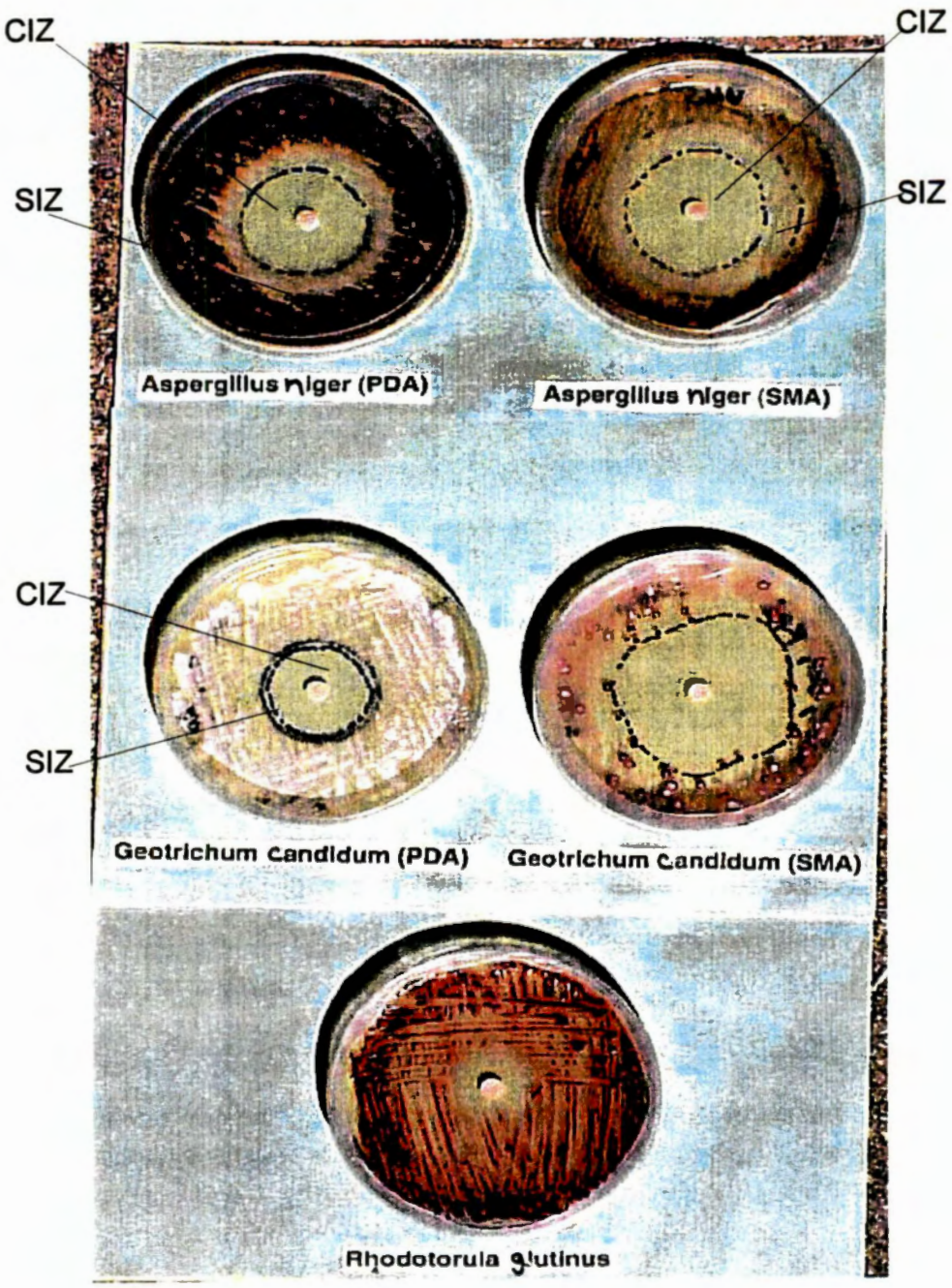


Figure 7-3: Illustration of the Effect of PP Products on 3 Fungi Grown on 2 Different Media

CIZ : Complete Inhibition Zone

SIZ : Sporulation Inhibition Zone

if their concentration use is too small to allow total inhibition. Inhibition of sporulation is very significant in fungi, since spores are essential for propagation of new fungi.

VII-4 Conclusion

As mentioned previously, the primary use of PP is flavoring. The fact that PP exhibited strong antimicrobial activity suggests it might help in reducing, or even eliminating the use of preservatives in products to which it is added. This dual functionality has a potential impact on both the economical aspects, and on the consumer attitude, where labels, such as "No preservative added", can often be a great buying incentive. However, first more studies are needed to evaluate the antimicrobial activity of PP within a food matrix.

The investigation of potential differences between the two enantiomers, did not show any significant difference in antimicrobial activity. Our initial hypothesis that enantiomers may show different levels of antimicrobial activity was disproven. Therefore, the least expensive of the three products (ie the racemic) should be used in future antimicrobial studies, which should be preceded by studies of the mutagenicity of PP. Reporting results, including negative ones, may encourage other workers to investigate other enantiomers of antimicrobial compounds. It would be interesting, also to investigate the minimum inhibitory concentration (MIC) for PP. Unfortunately, we were not able

to run such an experiment, because of time constraint and unavailability of large quantities of PP.

Chapter VIII

Summary and General Conclusions

In this study, simulated moving bed technology (SMB), and its suitable status with regard to enantiomer separation, has been evaluated. SMB has been shown to offer an array of advantages over conventional batch chromatography, such as a better use of the chromatographic bed, higher yield and purity for the recovered products, and most importantly, a tremendous saving in the volume of mobile phase. However, SMB, also, has a critical disadvantage, in its restriction to binary mixture separation. Fortunately, such a drawback vanishes, when SMB is applied to enantiomer separation.

Using a lab-scale SMB with eight column setting, we were able to separate enantiomers of three different flavor compounds (with three different separation factors), under linear conditions. The approach, based on the use of safety factors, was applied to determine, rather quickly and successfully, the appropriate experimental parameters for those separations. When the conditions were advanced to non-linear, the "triangle theory" approach, was used instead. Such approach seems to be a very useful tool, not only to determine operating conditions, but also to carry out a complete optimization procedure. However, the "triangle theory" seems to be limited to systems with Langmuirian adsorption

behavior, which, apparently, is hindering its use on a broader level.

For the adsorption isotherm study, the most important result we have obtained, may be the excellent agreement between parameters derived from single component data, and the parameters derived from the competitive ones. Such result suggests that isotherm parameters may be derived from measurements made **ONLY** with racemic mixture, allowing major savings in time and money for the determination of those critical competitive isotherm data, required for the successful modeling of enantiomeric separations. Furthermore, in many instances, either only the racemic mixture is commercially available, or if the active forms are available, they are outrageously expensive.

Finally the screening of PP products for antimicrobial activity, revealed that all three forms exhibit strong antimicrobial activity assessed by the disc diffusion assay. This result is very important, if we consider that PP is mainly added to food for flavoring. Further investigations, are needed to determine the minimum inhibitory concentration (MIC) for PP. If the MIC is found to be within the normal range of use of PP in food, then it will help promote the use of such flavoring compound, since it will help in reducing, or even eliminating, the use of preservatives in products to which PP is added.

REFERENCES

Andrade, J. D., Ed. 1985. Surface and Interfacial Aspects of Biomedical Polymers, 60, Chapter 1, pp 35-50, Plenum Press, New York, NY.

Anonymous. 1992. FDA policy statement for the Development of New Sterioisomeric Drugs. Chirality, (4):338-340.

Anonymous. 1997. Preparative chromatographic separation of enantiomers. URL address: http://www. merck.de/chromatography/chir_502.htm.

Anonymous. 1999. U.S. Food and Drug Administration, CFSAN, Office of Premarket Approval: EAFUS a Food Additive Database. URL address: http://vm.cfsan.fda.gov/~dms/eafus.html.

Armstrong, D.W., and Han, S.M. 1988. Enantiomeric separations in chromatography. CRC Critical Reviews in Analytical Chemistry, (19) 3:175-223.

Armstrong, D.W., Chang, C.D., and Li, W.Y. 1990. Relevance of enantiomeric separation in food and beverage analyses. J. Agric. Food Chem., (38):1674-1677.

Bauer, K., and Garbe, D. 1985. Common Fragrance and Flavor Materials: Preparation, Properties and Use. VCH Publisher, Deerfield Beach, FL.

Boelens, M.H., Boelens, H., and Van Gemert, L.J. 1993. Sensory properties of optical isomers. Perfumer and flavorist, (18) 6:1-16.

Broughton,D.B., and Gerhold, C.G. 1961 US Patent 2,985,589, May 23, 1961.

Carson, C.F., and Riley, T.V. 1995. Antimicrobial activity of the major components of the essential oil of Melalenca alterifolia. Journal of Applied Bacteriology (78):264-269.

Charton, F., Jacobson, S.C., and Guiochon, G. 1993. Modeling of the adsorption behavior and the chromatographic band profiles of enantiomers. Behavior of methyl mandelate on immobilized cellulose. J. Chromatography, (630):21-35.

Charton, F., Bailly, M., and Guiochon, G. 1994. Recycling in preparative liquid chromatography. J. Chromatography A, (687):13-31.

Chen,Y., Kele, M., Sajonz, P., Sellergren, B., and Guiochon, G. 1999. Influence of thermal annealing on the thermodynamic and mass-transfer kinetic properties of D- and L-phenylalanine anilide on imprinted polymeric stationary phase. Anal. Chem., (71):928-938.

Cherrak, D.E., Khattabi, S., and Guiochon, G. 1999. Adsorption behavior, and prediction of the band profiles of 3-chloro-1-phenyl-1propanol. Influence of the mass transfer kinetics. Submitted to the J. Chromatography A.

Cherrak, D.E. 1999. Personal discussion.

Ching, C.B., Lim, B.G., Lee, E.J.D., and Ng, S.C. 1993. Preparative resolution of praziquantel enantiomers by simulated counter-current chromatography. J. Chromatography, (634):215-219.

Cuong, N.D., Xuyen, T.T., Molt, O., Stransky, K., Presslova, J., Jedlickova, Z., and Sery, V. 1994. Antibacterial properties of Vietnamese cajuput oil. J. Essential Oil Res., (6):63-67.

Dufosse, L., Latrasse, A., and Spinnler H.E. 1994 Importance des lactones dans les aromes alimentaires: structure, distribution, propriétés sensorielles et biosynthese. Science des aliments, (14):17-50.

Elgayyar, M. 1999. Master 's Dissertation. Antimicrobial Activity of Essential Oils from Herbs and Spices, and Application of Black Cumin to Rainbow Trout Fillet. Department of Food Science and Technology, University of Tennessee.

Felinger, A., and Guiochon, G. 1994. Optimizing experimental conditions for minimum production cost in preparative chromatography. AIChE Journal, (40) 4:594-604.

Fornstedt, T., Zhong, G., Bensetiti, Z., and Guiochon, G. 1996. Experimental and theoretical study of the adsorption behavior and mass transfer kinetics of propanolol enantiomers on cellulase protein as the selector. Anal. Chem., (68): 2370-2378.

Fornstedt, T., Sajonz, P., and Guiochon, G. 1997. Thermodynamic study of an unusual chiral separation: Propanolol enantiomers on immobilized cellulase. J. Am. Chem. Soc., (119):1254-1264

Francotte, E.R. 1993. Preparative Chromatographic Resolution of Racemates. pp 35-53. In Simulated Moving Bed: Basics and Applications, European Meeting, I.N.P.L, Nancy, France.

Francotte, E.R., and Richert, P. 1997. Applications of simulated moving-bed chromatography to the enantiomers of chiral drugs. J. Chromatography A, (769):101-107.

Francotte, E.R., Richert, P., Mazzotti, M., and Morbidelli, M. 1998. Simulated moving bed chromatographic resolution of a chiral antitussive. J. Chromatography A, (796):239-248.

Furia, T.E., and Bellanca, N. 1971. Fenaroli's Handbook of Flavor Ingredients. 2nd Edition. CRC Press Publisher.

Ganestos, G., and Barker, P.E. 1993. Preparative and Production Scale Chromatography. Chromatographic Science series, volume 61. Marcel Dekker Inc., New York, NY.

Guichard, E, Kustermann, A., and Mosandl, A. 1990. Chiral flavor compounds from apricots. Distribution of γ-lactone enantiomers and stereo-differentiation of dihydroactinidiolide using multi-dimensional gas chromatography. J. Chromatography, (498): 396-401.

Guiochon, G., Golshan-Shirazi, S., and Katti, A.M. 1994. Fundamentals of Preparative and Nonlinear Chromatography, Academic Press, Boston, MA.

Jay, J.M. , and Rivers, G.M. 1984. Antimicrobial activity of some food flavoring compounds. J. Food Safety, (6):129-139.

Jacobson, J., Frenz, J.H., and Horváth, Cs. 1987. Measurement of competitive adsorption isotherms by frontal chromatography. Ind. Eng. Chem. Res., (26):43-50.

Jacobson, S.C., Golshan-Shirazi, S., and Guiochon, G. 1990. Chromatographic band profiles and band separation of enantiomers at high concentration. J. Am. Chem. Soc., (112):6492-6498.

Jacobson, S.C., Golshan-Shirazi, S., and Guiochon, G. 1991. Isotherm selection for band profile simulations in preparative chromatography. AIChE Journal, (37) 6:836-844.

Karl,V., Schumacher,K., and Mosandl, A. 1992. Enantiomeric 2-Methylbutanoates: Sensory evaluation and chirospecific analysis. Flavor and Fragrance Journal, (7):283-288.

Koppenhoefer, B., Behmisch, R., Epperlein, U., Holzschuh,H., Bernreuther, A., Piras, P., and Roussel, C. 1994. Enantiomeric odor differences and gas chromatographic properties of flavors and fragrances. Perfumer and Flavorist, (19) 5:1-14.

Küsters, E., Gerber, G., and Antia, F.D. 1995. Enatioseparation of a chiral epoxide by simulated moving bed chromatography using chiracel-OD. Chromatographia, (40):387-393.

Mazzotti, M., Pedeferri, M.P., and Morbidelli, M. 1996. Design of optimal and robust operating conditions for chiral separations using simulated moving beds. pp 103-112, Proceedings of the Chiral Europe'96 Symposium, Spring Innovations, Stockport. UK.

Mazzotti, M., Storti, G., and Morbidelli, M. 1997. Optimal operation of simulated moving bed units for nonlinear chromatographic separations. J. Chromatography A, (769):3-24.

Meena, M.R., and Sethi, V. 1994. Antimicrobial activity of essential oils from spices. J. Food Sci. Technol., (31) 1:68-70.

Migliorini, C., Mazzotti, M., and Morbidelli, M. 1998. Continuous chromatographic separation through simulated moving beds under linear and nonlinear conditions. J. Chromatography A, (827):161-173.

Migliorini, C., Gentilini, A., Mazzotti, M., and Morbidelli, M. 1999. Design of simulated moving bed units under non-ideal conditions. Ind. Eng. Chem. Res. (38):2400-2410.

Mihlbachler, K. 1999. Personal discussion.

Miyabi, K., and Guiochon, G. 1999. Analysis of surface diffusion phenomena in reversed-phased liquid chromatography. Anal. Chem., (71):889-896.

Mosandl, A., Heusinger, G., and Gessner, M. 1986. Analytical and sensory differentiation of 1-Octen-3-ol enantiomers. J. Agric. Food Chem., (34):19-122.

Mosandl, A., Braunsdorf, R., Dietrich, A., Faber, B., Karl,V., Kopke, T., Lehmann, D., and Maas, B. 1994. Recent Developments in the Authenticity Control of Flavours and Fragrances, pp 89-98. In Trends in Flavour Research, Maarse, H. (Editor). Elsevier Science B.V., New York, NY.

Mussinan, C.J. 1993. Instrumental Analysis, pp 211-224. In Flavor Science: Sensible Principle and Techniques. American Chemical Society (Publisher), Washington,D.C.

Negawa, M., and Shoji, F. 1992. Optical resolution by simulated moving bed adsorption technology. J. Chromatography, (590):113-117.

Nicoud, R.M. 1993. Simulated Moving Bed (SMB) in Preparative Chromatography. Basics, Limitations and Use, pp 54-64. In Simulated Moving Bed:Basics and Applications, European Meeting, I.N.P.L Nancy, France.

Nicoud, R.M., Fuchs, G., Adam, P., Bailly, M., Küsters, E., Antia, F.A., Reuille, R., and Schmid, E. 1993. Preparative scale enantioseparation of a chiral epoxide: Comparison of liquid chromatography and simulated moving bed adsorption technology. Chirality, (5):267-271.

Pais, L. S., Loureiro, J.M., and Rodrigues, A.E. 1998. Separation of enantiomers of a chiral epoxide by simulated moving bed. J. Chromatography A, (827):215-233.

Pedeferri, M.P., Zenoni, G., Mazzotti, M., and Morbidelli, M. 1999. Experimental analysis of a chiral separation through simulated moving bed chromatography. Chem. Eng. Sci., (54):3735-3748.

Prochrom, Inc. 1997. Chrosoft manual, Technical documentation, Prochrom, Champineulles, France.

Pickenhagen, W. 1989. Enantioselectivity in Odor Perception, pp 151-157. In Flavor Chemistry Trends and Developments. ACS symposium series, American chemical society, Washington D.C.

Pynnonen, B. 1998. Simulated moving bed processing: escape from the high-cost box. J. Chromatography A, 827:143-160.

Rios, J.L., Recios, M.C., and Villard, A. 1988. Screening methods for natural products with antimicrobial activity. A review of literature. J. of Ethnopharmacology, (23):127-149.

Russel, G.F., and Hills, J.I. 1971. Odor differences between enantiomers. Science, (172):1043-1044.

Ruthven, D.M., and Ching, C.B. 1989. Counter-current and simulated counter-current adsorption separation processes. Chem. Eng. Sci., (44):1011-1038.

Sajonz, P., Zhong, G., and Guiochon, G.1996. Influence of the concentration dependence of the mass transfer properties on chromatographic band profiles. II- Accuracy of the determination of isotherm data by frontal analysis. J. Chromatography A, (731):1-25.

Sarker, M., and Guiochon, G.1995a. Study of the packing behavior of axial compression columns for preparative chromatography. J. Chromatography A, (702):27-44.

Sarker, M., and Guiochon, G.1995b. Study of operating conditions of axial compression columns for preparative chromatography. J. Chromatography A, (709):227-239.

Sarker, M., Katti, A.M., and Guiochon, G. 1996. Consolidation of the packing material in chromatographic columns under dynamic axial compression. II- Consolidation and breakage of several packing material J. Chromatography A, (719):275-289.

SAS Institute. 1996. SAS, version 6.12, SAS Institute, Cary, NC.

Seidel-Morgenstern, A., and Guiochon, G. 1993. Modeling of the competitive isotherms, and the chromatographic of the two enantiomers. Chem. Eng. Sci., (48): 2787-2797.

Stinson, S.C. 1995. Chiral drugs. Chem. & Eng. News, Oct. 09, 44-74.

Stinson, S.C. 1997. FDA may confer new status on enantiomers. Chem. & Eng. News, June 02, 28-29.

Storti, G., Mazzotti, M., Morbidelli, M., and Carra, S. 1993. Robust design of binary countercurrent adsorption separation processes. AIChE Journal, (39) 3:471-492.

Storti, G., Baciocchi, R., Mazzotti, M., and Morbidelli, M. 1995. Design of optimal operating conditions of simulated moving bed adsorptive separation units. Ind. Eng. Chem. Res., (34):288-301.

Streitweiser, A., and Heathcock, C.H. 1976. Introduction to Organic Chemistry. MacMillan Publishing Co., New York, NY.

White, C.A., and Subramanian, G. 1994. An Introduction to Enantioseparation by Liquid Chromatography, pp 1-17. In A Practical Approach to Chiral Separation by Liquid Chromatography, G. Subramanian (editor), VCH publishers, New York, NY.

Yun, T. 1996. PhD thesis. A Fundamental Study of Simulated Moving Bed Chromatography under Linear Conditions. Department of Chemical Engineering, University of Tennessee.

Yun, T., Zhong, G., and Guiochon, G. 1997. Simulated moving bed under linear conditions: Experimental versus calculated results. AIChE Journal, (43) 4:935-945.

Zhong, G., and Guiochon, G. 1996. Analytical solution for the linear model of simulated moving bed chromatography. Chem, Eng. Sci., (51): 4307-4319.

Zhong, G., and Guiochon, G. 1997. Simulated moving bed chromatography. Comparison between the behaviors under linear and nonlinear conditions. Chem, Eng. Sci., (52): 4403-4418.

Zhong, G., and Guiochon, G. 1998. Fundamentals of Simulated Moving Bed Chromatography under Linear Conditions, pp 351-400. In Advances in Chromatography. Volume 39.Grushka, E., and Brown, P.R. (Editors), Marcel Dekker Inc., New York, NY.

Zhong, G., Yun, T., Khattabi, S., and Guiochon, G. 1997. Simulated Moving Bed chromatography under linear conditions. Chromatographia. 45:109-115.

Vita

Saad Khattabi was born in Casablanca, Morocco. Upon graduating from high school in 1979, he left to Grenoble, France where he earned a Bachelor's degree in Metabolic Physiology in 1984, and a D.E.S.S. in Quality Control of Food in 1986. After graduation, he returned to Morocco, where he worked as a lab supervisor, then as a production manager, in a beer and soft drink bottling company (Brasserie du Maroc), which was licenced by Coca Cola Co. to bottle its products. In January 1996, he started his graduate studies in the department of Food Science and Technology at the University of Tennessee, Knoxville, where he received his Ph.D. degree in the last semester of the century (Fall 1999).

1150 7258 49
04•27•00 MAB
INFORMATION CONSERVATION, INC.